PDF issue: 2024-07-29

圧電素子を利用した睡眠状態無拘束観察法の提案

篠, 敏弘 / SHINO, Toshihiro

2011 年度　修士論文

圧電素子を利用した

睡眠状態無拘束観察法の提案

指導教員：渡辺　嘉二郎 教授

大学院工学研究科

システム工学専攻(システム系)修士課程

10R6116

シノ　トシヒロ

篠　敏弘

A Study of Noninvasive Bed Monitoring Method Using Piezoceramics

Toshihiro Shino

Abstract

This paper describes a noninvasive human monitoring using piezoceramics who is in bed. Sensors built in piezoceramics are set beneath the bed feet. This monitoring can detect body movement, scratching motion, respiration and heartbeat. These bio signals provide not only basic medical information but also details about sleep conditions. Thus, the bed sensing method can be used to monitor the health condition of people sleeping at home as well as that of patients in the hospital. The device has a wide dynamic range enabling the detection of micro vibrations from the heartbeat by the change in acting force, without saturation from body movements. Scratching motion is often monitored in various ways to evaluate an itching which appears as a symptom of various diseases. It is known that the length of the scratching time is related to the altitude of skin diseases accompanied by itching.

Key word

noninvasive sensing, bed sensing, piezoceramics, scratch monitoring

<h1>～ ～ 目 次 ～ ～</h1>

1 概要

本研究は睡眠中の人を無拘束で観察する事を目的としている．観察する目的はその人の健康管理である．観察は，圧電素子を利用したセンサをベッドの脚の下に設置して，ベッドの振動を計測する事によって行う．この計測に用いるセンサは，脈拍による微小振動も寝返りによって発生する大きな力の変化も，飽和する事なく計測可能な広いレンジを有する．この方法により，その人の寝返り・掻破・呼吸・脈拍によるベッドの振動を計測する事が出来る．これらの基本的な情報である生体信号から，睡眠の細かな様子を知る事が可能である事が知られている．掻破行動は様々な病気の症状として現れる．掻破にかける時間は，痒みを伴う皮膚病の皮膚の症状と相関がある事が知られており，その事を利用して，痒みの評価の為に多くの計測方法が提案されている．本論文ではベッドの振動から状態毎の振動を計測し，その時の状態に応じた信号処理法を提案する．このベッド計測システムを利用して，家庭生活に於いても病院の様に健康管理を行う事が出来る．

2 はじめに

高齢社会に於いて，高齢者が自らの健康を維持・管理する事はとても重要である．健康の維持は高齢者に限らず大切な事である．健康を管理するには，健康状態を定期的に観察する必要がある．これには日常的な生体信号計測が有意義である．また，健康を保つには睡眠が不可欠である．一方で，睡眠中には無意識に体を動かしており，その行動が病気の症状である事もある．一例として掻破行動が挙げられるが，掻破行動は痒みを伴う病気に対して表れ，特に皮膚病においては，皮膚の状態と患部を掻く時間に相関関係があることが知られている [1 - 3]．この時痒みを評価する指標として TST%が利用されている．これは総計測時間に占める総掻破時間の割合で表現される．これまで，健康管理を目的として，前腕の加速度や角速度の終日計測や，心電や脳波等のバイタルサインの計測，睡眠中のベッドに敷いたエアマット内の圧力の計測等が [4 - 15]，掻破行動の観察を目的として，睡眠中の様子を赤外線カメラで撮影し観察する方法や，指の曲がり具合の計測，手背の圧力の計測等が研究されてきた [16 - 23]．これら従来法は，大規模な装置と専門家が必要である事や，体に装着するセンサによる拘束，カメラ撮影におけるプライバシーに関する問題等の課題が挙げられる．そこで，我々は睡眠中の人を対象とし，人に直接触れずに，ベッドの振動を通して脈拍リズム及び呼吸リズム，掻破や寝返りを計測する装置及び，その計測結果よりその時の状態を推定する方法を開発した．

3 システム

3.1 ベッド計測システム

　図1に本研究に於いて提案するベッド計測システムを示す．ベッドの上にいる人の動作によるベッドの振動を計測する．センサは圧電素子が貼り付けられたステンレスの円板であり，ベッドの脚と床の間に円板を上にして設置される．ベッドと人の全ての荷重を4つのセンサが支える．センサに利用されている圧電素子には，加えられた圧力の変化量に比例した電圧を発生させる圧電特性がある．変化量に比例する為，出力電圧は定常状態に於いて 0V を基準とした極微小変化を示す．人が動くとベッドが振動し，ベッドの振動によりセンサが歪み，その歪み変化に比例した電圧が発生する．このシステムの変数と定数を以下に説明する．
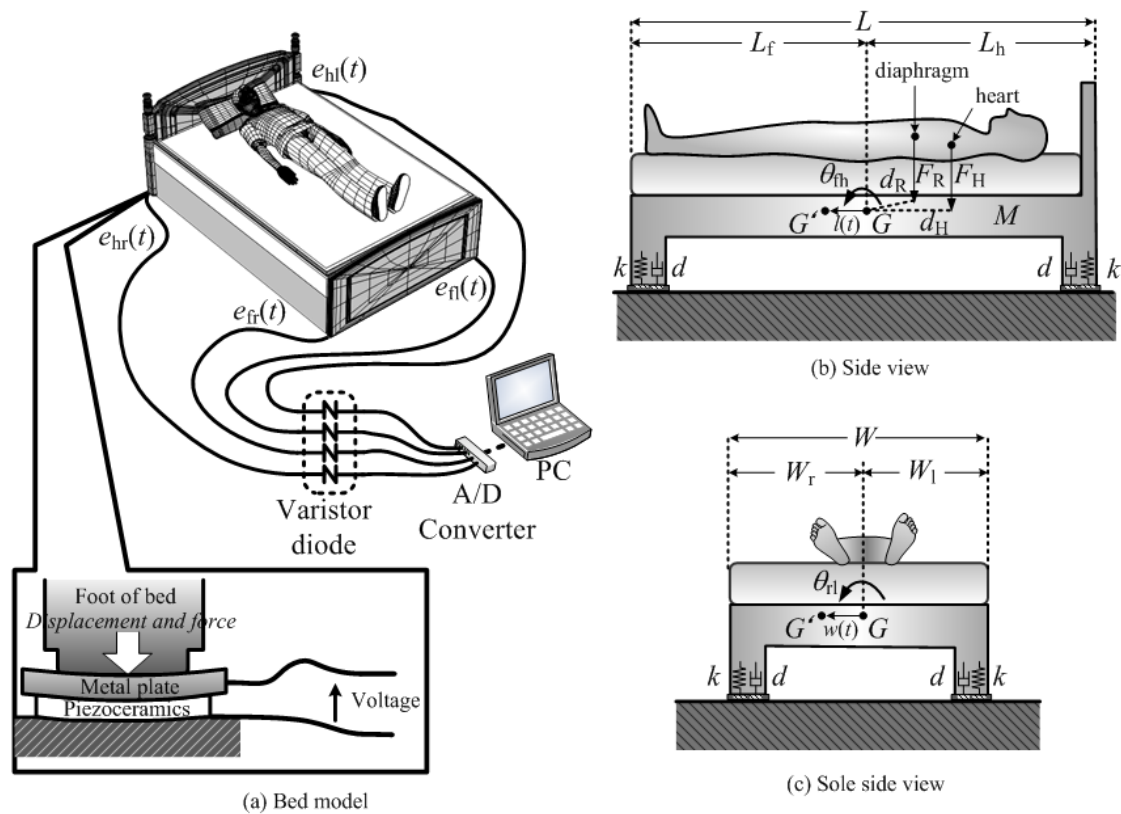

図1　ベッド計測システム

t [s]：時間

g [m/s^2]：重力加速度

<ベッド部分>

G, G'：ベッドと人の重心(C.G.)

$F_H(t)$ [N]：脈拍がベッドを押す力

$F_R(t)$ [N]：呼吸がベッドを押す力

M [kg]：ベッドと人の質量

W [m]：ベッドの幅

W_l [m]：C.G.から左の端までの長さ

W_r [m]：C.G.から右の端までの長さ

L [m]：ベッドの長さ

L_f [m]：C.G.から足元の端までの長さ

L_h [m]：C.G.から枕元の端までの長さ

$w(t)$ [m]：人の移動による C.G.変位の左右方向成分

$l(t)$ [m]：人の移動による C.G.変位の上下方向成分

d_H [m]：C.G.から心臓直下までの距離

d_R [m]：C.G.から横隔膜直下までの距離

$\theta_{rl}(t)$：ベッドの左右方向の俯角

$\theta_{fh}(t)$：ベッドの上下方向の俯角

<圧電素子部分>

A [C/m] or [N/V]：圧電素子の圧力-電圧変換係数

k [N/m]：センサのバネ係数

d [Ns/m]：センサのダンパ係数

C [F]：圧電素子の静電容量

R [Ω]：計測機器の入力インピーダンス

$f(t)$ [N]：圧電素子が発生する力

$q_i(t)$ [C]：外部歪みにより蓄えられる電荷量

$q(t)$ [C]：蓄えられる合成電荷量

$x_{hl}(t), x_{hr}(t), x_{fl}(t), x_{fr}(t)$ [m]：センサ円板の変位（添え字は其々枕元左側，枕元右側，足元左側，足元右側に設置されたセンサの変位である事を意味する）

$e_{hl}(t), e_{hr}(t), e_{fl}(t), e_{fr}(t)$ [V]：其々 $x_{hl}(t), x_{hr}(t), x_{fl}(t), x_{fr}(t)$ の出力電圧

3.2 計測原理

図 1 (b), (c) にベッドの上に人が寝ている様子を示す. 心臓は C.G. から d_H の距離に在り, 横隔膜は C.G. から d_R の距離に在る. 脈拍及び呼吸に伴う運動は其々 $F_H(t), F_R(t)$ の力でベッドを押す. 更に, この人が足元に向かって動いたり, 右に向かって動いたりすると, C.G. は G から G' へ距離 $l(t), w(t)$ だけ移動する. そしてベッドの足元は $\theta_{fh}(t)$ 沈み込み, 右側は $\theta_{rl}(t)$ 沈み込む.

まず, 図 1 (b) に於けるベッドの動きとセンサ出力について述べる.

$l(t)$ は非常に小さく $l(t) << L_f, L_h, L$ であり, G 周りの $\theta_{fh}(t)$ は G' 周りの $\theta_{fh}(t)$ と等しい. ベッドと人を考慮した C.G. 周りの慣性モーメント I_{fh} は, ベッドと人の質量及びベッドの寸法により与えられる. そして, このベッドの運動に関するバネ係数 K_{fh} とダンパ係数 D_{fh} は以下の式(1)で与えられる.

$$
\begin{aligned}
I_{\mathrm{fh}} &= M \cdot \frac{L_{\mathrm{f}}-l}{3L} \cdot (L_{\mathrm{f}}-l)^2 + M \cdot \frac{L_{\mathrm{h}}+l}{3L} \cdot (L_{\mathrm{h}}+l)^2 \cong \frac{M}{3L}\left(L_{\mathrm{f}}^3 + L_{\mathrm{h}}^3\right) \\
D_{\mathrm{fh}} &= d\left\{(L_{\mathrm{f}}-l)^2 + (L_{\mathrm{h}}+l)^2\right\} \cong d\left(L_{\mathrm{f}}^2 + L_{\mathrm{h}}^2\right) \\
K_{\mathrm{fh}} &= k\left\{(L_{\mathrm{f}}-l)^2 + (L_{\mathrm{h}}+l)^2\right\} \cong k\left(L_{\mathrm{f}}^2 + L_{\mathrm{h}}^2\right)
\end{aligned}
\tag{1}
$$

定常状態に於ける C.G. 周りの運動は式(2)で示される.

$$
I_{\mathrm{fh}} \frac{d^2\theta_{\mathrm{fh}}(t)}{dt^2} + D_{\mathrm{fh}} \frac{d\theta_{\mathrm{fh}}(t)}{dt} + K_{\mathrm{fh}}\theta_{\mathrm{fh}}(t) = Mgl(t) + d_{\mathrm{H}}F_{\mathrm{H}}(t) + d_{\mathrm{R}}F_{\mathrm{R}}(t) + Lf(t)
\tag{2}
$$

枕元及び足元に設置されたセンサの変位は以下で与えられる.

$$
\begin{aligned}
x_{\mathrm{f}}(t) &= (L_{\mathrm{f}}-l)\theta_{\mathrm{fh}}(t) \cong L_{\mathrm{f}}\theta_{\mathrm{fh}}(t) \\
x_{\mathrm{h}}(t) &= -(L_{\mathrm{h}}+l)\theta_{\mathrm{fh}}(t) \cong -L_{\mathrm{h}}\theta_{\mathrm{fh}}(t)
\end{aligned}
\tag{3}
$$

圧電素子の持つ圧電効果は可逆性を有しており，この変位により式(4)の力が生じる．

$$
\begin{aligned}
q_i(t) &= A x_{\mathrm{f}}(t) = A L_{\mathrm{f}} \theta_{\mathrm{f\,h}}(t) \\
R \frac{dq(t)}{dt} + \frac{1}{C} q(t) &= \frac{1}{C} q_i(t) \\
e_{\mathrm{f}}(t) &= R \frac{dq(t)}{dt} \\
f(t) &= -A e_{\mathrm{f}}(t)
\end{aligned}
\tag{4}
$$

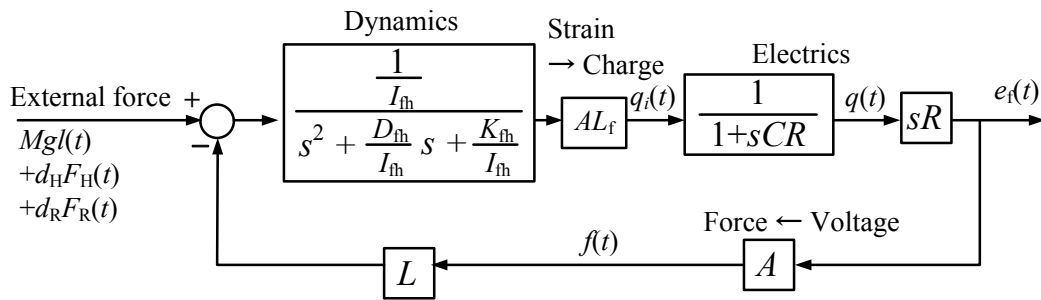図2は，このベッド計測システムの力学入力から計測信号となる電気出力までをブロック線図で表したものである．このベッド計測システムが有する変換関数を機能毎に式(5)に定義する．

図2 ベッド計測システムのブロック線図

$$
\begin{aligned}
G_1(s) &= \frac{A}{C} \\
G_2(s) &= \frac{sCR}{1 + sCR} \\
G_3(s \mid L_{\mathrm{f}}) &= \frac{\dfrac{L_{\mathrm{f}}}{I_{\mathrm{fh}}}}{s^2 + \dfrac{D}{I_{\mathrm{fh}}} s + \dfrac{1}{I_{\mathrm{fh}}} \left\{ K_{\mathrm{fh}} + \dfrac{sRLL_{\mathrm{f}} A^2}{(1 + sCR)} \right\}}
\end{aligned}
\tag{5}
$$

従って，力学入力 $Mgl + d_H F_H + d_R F_R$ に対して，足元に設置されたセンサの出力 $e_f(t)$ は式(6)で与えられ，(4)式から(7)式により，同様に枕元に設置されたセンサの出力 $e_h(t)$ は式(7)で与えられる．

$$e_f = G_1(s) \cdot G_2(s) \cdot G_3(s \mid L_f)(Mgl + d_H F_H + d_R F_R) \tag{6}$$

$$e_h = -G_1(s) \cdot G_2(s) \cdot G_3(s \mid L_h)(Mgl + d_H F_H + d_R F_R) \tag{7}$$

3.3 計測

計測には入力インピーダンス R が 1 から $10\,M\Omega$ の一般的な計測機器を用いると想定する．この時，式(5) $G_2(s)$ による遮断周波数 $\dfrac{1}{2\pi CR}$ は，脈拍の周波数よりも十分低く設定出来る．更に，式(5) $G_3(s)$ の共振周波数は

$$f = \frac{1}{2\pi}\sqrt{\frac{K_{fh} + (LL_f A^2/R)}{I_{fh}}} = \frac{1}{2\pi}\sqrt{\frac{3Lk(L_f^2 + L_h^2)}{M(L_f^3 + L_h^3)}} \tag{8}$$

により設定出来る．ここで，式(1), (5), (6), (7)から，$\dfrac{1}{2\pi CR}$ よりも低い周波数帯域において，式(9)の近似式が得られる．同様に，図1(c)に示した左右方向の運動による出力電圧 $e_l(t), e_r(t)$ も以下の様に得られる．これらセンサ出力は図1の $e_{hl}(t), e_{hr}(t), e_{fl}(t), e_{fr}(t)$ に対応している．

$$e_f(t) = AR\frac{L_f}{k(L_f^2 + L_h^2)}\frac{d}{dt}\{Mgl(t) + d_H F_H(t) + d_R F_R(t)\}$$

$$e_h(t) = -AR\frac{L_h}{k(L_f^2 + L_h^2)}\frac{d}{dt}\{Mgl(t) + d_H F_H(t) + d_R F_R(t)\} \tag{9}$$

$$e_r(t) = AR\frac{W_r}{k(W_r^2 + W_l^2)}\frac{d}{dt}\{Mgw(t) + d_H F_H(t) + d_R F_R(t)\}$$

$$e_l(t) = -AR\frac{W_l}{k(W_r^2 + W_l^2)}\frac{d}{dt}\{Mgw(t) + d_H F_H(t) + d_R F_R(t)\} \tag{10}$$

3.4 状態の定義

　睡眠中の人は安静状態又は，掻破状態，寝返り状態のいずれかの状態にあるとする．以下に各状態の定義とその状態に於ける人の動きを記述する．

　安静状態は何も動作をしていない状態である．この時もその人の心臓や横隔膜は動いている．この脈拍や呼吸により人の体は其々の周期で小さく振動している．この時のベッド計測システムへの主な入力は $d_H F_H(t) + d_R F_R(t)$ である．

　掻破状態はその人が体の痒い箇所を指で繰り返し掻いている状態である．本研究では足同士をこすり合わせる動作も掻破行動とする．この状態では人の四肢が大きく周期的に動いている．この時の主な入力は $Mgl(t), Mgw(t)$ であり，周期的に変化している．

　寝返り状態は，仰臥位又は右左の側臥位，長座位等へと体位を変え，ベッド上を移動している状態である．掻破の為に四肢を掻破したい箇所へ動かしている状態や，その逆に掻破箇所から遠ざけている状態も寝返り状態とする．この状態のベッド上における人の動きは，ある体位から別のある体位へ動く大きな非周期或いは長周期的動作である．この時のベッド計測システムへの主な入力は $Mgl(t), Mgw(t)$ である．

3.5 信号処理

　ここでは各状態に対して必要な信号処理について述べる．尚，システムの外乱として，ベッドの固有振動による振動及び計測時の電気的ノイズが存在する．

・安静状態

　脈拍及び呼吸による振動 $d_H F_H(t) + d_R F_R(t)$ のみが計測される．脈拍や呼吸は周期的に動いており，その周波数成分を抽出する事によって，脈拍や呼吸の情報が得られる．

・掻破状態

　掻破行動を通した痒み観察の為の処理を行う．まず掻破状態であった時間を決定する．時間が決定されたら，痒みの指標である TST%を算出する．TST%は総計測時間に対する，総掻破時間の割合で表される．

・寝返り状態

　ベッド上で人が大きな寝返りをすると，入力 $Mgl(t), Mgw(t)$ が大きく

$$Mgl(t) >> d_H F_H(t) + d_R F_R(t)$$
$$Mgw(t) >> d_H F_H(t) + d_R F_R(t)$$

となる．

その為，式(9)，（10)は式(11)となる．

$$e_f(t) = AR \frac{L_f}{k(L_f^2 + L_h^2)} \frac{d}{dt}\{Mgl(t)\}$$

$$e_h(t) = -AR \frac{L_h}{k(L_f^2 + L_h^2)} \frac{d}{dt}\{Mgl(t)\}$$

$$e_r(t) = AR \frac{W_r}{k(W_r^2 + W_l^2)} \frac{d}{dt}\{Mgw(t)\}$$

$$e_l(t) = -AR \frac{W_l}{k(W_r^2 + W_l^2)} \frac{d}{dt}\{Mgw(t)\}$$

(11)

この式(11)利用して，式(12)が導かれる．

$$P_{fh}(t) = \int_o^t \{e_{fl}(\tau) - e_{hl}(\tau)\}d\tau = \frac{ARLMg}{k(L_f^2 + L_h^2)} l(t)$$

$$P_{rl}(t) = \int_o^t \{e_{hr}(\tau) - e_{hl}(\tau)\}d\tau = \frac{ARWMg}{k(W_r^2 + W_l^2)} w(t)$$

(12)

これは其々，上下，左右方向の C.G の変位に比例している．これを利用して，ベッド上の重心移動を推定する事が出来る．

3.6 本研究に使用したシステム

　図 3 に本研究で利用した実験システムを示す．センサには直径 25mm の真鍮円板に張り付けられた直径 20mm の円形の素子を使用している．これは小型のブザーとして市販されていた物である．この圧電素子を厚さ 1mm，直径 50mm のステンレス円板の中心に同心円を描くように接着した．そして，直径 50mm のアルミニウム円板に厚さ 2mm，外径 50mm，内径 40mm のワッシャーを接着したものを，圧電素子保護用のカバーとして接着した．本研究で使用している圧電素子の圧電素子の圧力-電圧変換係数 A は 1×10^{-3} [C/m]であり，その静電容量 C は $0.01 \mu F$ である．図 3 に示す様に 4 つのセンサを 1 つずつベッドの脚の下に設置する．使用しているベッドはコイルクッションタイプのものであり，重さ 60kg，縦 2.1m，横 1.0m である．4 つのセンサからの信号はサンプリング周期 1ms，計測レンジを ±1V と設定し，AD 変換器(NR2000, Keyence Co. Ltd.)で計測した．

ベッドの振動特性を調べる為に，ベッドの隅を軽く叩き，インパルス状の振動を入力した．その時の出力 $e_{hr}(t)$ の時間的変化の様子とその 1024 点をフーリエ変換した時の周波数分布を図 4 に示す．この結果より，このベッド計測システム全体の共振周波数は 10.73Hz である．
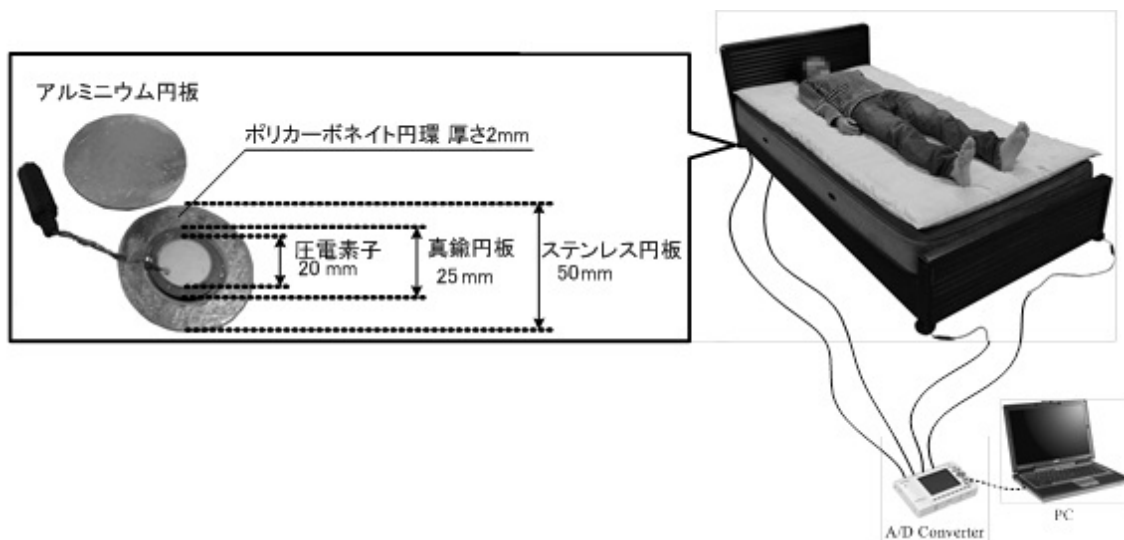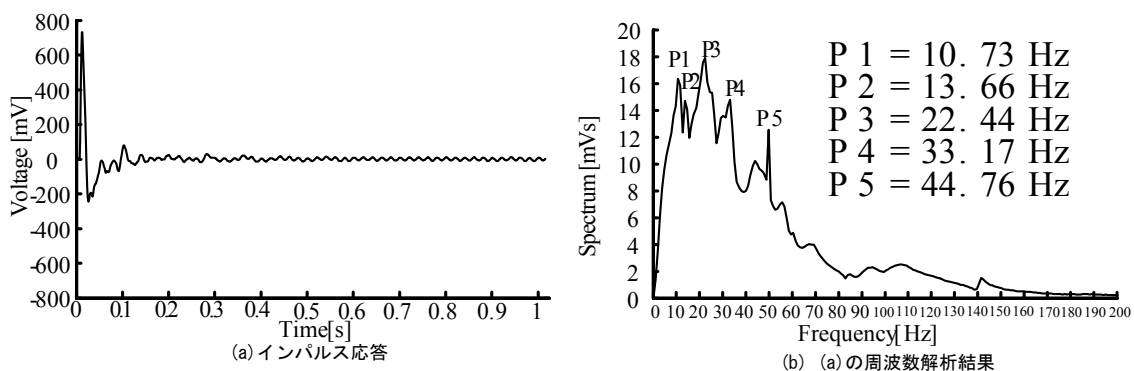

図 3　実験システム

図 4　インパルス応答

　このシステムを用いて出力信号 $e_{hl}(t), e_{hr}(t), e_{fl}(t), e_{fr}(t)$ から脈拍や呼吸を計測し，寝返りや掻破を観察する．

4 実験

4.1 安静状態に関する実験

4.1.1 安静状態に関する実験―方法

安静状態に得られた信号から脈拍及び呼吸の信号を取り出す事が本実験の目的である．被験者はベッドに横たわり，安静状態を保つ．この時，計測対象の基準データ計測用として脈拍信号用に脈波測定器を耳たぶに，呼吸用に低周波マイクロフォンを鼻孔の下に装着して実験を行う．脈拍及び呼吸はそれぞれおよそ 1Hz，0.3Hz である．また，脈拍による振動には約 1Hz の基本波成分よりも 3〜7Hz 程度の高周波成分が多く含まれる特徴がある．呼吸信号については高調波成分が殆ど無い．其々をフィルタリング処理により取り出す．

脈拍信号については，計測信号をフーリエ変換し，脈拍の特徴から 3Hz から 7Hz の成分のみを取り出し，逆フーリエ変換する．抽出した脈拍成分の高調波信号を低周波帯域へシフトさせる為に全波整流し，150 点の移動平均を取る．

呼吸信号については，脈拍信号と同様に呼吸の特徴から 0.1Hz から 0.5Hz の成分のみを取り出す．呼吸信号は一度のフィルタリング処理のみである．

4.1.2 安静状態に関する実験―結果

図 5 に脈拍成分の抽出した結果を示す．(a)は基準である脈波計測器によって計測された信号であり，(b)は上述の二度のフィルタリング処理によって得られた信号である．この信号を計測した箇所は被験者の足元左側である．センサ出力から抽出された脈拍信号の振幅は 10mV 程度であり，リファレンスと同期している．フィルタ処理をした脈拍信号の中にも呼吸信号による変化が含まれている．この箇所以外に設置されたセンサからも，フィルタリングにより，同様の信号を得られた．従って，4 箇所に設置されたセンサに於いても脈拍信号が計測された．

図 6 に呼吸成分を抽出した結果を示す．図 5 と同様(a)にはリファレンスとして使用した低周波マイクロフォンの計測結果を，(b)に枕元右側に設置されたセンサから得られた信号の処理結果を示す．圧電センサ出力から得られた呼吸信号の振幅は 0.5mV 程度であり，リファレンス信号と同期している．図に示すセンサ以外の 3 つのセンサからも同様の信号が得られた．しかし，枕元に設置されたセンサから抽出された信号はリファレンスと同期しており，足元に設置されたセンサから得られた信号は枕元のものとは正負が逆転していた．
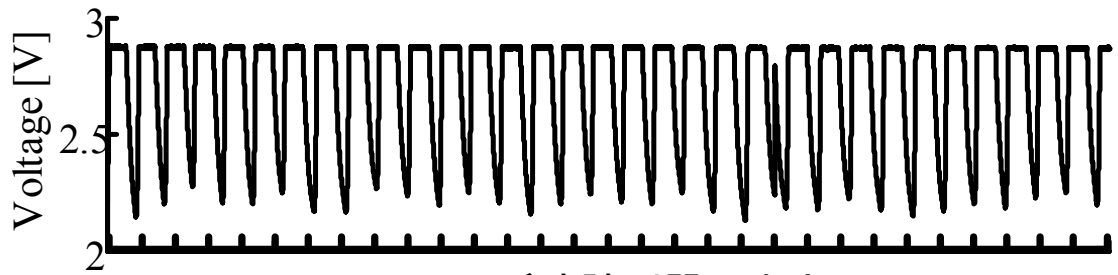
(a) 脈波計測器の出力
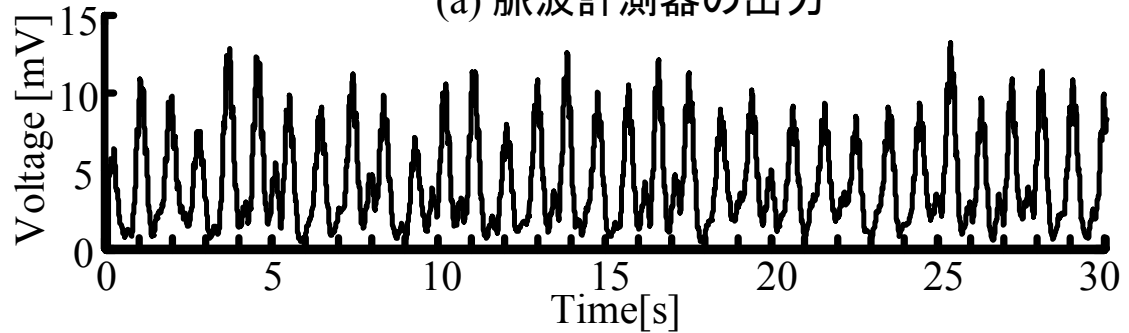
(b) フィルタリング後のセンサ信号

図5　脈拍信号抽出結果

(a) 低周波マイクロフォンの出力

(b) フィルタリング後のセンサ信号

図6　呼吸信号抽出結果

4.1.3 安静状態に関する実験―考察

　センサ出力から抽出された呼吸の信号が枕元と足元で正負逆転して変化していたが，これはフィルタ処理を施す前の計測された変化そのものにも見られた特徴である．この原因は呼吸の際に動く横隔膜や脈拍を生み出す心臓が C.G. よりも枕元に近いところでベッドに力を与えているからである（式(9)参照）．脈拍信号にこの特徴が表れない理由は，脈拍信号を抽出する際に全波整流処理を施しているからである．脈拍信号も呼吸信号も計測結果が基準と同期している事から，この計測システムを利用して脈拍及び呼吸のリズムを計測することが出来た．
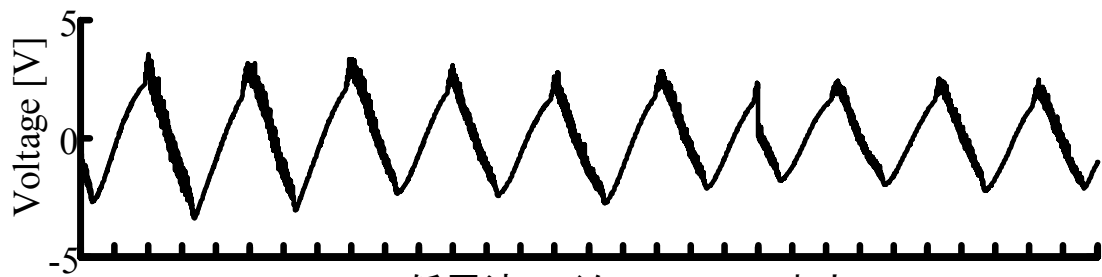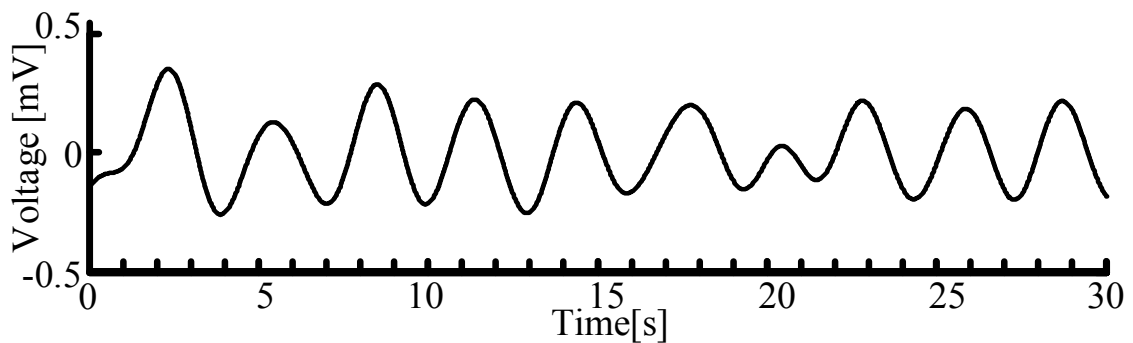
4.2 寝返り状態に関する実験

4.2.1 寝返り状態に関する実験―方法

　重心移動が推定可能である事を検証する事が目的である．被験者は安静に横たわった状態から左右の側臥位や長座位へと寝返りをする．実験は，その様子をカメラ(EX-F1, Casio)で撮影しながら行われた．寝返り状態を計測し，計測結果について 3.5 式(12)を適用する．

$$P_{\mathrm{fh}}(t) = \int_o^t \{e_{\mathrm{fl}}(\tau) - e_{\mathrm{hl}}(\tau)\} d\tau$$

$$P_{\mathrm{rl}}(t) = \int_o^t \{e_{\mathrm{hr}}(\tau) - e_{\mathrm{hl}}(\tau)\} d\tau$$

（3.5 式(12)）

4.2.2 寝返り状態に関する実験―結果

　図７から１１までは本実験の結果の一部とそのときの様子と併せて示した物である．図中では，最上段にその時の体位の写真，中段に $P_{fh}(t)$，下段に $P_{rl}(t)$ を示している．この計測中，４つのセンサはいずれも飽和する事は無かった．

　図７では被験者はまず仰臥位であり，そこからベッド右側へ移動して右側臥位となった．その後，ベッド左側へ寝返りをして左側臥位になり，再び仰臥位へ戻った．この実験動作では枕‐足方向の動作がほとんど無いので，$P_{fh}(t)$ の変化は極めて小さい．一方で左‐右方向の動きに合わせて $P_{rl}(t)$ が変化している．被験者が右向きに動き始めた時，$P_{rl}(t)$ は 0mVs から正の領域に増加し，反対に左向きに動き始めた時には減少を始める．被験者が一定の場所で停止しているとき，$P_{rl}(t)$ はそのときの一定の値をとり続け，あまり変化しない．最終的に仰臥位に戻った時には，$P_{rl}(t)$ は始めと同じ約 0mVs をとった．$P_{rl}(t)$ はベッド上で動く被験者の左右方向の重心移動に比例している．
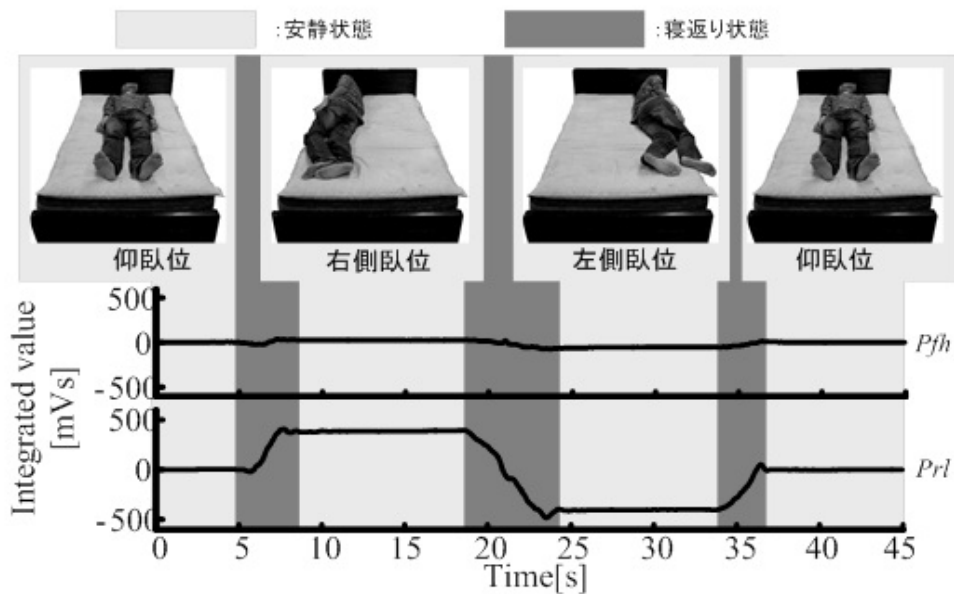
図7　横方向の寝返り

　図8から図11までは仰臥位であった被験者が長座位へ移動し，戻った様子を示している．但し，図8には実験の際には手をつかずに起き上がった場合を，図9には左手で体を支えながら起き上がった場合を，図10には右をついた場合を，図11には両手をついた場合を其々示す．

　図8に示す場合では，左右方向の動きが少なく$P_{rl}(t)$は少ししか変化をしない．$P_{fh}(t)$は被験者が起き上がり始めた時に増加を始め，長座位や仰臥位で動いていない時間にはほぼ一定値を取り，仰臥位へ戻り始めた際には減少を始めた．この実験より，$P_{fh}(t)$はベッド上で動く被験者の枕-足元方向の重心移動に比例している．

　図8～11では，$P_{fh}(t)$は同様な変化をしている．しかし，被験者がベッドを押した際に$P_{rl}(t)$が其々異なる変化をしている．図9では左手でベッドを押した事により，ベッドと人の重心が左側へ移動した事を意味している．図10では右手でベッドを押した事により，ベッドと人の重心が右側へ移動した事を意味している．図11では両手をついた為，左右どちらか一方だけに力が偏らず，重心も左右に大きく動くこと無く起き上がった事を示している．
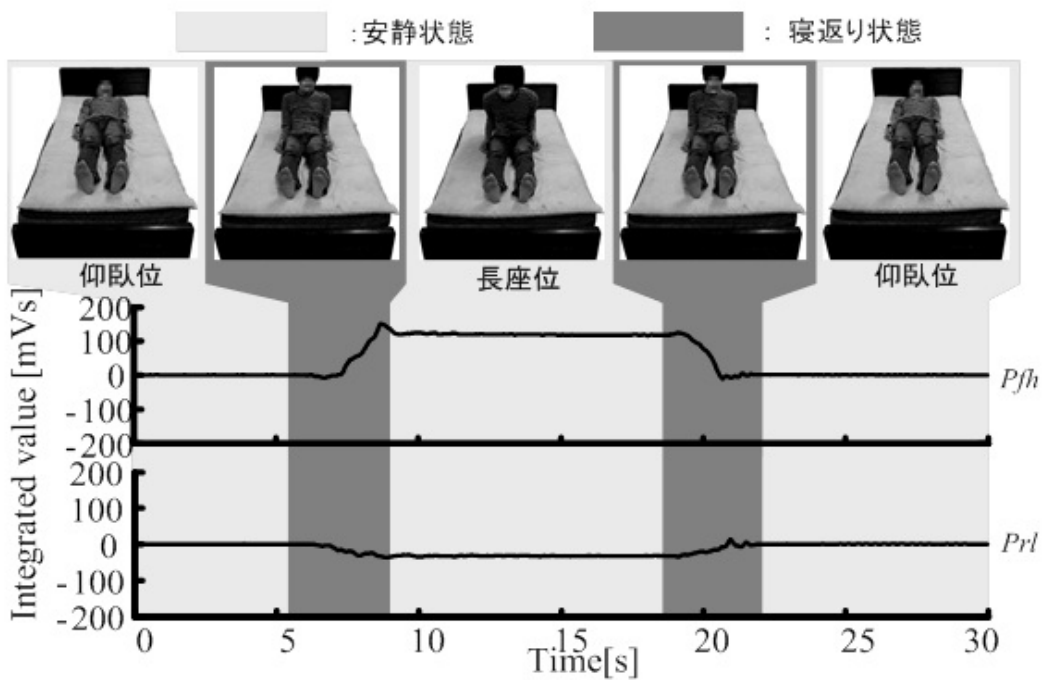
図8　縦方向の寝返り—手を使わない場合
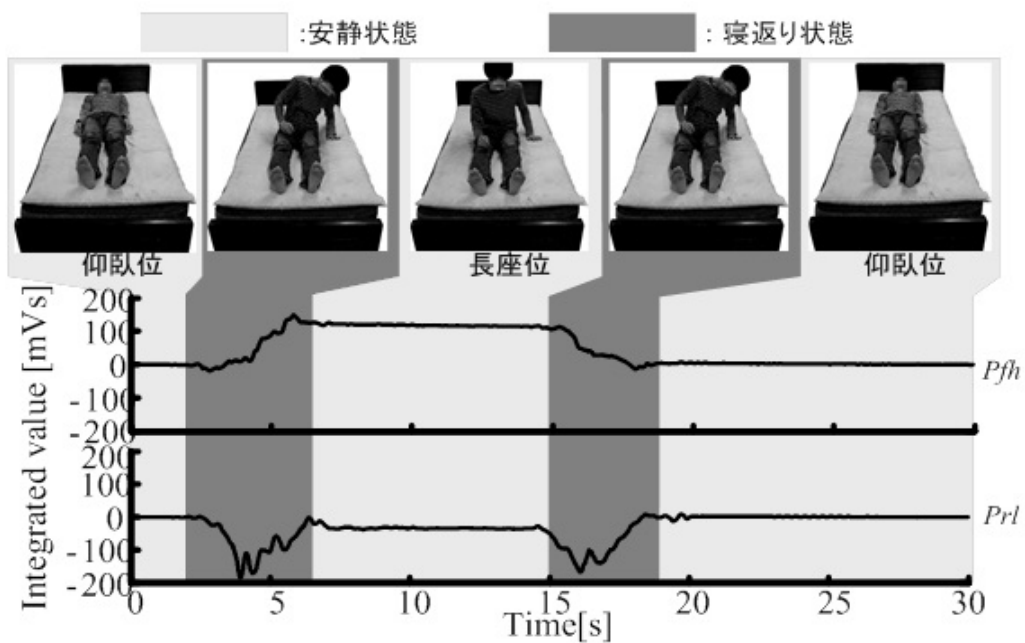
図9　縦方向の寝返り—左手を使う場合
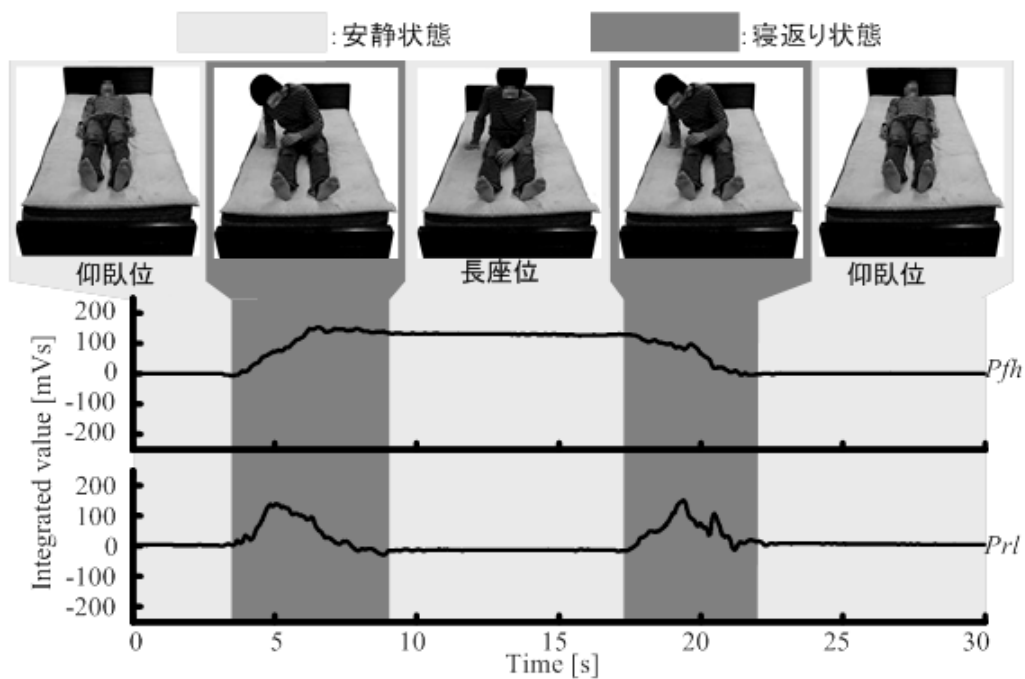
図１０　縦方向の寝返り—右手を使う場合
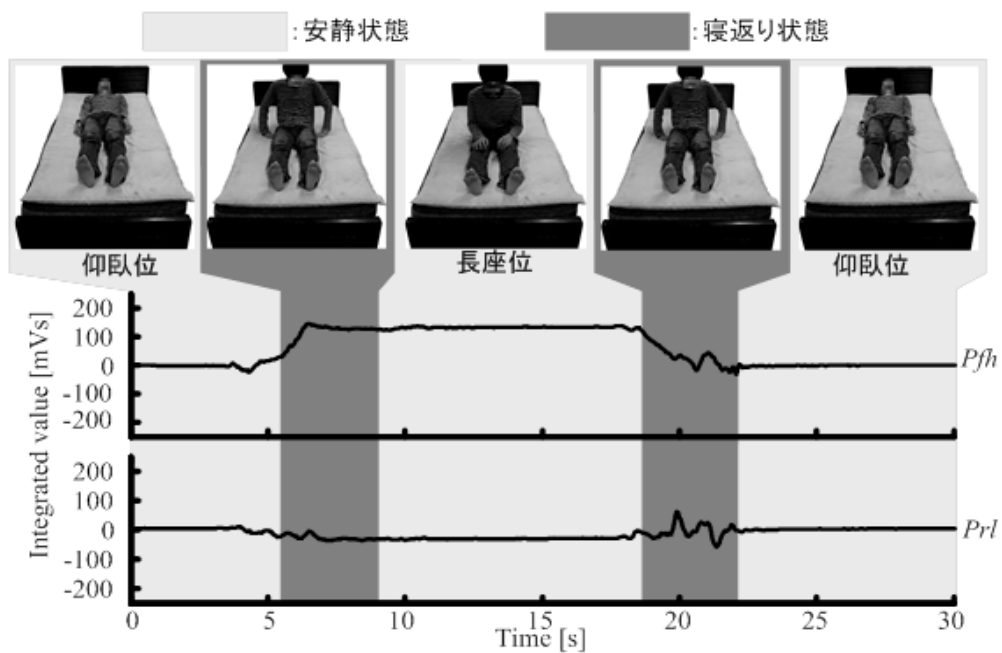
図１１　縦方向の寝返り—両手を使う場合

4.2.3 寝返り状態に関する実験—考察

結果では省略したが，寝返りよりも更に大きな振動を発生させる動作であるベッドの出入りも飽和することなく大きな信号として計測される．このセンサは広いレンジを持ちながら，圧電効果により，センサ部に電源が不要である．そして，3.5 式(12)を用いる事でベッド重心移動を推定する事が可能である．3.5 式(12)の通り，$P_{fh}(t), P_{rl}(t)$はベッドの上の人の変位に比例している．睡眠中の寝返りや脈拍，呼吸の変化から睡眠段階を推定する方法があるが [11]，そのセンサ部として利用可能である．この計測に用いているセンサはただ生体信号を計測するだけでなく，計測用マイコンのイベントトリガとしても使用可能である．トリガとしての利用は1年程度電池の持つ低消費電力のマイコンによる処理を開発する上で優れている．

4.3 掻破状態に関する実験

4.3.1 掻破状態に関する実験―方法 [16 – 23]

　提案システムによる掻破計測の精度を従来法と比較する事が目的である．本実験では，計測時に入り込む高周波ノイズを減衰させる為に遮断周波数 12Hz の一次ローパスフィルタを使用した．掻破計測に従来用いられてきたセンサと同時に模擬計測し，精度の比較をする．掻破行動を記録する為に，被験者の右手をビデオカメラ(EX-F1, Casio)で撮影する．カメラは動かないように固定する．図１２に掻破実験の様子を示す．使用する従来センサについて説明する．従来用いられているセンサは，筋電位計，加速度センサ，角速度センサ，マイクロフォン，圧力計及び歪ゲージである．

　筋電位センサは掻破による前腕の筋電位の変化を計測する為に使用されてきた．今回は，Medical Electronic Science Institute Co., Ltd の RF-ECG を右前腕にテープで固定した．サイズは 40×35×7.2mm である．

　加速度センサは掻破時に動く前腕の加速度を計測する為に用いられている．今回は，Medical Electronic Science Institute Co., Ltd の RF-ECG を右前腕にテープで固定した．このセンサは筋電位と 3 軸加速度が計測出来る．筋電位と加速度の情報は 204Hz で AD 変換され，ブルートゥース通信を利用してパソコンに送られる．3 軸の方向は図１２に示す．計測レンジは±3G とした．このセンサは重力加速度も計測する．

　角速度センサも加速度センサ同様前腕の角速度を計測する為に使われる．今回は富士通製 3 軸角速度センサ(FMS-001)を使用し，図１２の様にテープで固定した．サイズは 40×45×13mm であり，2ms で計測されたデータはブルートゥース通信でパソコンに送られる．

　マイクロフォンは掻破に伴う音を計測する目的で開発された．今回は低周波マイク(MX4836, Primo Co. Ltd)を右手の甲に固定した．出力信号はアンプを通してから，サンプリング間隔 1ms，計測レンジ±10V で AD 変換した．

　掻破による手の甲の圧力変化を計測する為に，今回セラミックシート (Flicker, Measurement Specialties Inc.)を右手の甲にテープで固定した．出力信号はサンプリング間隔 1ms，計測レンジ±1.0V で AD 変換される．

　歪ゲージは指に沿って固定する事により，掻破による指の曲げ伸ばしを計測する．今回は右手人差し指につけた．サンプリング間隔 1ms，計測レンジ±5V で計測した．

　被験者は身長約 170cm，体重約 50kg，右利きの男性である．
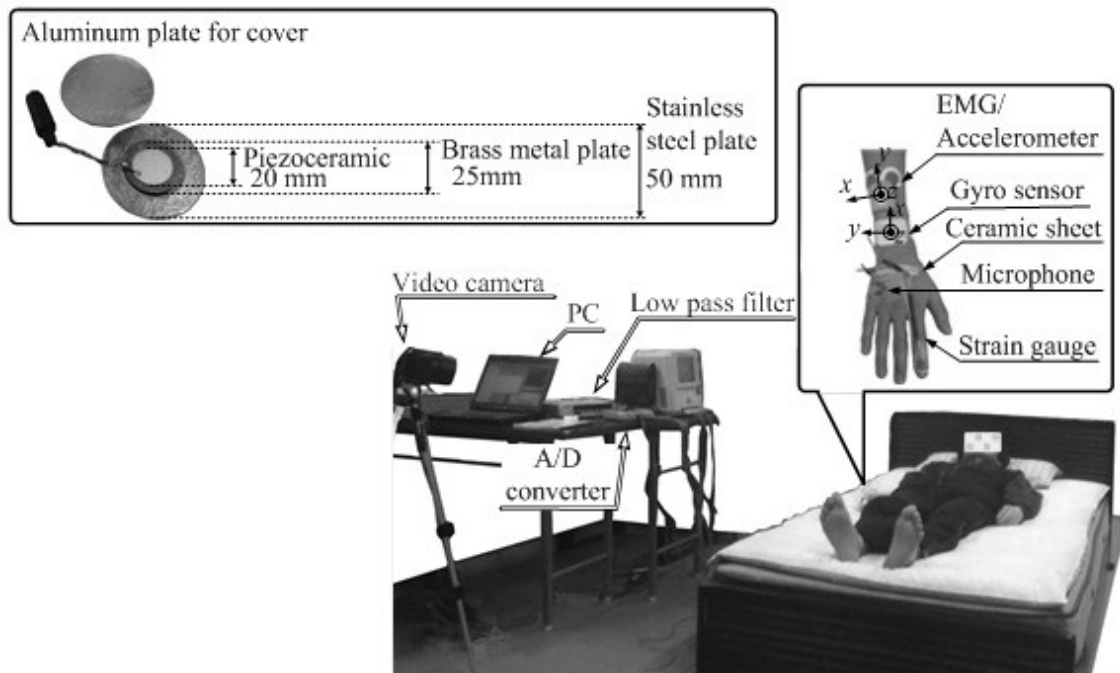
図１２　掻破状態に関する実験の計測装置

4.3.2 掻破状態に関する実験―手順

　図１２の様なベッド中央での自然な仰臥位を基本姿勢とする．被験者は基本姿勢から右肘を曲げて右頬を 20 回掻破する．顔を掻破する理由はアトピー性皮膚炎の患者が最も頻繁に掻破する箇所が首より上だからである [16]．20 回掻破したら基本姿勢に戻り，およそ 5 秒安静にし，再び右頬を 20 回掻破する．この行動を 35 回繰り返す．計測開始から，計測終了までの時間を T_{total} とする．掻破行動は指の往復運動であるので，センサ出力から信号が周期的に大きく変化している時間を掻破時間として読み取ることが出来る．その特徴から読み取った 35 回分の掻破時間の和である Total Scratching Time [s]を $T_{scratch}$ とする．すると，皮膚病の痒みの指標として使用されている TST%は以下より求まる．

$$TST\% = \frac{T_{scratch}}{T_{total}} \times 100$$

　以上の手順を全てのセンサについて行い，カメラで撮影された映像より求まる正しい Total Scratching Time との比較を行う．

4.3.3 掻破状態に関する実験―結果

図１３にある一区間の掻破計測結果を示す．グラフは上から順に，筋電位計，セラミックシート，マイクロフォン，歪ゲージ，3 軸加速度センサ(X, Y, Z 軸の順)，3 軸角速度センサ(X, Y, Z 軸の順)，提案するシステム($e_{hl}(t), e_{hr}(t), e_{fl}(t), e_{fr}(t)$ の順)の出力を示している．

図中の 0 秒から 1 秒までは安静状態であり，提案するシステムだけが，脈拍による信号を検知している．

1 秒から 2 秒までの間に被験者は手を顔に向かって動かした．この時，多くのセンサ出力が変化した．提案システムについては，ベッドの右側に設置されたセンサ出力 $e_{hr}(t), e_{fr}(t)$ がそれまでとは異なる不規則な変化をした．

2 秒から 7.5 秒までの間に被験者は 20 回の掻破を行った．$e_{hl}(t), e_{hr}(t), e_{fl}(t), e_{fr}(t)$ は掻破によって大きく周期的に変化している．この時の提案センサの振幅は，比較的掻破箇所に近い枕元に設置されたセンサ出力である $e_{hr}(t), e_{hl}(t)$ が足元のものよりも大きい．提案センサの中で最も掻破箇所に近い $e_{hr}(t)$ の振幅が最大となった．他の従来センサも掻破時には周期的に変化している．

7.5 秒から 9 秒までは，被験者は基本姿勢に戻っている途中である．この時の出力変化は掻破前の変化より滑らかである．

9 秒から 10 秒までは安静状態であり，0 秒から 1 秒までと同様，従来センサには大きな変化は無く，提案センサでは脈拍による振動を計測している．
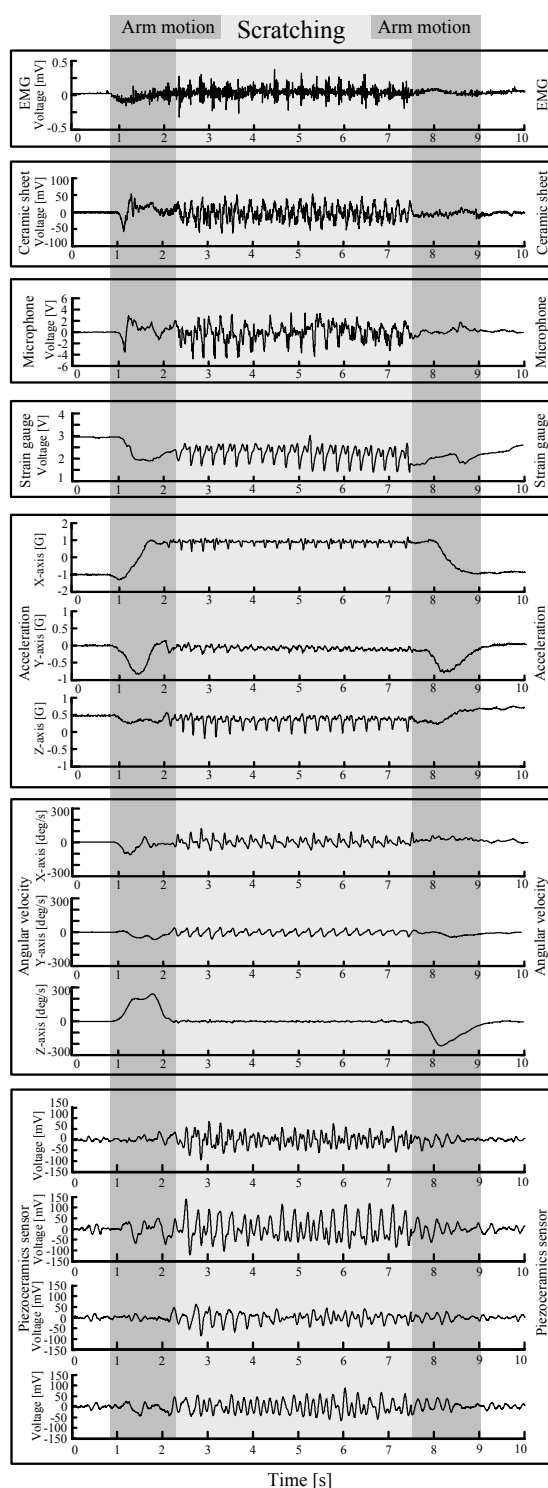
図１３　掻破計測結果

表１は図１３の区間について，各センサから得られた掻破時間と映像によって求めた掻破時間との誤差を示している．筋電位計について，掻破時の波形と掻破前の腕の動きによる信号の変化が似ている為，掻破時間を正確に決定するのは難しく，この区間での誤差は+1.16秒であった．セラミックシートとマイクロフォン，歪ゲージの出力について，これらは掻破による変化と腕の動きによる変化の違いがはっきりしている為，掻破時間の決定が簡単である．其々の誤差は，+0.02秒，+0.05秒，+0.11秒であった．加速度の計測結果について，3軸とも腕の動きによる出力変化と掻破による変化の仕方は明確に異なるが，二つの動作の間の変化が滑らかである為，掻破時間決定が多少難しい．誤差はX, Y, Z軸の順に+0.06秒，-0.22秒，+0.18秒である．角速度の変化については，X, Y軸では掻破が終わった時刻を判断するのが困難であり，誤差は其々+0.42秒，+0.48秒となった．Z軸角速度については，掻破区間がその前後と明らかに異なる為分かり易く，誤差は+0.03秒となった．そして提案するシステムによる結果，掻破区間の決定は足元に於いて難しく，誤差は$e_{hl}(t), e_{hr}(t), e_{fl}(t), e_{fr}(t)$の順に+0.15秒，-0.02秒，+1.12秒，+1.00秒であった．

　また，この実験ではT_{total}は385秒であった．センサ毎にTST%を計算した．表２は$T_{scratch}$とTST%，其々の誤差を示した物である．提案システムの中では，掻破箇所に近くに設置された$e_{hl}(t)$の誤差が最小の-0.8%であり，足元に設置された$e_{fl}(t)$の誤差が最大の+6.5%であった．従来センサと比較すると，最小の誤差は-0.3%であり，最大誤差は12.7%である．

表１　掻破時間とその誤差

Sensor		Time during scratching [s]	Error [s]
Video camera		5.22	-
EMG		6.38	1.16
Ceramic sheet		5.24	0.02
Microphone		5.27	0.05
Strain gauge		5.33	0.11
Acceleration	x	5.28	0.06
	y	5.00	-0.22
	z	5.40	0.18
Angular velocity	x	5.64	0.42
	y	5.70	0.48
	z	5.25	0.03
Piezoceramics sensor	e_{hl}	5.20	-0.02
	e_{hr}	5.37	0.15
	e_{fl}	6.22	1
	e_{fr}	6.34	1.12

表２　$T_{scratch}$とTST%とそれらの誤差

Sensor		$T_{scratch}$ [s]	Error [s]	TST [%]	Error of TST [%]
Video camera		179	-	46.5	-
EMG		228	49	59.2	12.7
Ceramic sheet		177	-2	46.0	-0.5
Microphone		176	-3	45.7	-0.8
Strain gauge		186	7	48.3	1.8
Acceleration	x	159	-20	41.3	-5.2
	y	151	-28	39.2	-7.3
	z	162	-17	42.1	-4.4
Angular velocity	x	178	-1	46.2	-0.3
	y	178	-1	46.2	-0.3
	z	167	-12	43.4	-3.1
Piezoceramics sensor	e_{hl}	176	-3	45.7	-0.8
	e_{hr}	186	7	48.3	1.8
	e_{fl}	204	25	53.0	6.5
	e_{fr}	201	22	52.2	5.7

4.3.4 掻破状態に関する実験―考察

掻破状態計測信号は比較的大きな振幅のある周期的変化を示した．この特徴から，掻破時間を計測する事が可能であり，TST%を求める事が出来る．提案する方法は，センサをベッドの脚の下に設置する為，従来法よりも拘束性が非常に低い．

提案するシステムでは，掻破箇所に近いところに設置されたセンサの出力程掻破による信号の振幅が大きい．振幅が小さいと掻破区間決定が難しくなり誤差の原因となる．足元に設置されたセンサの誤差が提案法の中で最大となった理由は，掻破区間の振幅が小さかったからである．顔を掻破していた為，足元は掻破箇所から遠い．その為，掻破信号と掻破前後の動作の信号の区別が困難となった．枕元に設置されたセンサの誤差が小さかった理由は，掻破箇所に近く，振幅が大きくなり，掻破区間の判断が容易であった為である．角速度センサの誤差が最小であったが，角速度センサは掻破をしている手に固定され，直接計測を行っているからである．直接計測に対し，提案システムはベッドの振動を通じた間接計測である．その為直接計測のセンサよりも大きな誤差となってしまった．

4.4 掻破箇所推定実験

4.4.1 掻破箇所推定実験―方法

　提案システムを用いて，被験者が掻破している場所を推定する事が目的である．本実験では，計測時に入り込む高周波ノイズを減衰させる為に遮断周波数 12Hz の一次ローパスフィルタを使用した．掻破行動を記録する為に，被験者の右手をビデオカメラ(EX-F1, Casio)で撮影する．カメラは動かないように固定する．図１４に今回の実験の様子を示す．本実験では，計測結果について３.５式(12)を適用する事で，掻破前後の四肢の動きによるベッド上の重心移動を計算する．
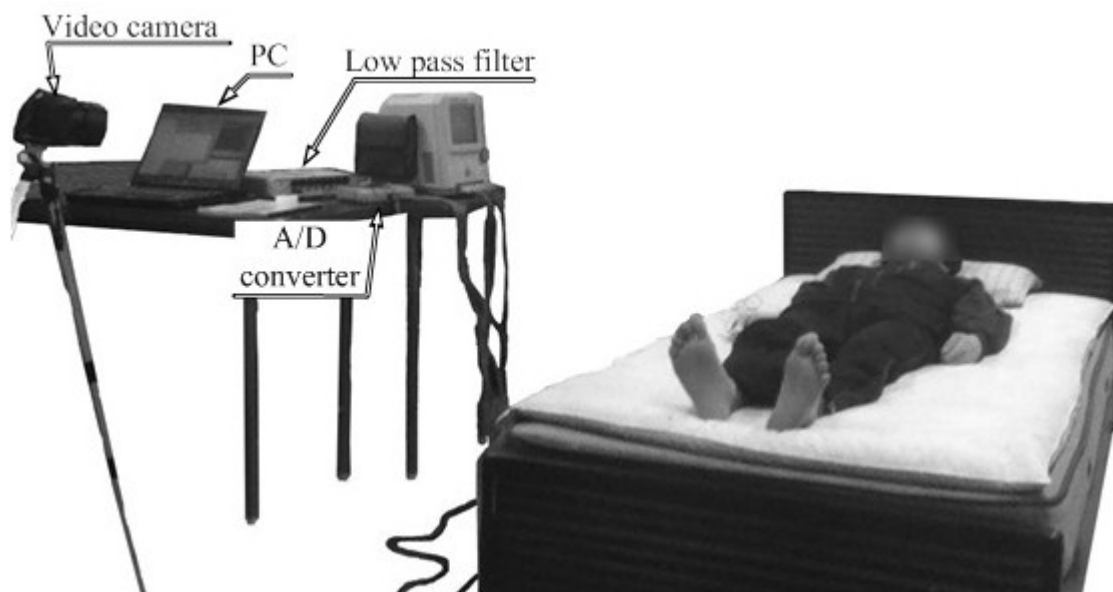
図１４　実験装置

$$P_{\mathrm{fh}}(t) = \int_o^t \{e_{\mathrm{fl}}(\tau) - e_{\mathrm{hl}}(\tau)\} d\tau$$

$$P_{\mathrm{rl}}(t) = \int_o^t \{e_{\mathrm{hr}}(\tau) - e_{\mathrm{hl}}(\tau)\} d\tau$$

（３.５式(12)）

4.4.2 掻破箇所推定実験—手順

ベッド中央での仰臥位を基本姿勢とする．本実験では,被験者は次の 3 箇所を掻破する．

(Case 1)　頬

被験者は右頬を 20 回掻破し，基本姿勢に戻り，5 秒後に再び掻破する，という一連の動作を 5 回繰り返す．

(Case 2)　背

被験者は左側臥位になり，背中を右手で 20 回掻破し，基本姿勢へ戻る．その 5 秒後，再び左側臥位で背中を掻く．これを 5 セット行う．

(Case 3)　脛

被験者は左脛 10 回右足の裏でこする．右足を戻し，基本姿勢で 5 秒安静状態を保つ．そして，再び 10 回左脛を擦る．このセットを 5 回繰り替えしたら，同じ様に左足の裏で右脛を 10 回擦る動作を 5 セット行う．

4.4.3 掻破箇所推定実験—結果

(Case 1)　頬

図１５にある一区間の結果を示す．図 (a) は上から $e_{hl}(t), e_{hr}(t), e_{fl}(t)$ の変化，(b) は上から $P_{fh}(t), P_{rl}(t)$ の変化を示したグラフである．被験者は 4 秒から 7.5 秒まで掻破状態であった．掻破前後寝返り状態である 3 秒から 4 秒及び 7.5 秒から 9 秒において，被験者の右腕が動いていた．この時，全てのセンサの出力信号が大きく変化した．被験者が安静状態にあるときはセンサの出力信号は大きく変化しない．掻破状態の時は，全てのセンサの出力が大きく周期的に変化している．図１５ (a) の 0 秒から 3 秒まで，安静状態であり，被験者の右手は被験者の体の横にあった．この時脈拍信号が計測されている．3 秒から 4 秒の間に顔に向かって手が動いていた．掻破中は 20 回の掻破に合わせてセンサ出力 $e_{hl}(t), e_{hr}(t), e_{fl}(t)$ が大きく周期的に変化している．掻破箇所に近い枕元に設置されたセンサの出力信号 $e_{hl}(t), e_{hr}(t)$ の方が足元に設置された $e_{fl}(t)$ よりも大きい．最も掻破箇所に近い $e_{hr}(t)$ の振幅が最大である．提案するシステムではセンサ出力は掻破箇所から遠ければ遠い程振幅が小さくなる．7.5 秒から 9 秒までの振幅は基本姿勢へ腕を戻している動作による変化である．この時，3 秒から 4 秒までの変化よりも滑らかな変化が発生している．9 秒から 12 秒までの間，被験者は再び安静状態となり，再び脈拍成分が計測されている．

搔破による信号の変化から搔破時間を確認出来る．被験者の手が動いていないとき，$P_{fh}(t), P_{rl}(t)$は両方とも変化は小さく，およそ 0mVs である．被験者の腕が動く，寝返り状態では$P_{fh}(t), P_{rl}(t)$は大きく変化し，搔破状態に於いては搔破に合わせて変化している．寝返り状態に注目すると，搔破前に$P_{fh}(t), P_{rl}(t)$が共に負へシフトした．搔破後に基本姿勢に戻ると，$P_{fh}(t), P_{rl}(t)$も搔破前同様およそ 0mVs を中心として変化している．

Voltage [mV]

$e_{hl}(t)$

$e_{hr}(t)$

$e_{fl}(t)$

Time [s]

(a) The outputs of piezoceramic sensors

Integrated values [mVs]

$P_{fh}(t)$

$P_{rl}(t)$

Time [s]
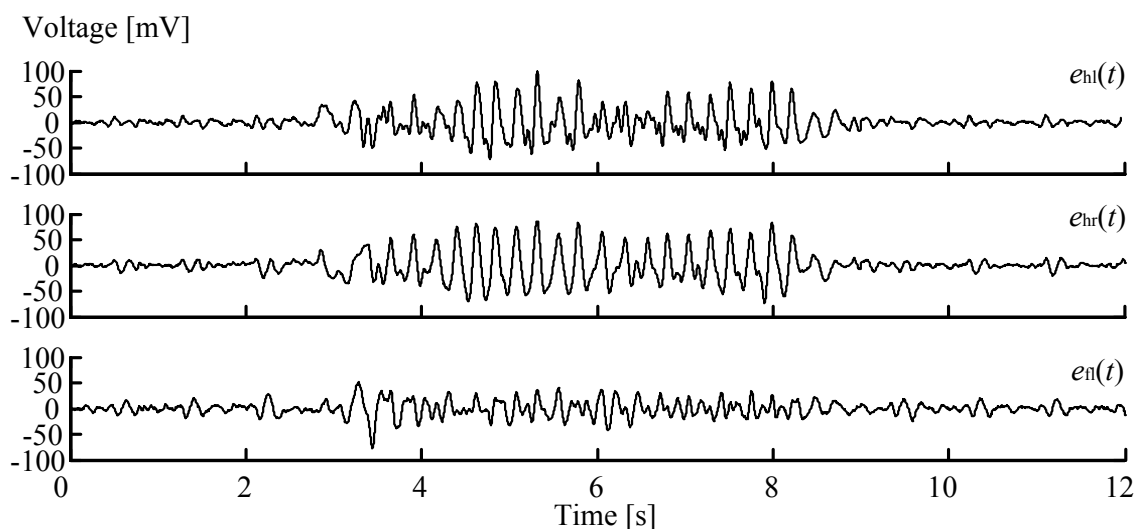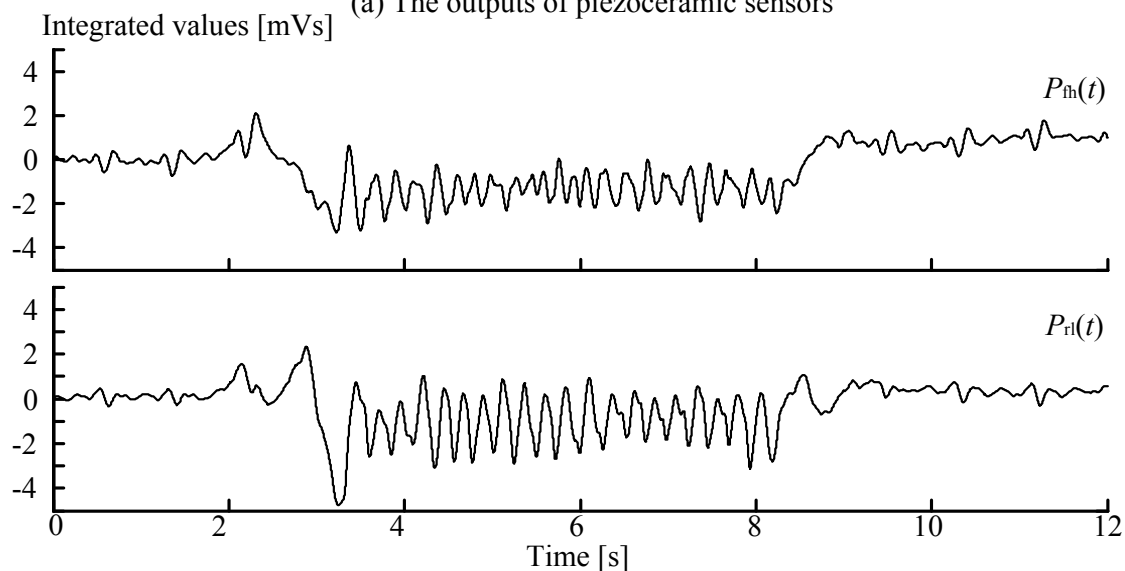
(b) The integrated values of the outputs

図１５　（Case 1)頬を搔破

(Case 2)　背

　図１６に結果を示す．被験者は基本姿勢から左に寝返りをして，背を掻破して戻った．(a)に示す様に掻破中の出力信号は，Case 1 と同様に，掻破の振動に同期している．しかし，Case 1 との違いは掻破の前後に，寝返りによる大きな変化が有る事である．掻破前の寝返り状態では，ベッドの左側に設置されたセンサの出力 $e_{hl}(t), e_{fl}(t)$ が大きな正の信号を発し，右側では，$e_{hr}(t)$ が大きな負の信号を発していた．掻破後の寝返り状態に於いては，被験者は基本姿勢に戻る為に右向きに寝返りをした．この時掻破前とは逆に左側から負の信号，右側から正の信号が得られた．

　掻破前の寝返り状態にある時，$P_{rl}(t)$ は大きくマイナスにシフトし，$P_{fh}(t)$ はわずかながらプラスにシフトしている．

(Case 3)　脛

　図１７に結果のある一区間を示す．上記の掻破の様に足の動きに伴う周期的信号から掻破区間を判断することが出来る．ベッド上で足を動かすと，足元に設置されたセンサの出力が枕元に設置されたセンサの出力より大きくなる．掻破時に積分値は $P_{fh}(t) \geq P_{rl}(t)$ という大小関係になった．寝返り状態によって，掻破状態の際には，$P_{rl}(t)$ はプラス領域で変化している．一方 $P_{fh}(t)$ は正負に大きく振動している．

Voltage [mV]

$e_{hl}(t)$

$e_{hr}(t)$

$e_{fl}(t)$

Time [s]

(a) The outputs of piezoceramic sensors

Integrated values [mVs]

$P_{fh}(t)$

$P_{rl}(t)$

Time [s]
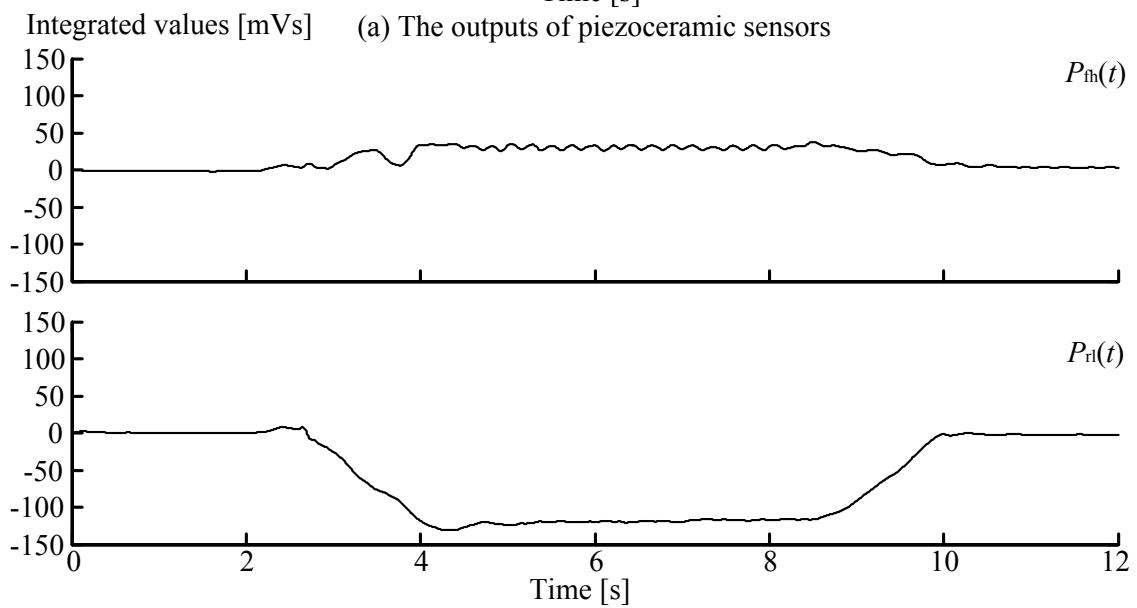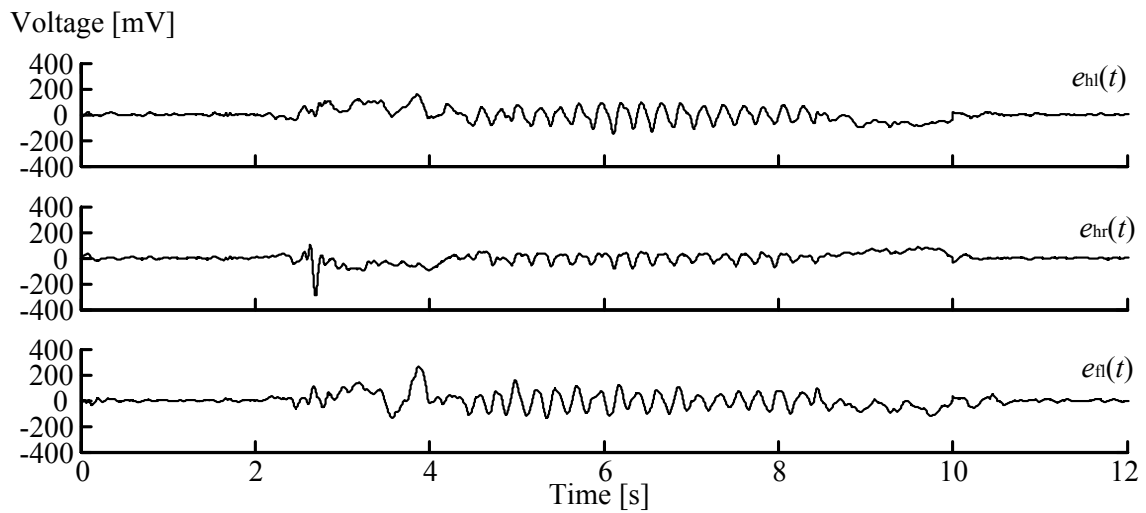
(b) The integrated values of the outputs

図16　（Case 2）背を掻破
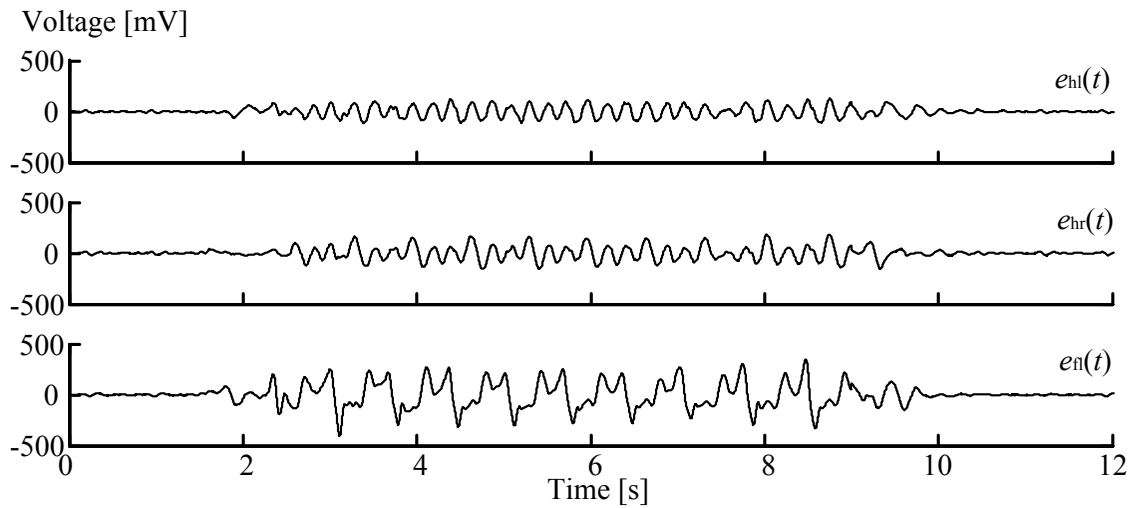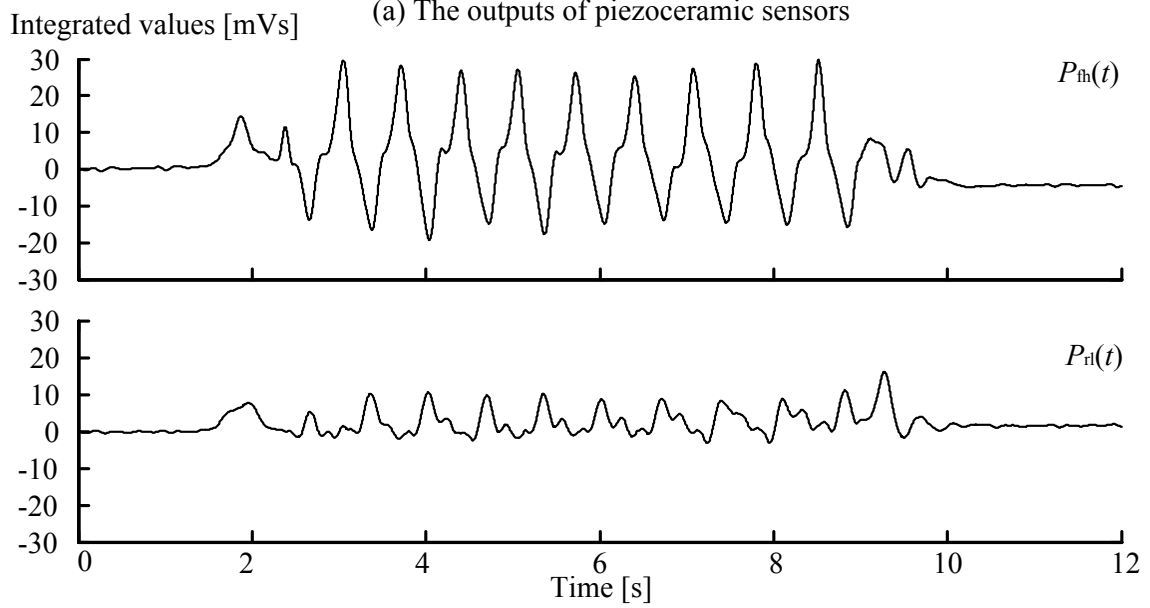
Voltage [mV]

$e_{hl}(t)$

$e_{hr}(t)$

$e_{fl}(t)$

Time [s]

(a) The outputs of piezoceramic sensors

Integrated values [mVs]

$P_{fh}(t)$

$P_{rl}(t)$

Time [s]

(b) The integrated values of the outputs

図１７　（Case 3）左脛を掻破

4.4.4 掻破箇所推定実験—考察

掻破計測結果は全ての箇所に於いて，比較的大きな周期変化を示した．この特徴から，場所に寄らず掻破時間を計測する事が可能である．$P_{fh}(t), P_{rl}(t)$ より寝返りによるベッド上の重心移動の変遷を取得することが出来る．3.5 式(12)が示す様に $P_{fh}(t)$ は枕-足方向の重心移動に対応し，$P_{rl}(t)$ は左-右方向の重心移動に対応している．$P_{fh}(t)$ が負へシフトしたという事はベッドと人の重心が枕のある向きに移動した事を意味し，$P_{rl}(t)$ が負へシフトしたという事はベッドと人の重心が左向きに動いた事を意味している．つまり，(Case 1)では，重心が枕向き且つ左向きへ少し移動してから掻破が行われたことを示している．この部分に有るのは首や顔である．同様に(Case 2)では左向きへの大きな重心移動と少しの枕向きの重心移動があった事が示されている．これは，左側臥位で上半身の掻ける箇所を掻破したと推定出来る．枕-足方向の重心移動が少ない事も考慮される．そして，(Case 3)では，少しだけ重心が右へ移動してから，$P_{fh}(t), e_{fl}(t)$ の大きさから足元で掻破が行われている事が示されている．これは，多少右に重心が移動している事から左足が右側に来ているか，右膝か曲がっているか，が考えられる．この様に，重心移動を利用して，その時掻破し得る箇所を推定する事が出来る．本実験では基本姿勢を指定し，そこから推定しているが，体位推定と併せれば良い．

また，足が動いていると $P_{fh}(t)$ が $P_{rl}(t)$ より大きくなる理由は，掻破箇所に近いセンサの出力が大きく，足元のセンサ出力を利用しているのは $P_{fh}(t)$ だけだからである．

この様に，今回 $P_{fh}(t), P_{rl}(t)$ を掻破前後の寝返り状態に適用する事で掻破箇所を推定出来る事を示した．本システムは掻破を計測出来るだけではなく，(Case 3)の様に，レストレスレッグス症候群の様な睡眠中の四肢の異常行動を検知する事にも利用可能である点で優れている．睡眠中の異常行動は睡眠障害を招く事も有る．

4.5 掻破状態分離アルゴリズムに関する実験

4.5.1 掻破状態分離アルゴリズムに関する実験—信号処理

　ここでは，睡眠中に計測された信号 $S(t)$ から掻破状態を自動分離する事を目的とする．信号分離処理について説明する．計測される信号は 3.3 式 (9)，(10) 式の様に，人の動きに比例しており，計測された信号の変化の特徴は 3.4 において記述した各状態における人の変化の特徴と同様である．図１８に各状態の時に計測される信号の周波数と振幅の関係を示す．
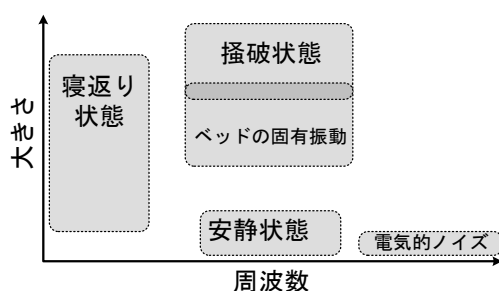
図１８　各状態における信号の主な成分の分布

(Step 1)

ベッドの固有振動及び計測時に含まれる電気的高周波ノイズの影響を低減する為に，ある時間 q の移動平均をとる事により高周波振動ノイズを除去する．

$$M(k) = \frac{1}{2q+1} \sum_{i=k-q}^{k+q} S_{(i)}$$

(Step 2)

ある区間 T を離散フーリエ変換し，その区間のピーク周波数をみる．この区間のピーク周波数が低周波であれば寝返り状態であるとし，高周波であれば掻破状態又は安静状態であるとする．

(Step 3)

Step 2 において高周波であった区間に対して処理を行う．掻破状態と安静状態では振動の大きさが異なるので，区間の振幅の大小比較を行う．小さければ安静状態の区間であり，大きければ掻破状態の区間であるとする．

4.5.2 掻破状態分離アルゴリズムに関する実験―方法

本実験では，アトピー性皮膚炎等皮膚病の患者の多くが掻破する首から上の部位のうち，頬を被験者に掻破してもらう [16]．まず，ベッドの中央での仰臥位を基本姿勢とする．この姿勢から右の4本の指を使って右の頬を20回掻破する．掻破をしたら腕を基本姿勢に戻して，5秒安静状態を保つ．そして，再度頬を20回掻破する．これを35セット繰り返す．一連の手の動きは滑らかに行う．そして時々寝返りをする．実験の様子を同時にビデオカメラ(EX-F1, Casio)で撮影する．計測終了後，総掻破時間T_sとTST%を提案するアルゴリズムによる決定と波形を目視して掻破時間を決定の二つの方法により計算する．総掻破時間T_sとTST%を，カメラで撮影された映像から判断された正しい値と比較する．センサ同士の誤差の比較には平均平方誤差とその誤差率を用いる．誤差率は平均平方誤差の総計測時間に占める割合とする．

変数の設定について，本実験でサンプリング間隔を1ms，Step 1でのqを250とする．また，Step 2では0.5秒間隔で1秒間を離散フーリエ変換して，周波数で分離する際の閾値を最低周波数(1Hz)とした．

4.5.3 掻破状態分離アルゴリズムに関する実験―結果

図19に掻破状態を分離した一例を示す．図中の(a)には枕元左側に設置されたセンサの出力，(b)には枕元右側に設置されたセンサの出力を示した．足元に設置されたセンサの結果は枕元のものと同様である為，割愛する．図には撮影された映像によって決定された区間と，本アルゴリズムによって決定された区間と，評価者が波形を見て決定した区間の3種類の区間が示してある．背景が灰色の範囲がカメラによる正しい掻破区間である．被験者が動いていない時にはセンサは被験者の脈拍による振動を検出している．掻破行動の前に横方向への寝返りを行ったが，この時，左右で正負の異なる大きな長周期信号が得られた．信号分離処理の結果，人がグラフを見て決定した区間より灰色の範囲に近づき，正確に掻破状態は寝返り状態や安静状態から分離され，決定された．

表3に掻破区間と判断された区間より得られたTSTの平均平方誤差(RMSE)及び，その誤差率を掲載する．表4にはTSTとTST%，TST%の誤差を示す．35回の試行による総掻破時間は179秒であった．4箇所のセンサ全てで，RMSEは1秒未満であった．誤差の大きさは足元に設置されたセンサにおいて小さくなった．
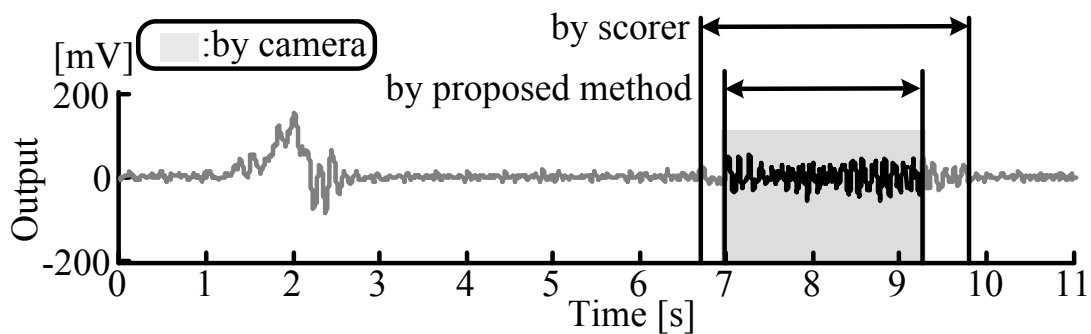
(a) The output of piezoceramics sensor set under the head-side left corner
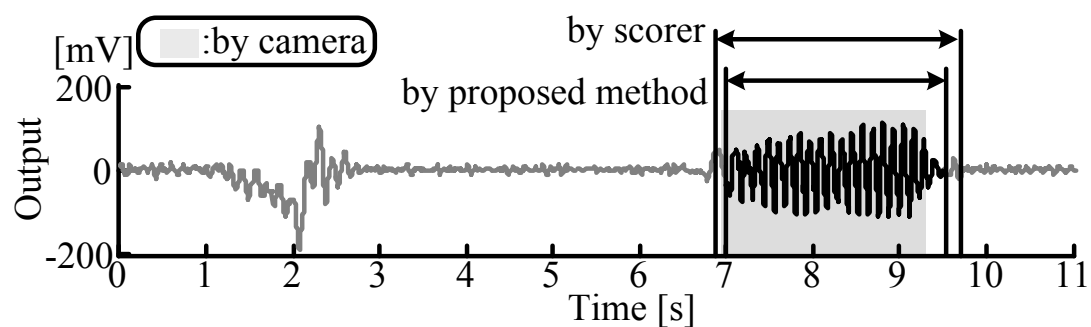
(b) The output of piezoceramics sensor set under the head-side right corner

図19 掻破状態分離結果

表3 総掻破時間の平均平方誤差とその誤差率

Sensors	Method	RMSE [s]	Error rate
Piezo-ceramics, head side left	Conventional	0.40	0.10
	Proposed	0.68	0.18
Piezo-ceramics, head side right	Conventional	0.64	0.17
	Proposed	0.74	0.19
Piezo-ceramics, foot side left	Conventional	0.92	0.24
	Proposed	0.73	0.19
Piezo-ceramics, foot side right	Conventional	0.94	0.24
	Proposed	0.79	0.20

表 4　TST と TST%及び TST%の誤差

Sensors	Method	TST [s]	TST%	Error [%]
Camera	Conventional	179.31	46.57	-
	Proposed	-	-	-
Piezo-ceramics, head side left	Conventional	176.12	45.75	0.82
	Proposed	168.50	43.77	2.81
Piezo-ceramics, head side right	Conventional	186.17	48.36	-1.79
	Proposed	184.50	47.92	-1.35
Piezo-ceramics, foot side left	Conventional	204.36	53.08	-6.51
	Proposed	187.50	48.70	-2.13
Piezo-ceramics, foot side right	Conventional	201.51	52.34	-5.77
	Proposed	163.50	42.47	4.11

4.5.4 掻破状態分離アルゴリズムに関する実験―考察

　本実験で提案しているシステムは掻破状態のみを他の状態から抽出することが出来た．尚，提案アルゴリズムが含む誤差も従来方法が含む誤差を同じくらいの大きさであった．これによって，従来法では評価者が波形を見て掻破状態か別の状態かを判断していたが，その判断の必要が無くなる．従来の掻破時間決定方法では，総掻破時間 T_s の誤差の主な原因は掻破による出力変化と掻破状態の前後の動作による変化の区別が難しい事である．提案するシステムによる掻破時間決定では，総掻破時間 T_s の分解能が信号処理 Step 2 でのある区間 T の始点と終点に依存している．また Step 3 での大小比較の方法も状態決定の失敗，つまり誤差の原因である．Step 2 はある区間のピーク周波数によってその区間を寝返り状態かその他の状態に分離する処理である．この処理の中で TST%算出に必要不可欠な T_s の始点と終点に成り得る時点が決定する．従って，より細かい間隔でピーク比較処理を行えば T_s の精度は向上する．Step 3 は安静状態と掻破状態を振幅の大小比較によって分離する処理である．今回は過去の寝返り状態の振幅の平均値を使用したが，寝返りによる信号と掻破による信号の振幅の大小関係は変化する事もある為，改善の余地がある．

5 おわりに

本研究では睡眠中の状態を無拘束で観察するベッドシステムを提案した．

このベッド計測システムでは，圧電素子を利用した4つのセンサをベッドの脚と床の間に設置して使用している．このセンサは歪を感知しており，電源は要らない．なぜなら，素子の有する圧電効果により歪の時間変化に比例した電圧を素子自らが発生するからである．また，このセンサは高感度であり，ベッド利用者の脈拍，呼吸，掻破，寝返りを計測する事が出来る．高感度である為，微小な生体信号を計測する時にも増幅器を使わない．このセンサは40dbのSN比で脈拍信号を検出し，14dbのSN比で呼吸信号を検出する．このセンサは生体信号によるベッドの微小振動から寝返りによる大きな圧力の変化まで飽和すること無く計測出来る高い感度と広いレンジを有している．センサ自体に電源が要らず，感度が高く，計測可能レンジが広いというこのセンサの特徴は，低消費電力の生体信号計測装置の開発に有利である．また，ベッド計測方法の一つとして，この方法は費用対性能が格段に高い．本研究で利用している圧電素子と同じ物は低価格で販売されており，微小振動から大きな圧力変化まで飽和せずに計測する事が出来る．

日常的に生体信号を計測する際，無拘束である事は重要である．本研究の提案するシステムでは，ベッド利用者が寝ている間に無拘束で生体情報を計測出来る．上述の実験を通して，脈拍と呼吸のリズムを観察する事や体位変更による重心移動の検出，掻破に掛かった時間の計測及び様々な従来法との比較，掻破箇所の推定，掻破状態の自動決定をした．脈拍や呼吸のリズムを利用して，睡眠時の呼吸停止検知や睡眠段階の推定が出来る．寝返り検知の一応用例として，障害者や高齢者がベッドから出ようとしている事を検知する事が挙げられる．掻破時間の比較では，特に掻破箇所の近くに設置されたセンサに於いて，従来法と同程度もしくはより高精度に総掻破時間を計測出来た．睡眠中に掻破にかけた時間から，痒みを評価する際の指標であるTST%を求める事が可能である．この指標は痒みを伴う皮膚病に対して有益な情報である．更に掻破箇所を推定する事も出来るが，この情報を利用して，今までよりも詳細な掻破観察が期待される．本研究で提案した掻破時間を決定するアルゴリズムは，掻破時の信号の特徴である大きな振幅と周期性の利用を基本としている．この信号処理は，カメラで撮影した映像からTST%を求める従来法と比べて，TST%算出に掛かる時間を短縮出来る．更に，カメラを利用する方法では，死角で掻破が行われた場合には，その時間を正確に計測出来ないが，本システムではその問題は無い．計測精度はほぼ変わらずに指標算出時間を短縮出来るのである．

参考文献

[1] Y. Ishibashi, K. Yoshikawa, "The skin diseases with strong itch, the manual for discernment and therapeutics," 1991.

[2] R. Miyaji, A. Ikoma, "Forefront of medical dermatologists series: Frontiers itching," 2006.

[3] R. Miyaji, "Q&A Itching," 2007.

[4] T. Morgenthaler et al., "Validity in actigraphic sleep assessment," Sleep, vol. 30, Standards of Practice Committee, American Academy of Sleep Medicine, no. 4, pp. 519–529, 2007.

[5] B. Sivertsen et al., "A comparison of actigraphy and polysomnography in older adults treated for chronic primary insomnia," Sleep, vol. 29, no. 10, pp. 1353–1356, 2006.

[6] N. L. Johnson et al., "Sleep estimation using wrist actigraphy in adolescents with and without sleep disordered breathing: A comparison of three data modes," Sleep, vol. 30, no. 7, pp. 899–905, 2007.

[7] K. Watanabe, et al., "Ubiquitous health monitoring at home—Sensing of human biosignals on flooring, on tatami mat, in the bathtub, and in the lavatory," IEEE Sensors J., vol. 9, no. 12, pp. 1847–1855, Dec. 2009.

[8] K. Watanabe, et al., "Noninvasive measurement of heartbeat, respiration, snoring and body movement of a subject in bed via a pneumatic method," IEEE Trans. Biomed. Eng., vol. 52, no. 12, pp. 2100–2107, Dec. 2005.

[9] K. Watanabe, et al., "Design of a low-frequency microphone for mobile phones and its application to ubiquitous medical and healthcare monitoring," IEEE Sensors J., vol. 10, no. 5, pp. 934–941, Mar. 2010.

[10] J. Alihanka, et al., "A static charge sensitive bed. A new method for recording body movement during sleep," Electroencephalogr. Clin. Neurophysiol., vol. 46, pp. 731–734, 1979.

[11] T. Watanabe, et al., "Noncontact method for sleep stage estimation," IEEE Trans. Biomed. Eng., vol. 51, no. 10, pp. 1735–1748, Oct. 2004.

[12] N. Bu, et al., "Monitoring of respiration and heartbeat during sleep using a flexible piezoelectric film sensor and empirical mode decomposition," Proc. IEEE Eng. Med. Biol. Soc., pp. 1362–1366, 2007.

[13] M. Ishijima, "Monitoring of electro-cardiograms in bed without utilizing body surface electrodes," IEEE Trans. Biomed. Eng., vol. 40, no. 6, pp. 593–594, Jun. 1993.

[14] X. Zhu, et al., "Real-time monitoring of respiration rhythm and pulse rate during sleep," IEEE Trans. Biomed. Eng., vol. 53, no. 12, pp. 2553–2563, Dec. 2006.

[15] D. C. Mack, et al., "Development and preliminary validation of heart rate and breathing rate detection using a passive, ballistocardiography-based sleep monitoring system," IEEE Trans. Inf. Technol. Biomed., vol. 13, no. 1, pp. 111–120, Jan. 2009.

[16] T. Ebata, et al., "The Characteristics of nocturnal scratching in adults with atopic dermatitis," British Journal of Dermatology Vol. 141, pp. 82-86, 1999.

[17] H. Izumi, et al., "A Simplified Method for the Measurement of Nocturnal Scratching with an Infrared Video Camera," The Skin Vol. 39, pp. 560-563, 1997.

[18] J. A. Savin, et al., "SCRATCHING DURING SLEEP," The Lancet Vol. August 11, pp. 296-297, 1973.

[19] T. Ebata, et al., "Use of a wrist activity monitor for the measurement of nocturnal scratching in patients with atopic dermatitis", British Journal of Dermatology Vol. 144, pp.305-309, 2001.

[20] N. V. Bergasa, et al., "Effects of Naloxone Infusions in Patients with the Pruritus of Cholestasis," Annals of Internal Medicin Vol. 123, No. 3, pp. 161-167, 1995.

[21] T. Aoki, et al., "Nocturnal scratching and its relationship to the disturbed sleep of itchy subject," Clinical and Experiment Dermatology Vol. 16, pp. 268-272, 1991.

[22] J. R. Burch, et al., "THE MEASUREMENT OF ITCH," Measurements we Couldn't Make Without a Micro, pp. 9-12, 1988.

[23] K. Endo, et al., "Evaluation of Scratch Movements by a New Scrath-Monitor to Analyze Nocturnal Itching in Atopic Dermatitis," Acta Derm Venereol (Stockh) Vol. 77, pp. 432-435, 1997.

謝辞

_____

本研究に当たり　ご指導ご鞭撻賜りました　渡辺　嘉二郎　教授　に
深く感謝致しております

また　研究の契機を下さいました　株式会社ジェピコ取締役　中村　哲夫　様
センサを作成して下さいました　株式会社内田製作所部長　甲斐　久順　様
並びにご協力して頂いた皆様　にお礼を申し上げます

修士課程における研究発表成果

(1) T. Shino, K. Watanabe, K. Kobayashi, K. Suzuki, and Y. Kurihara, "Noninvasive biosignal measurement of a subject in bed using ceramic sensors," SICE Annual Conference 2010 proceeding, pp. 1559-1562, 2010.

(2) S. Nukaya, T. Shino, Y. Kurihara, K. Watanabe, and H. Tanaka, "Noninvasive Bed Sensing of Human Biosignals via Piezoceramic Devices Sandwiched Between the Floor and Bed," Sensors Journal, early access.

(3) T. Shino, S. Nukaya, Y. Kurihara, K. Watanabe, and H. Tanaka, "Development of Unconstrained Biosignal Bed Sensing Method Using Piezoceramics to Detect Body Movement and Scratching Motion," SICE Annual Conference 2011 proceeding, pp. 2317-2321, 2011.

(4) T. Shino, Y. Kurihara, S. Nukaya, K. Watanabe, and H. Tanaka, "Unconstrained Bed Monitoring System for Scratching Motion," The Third International Symposium on Sensor Networks and Applications 2011 proceeding, pp. 135-140, 2011.

(5) T. Shino, Y. Kurihara, S. Nukaya, K. Watanabe, and H. Tanaka, "Unconstrained measurement system for scratching by limb and estimation for scratching area," International Conference on Intelligent Computational System 2012 proceeding, pp. 71-75, 2012.

(6) T. Shino, Y. Kurihara, S. Nukaya, K. Watanabe, and H. Tanaka, "Signal Processing Method for Extracting Scratching Time," International Conference on Electrical Engineering 2012 proceeding, early access.

Noninvasive biosignal measurement of a subject in bed using ceramic sensors

Toshihiro Shino, Kajiro Watanabe,
Kazuyuki Kobayashi and Kaoru Suzuki

System Control Engineering Department
Faculty of Engineering, Hosei University
Koganei-shi, Tokyo, Japan

Yosuke Kurihara

Department of Computer and Information Science
Faculty of Science and Technology, Seikei University
Musashino-shi, Tokyo, Japan

Abstract—**This paper describes a novel noninvasive method for sensing heartbeat, respiration and body-movement biosignals of a subject in bed by using ceramic piezo devices set under the legs of the bed.**

Keywords - ceramics; bed-sensing; heartbeat; respiration; body movement

I. Introduction

Elderly people in nursing homes and other care facilities are at risk of serious injury when they wake up and attempt to get out of bed in order to visit the bathroom. [1]

To prevent an accidental fall from bed, it would be necessary to predict the person's intention from signs of their waking up and moving, which would then allow time to assist them in getting out of bed.

This paper describes a novel sensing method for measuring the heartbeat, respiration and body movement of a person in bed by using ceramic piezo devices placed under the legs of the bed. Effective use of the device is confirmed through experiments.

II. Measurement conditions and problem description

A. Measurement conditions

Figure 1 shows the situation where a single person is lying in a typical bed. Four ceramic piezo sensors are set under the four legs of the bed for measuring the biosignals from the heartbeat, respiration and body movement. Any action on the bed is produced by the subject, with no other causes present.

B. Problem description

From the conditions described above, we considered the following three problems:

(1) How to measure the heartbeat;

(2) How to measure the respiration; and

(3) How to estimate the body position and movement.
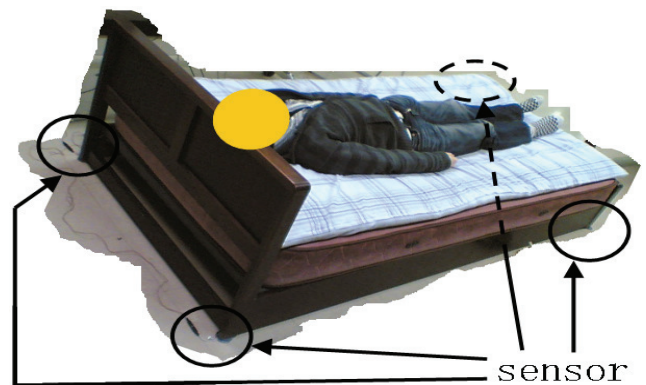
Figure 1. Measurement conditions
A person is in the bed, and ceramic sensors are under the legs of the bed.

III. Sensor

Physical displacement of the bed due to body movement or human-generated microvibration is transmitted to the piezo ceramic sensors set under the legs of the bed, and the displacement is converted to electrical signals. Figure 2 shows the structure of the sensor. When the sensor plate is pressed down, a positive voltage is generated with highpass filter characteristics.
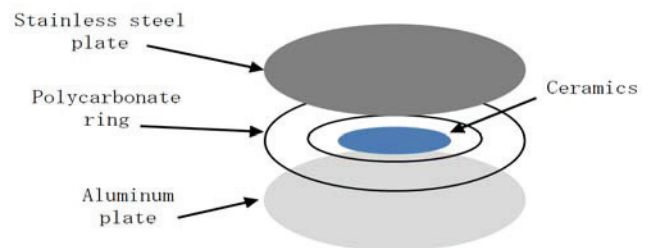
Figure 2. Structure of the sensor with built-in ceramics

IV. Experiments

A. Experimental system

Four ceramic sensors covered with rubber dampers are set under each leg of the bed. The subject lies on the bed and

moves occasionally. Output from the sensors is recorded on a PC via A/D converter. The sampling interval is set at 5 ms for measuring body movement, and 1 ms for measuring heartbeat and respiration. Data in the body movement experiment was acquired for the following actions of the subject:

- Sitting up and lying down

- Getting out of bed and getting back into bed

- Turning over in bed

- Moving one leg

The subject was asked to move one leg to the right or left from the center position without bending the knee. The leg could be moved either by lifting it from the bed or sliding it on the bed, and then allowing it to rest on the bed.

- Resting peacefully

Besides the ceramic sensors, we prepared and set a pulse oximeter and a low-frequency microphone, for reference data. The pulse oximeter was affixed to the subject's earlobe to count the heartbeats. The low-frequency microphone was set under the nostrils to count the respiration rate. We asked the subject to stop breathing for 35 [s], at 40[s] after starting.

B. Results of the experiment

At almost all movements, just after the motion, the output signals from the four ceramic sensors showed similar vibration characteristics.

- Sitting up and lying down

Figure 3 shows the typical output signals for the sitting up movement. When the subject first started this motion, the output from the upper-side sensor, near the head, generated a positive signal. For the lying down movement, the head-side output mainly showed a positive signal, whereas the foot-side showed a negative signal.

The frequencies of the vibration during these movements include 9 to 12 [Hz] as the dominant components.

After sitting up and staying in that position, the output from the four sensors showed similar vibration characteristics. The dominant frequency component is about 10 [Hz].

As will be shown later, the integrated value of the output from the ceramic sensors during movement shows a clear relationship to the movement. When sitting up, the integrated value of the head-side sensor was a negative constant, and that of the foot-side sensor was a positive constant. When the subject was lying down, the value of the head-side sensor was positive, and that of the foot-side sensor was negative.
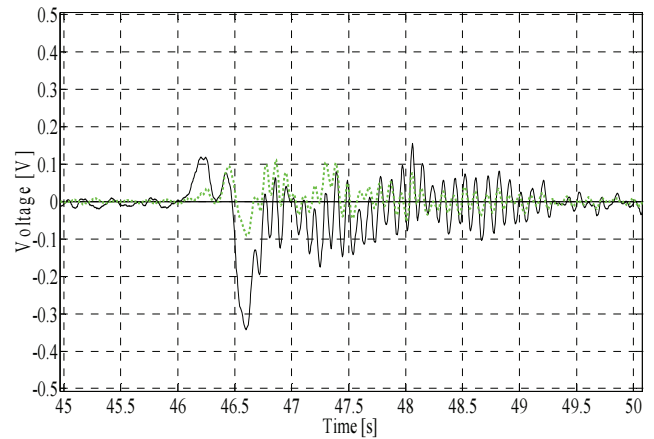
Figure 3. Sitting up movement
(Solid black line: upper left side / dotted green line: lower left side)

- Getting out of bed and getting back into bed

In this movement, only the right side of the bed was used to get out of bed and get back into bed.

During the movement of getting out of bed, the output from the right-side sensors was positive, and then all output was negative.

As the subject got back into bed, the output from the four sensors was synchronized as the same phase.

The integrated value showed a negative constant for getting out of bed, and was positive for getting back into bed. Figure 4 shows the output voltage and integrated value for the time from just before getting out of bed to just after getting back into bed. It can be determined from the figure that the subject was out of bed for about 13 s. Furthermore, the figure shows the time that the subject got out of bed and back into bed.
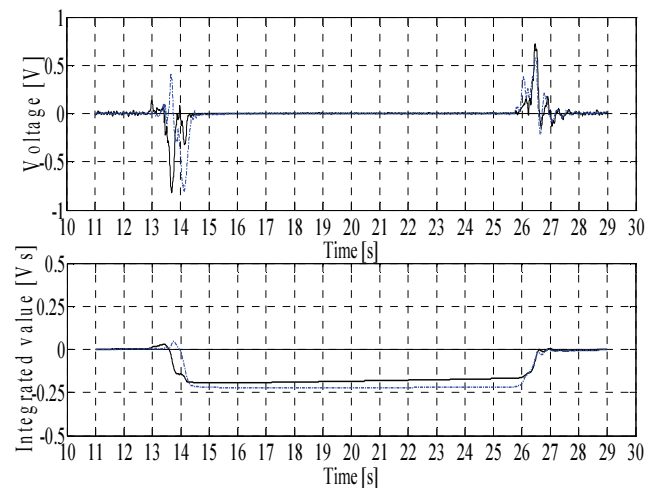
Figure 4. Getting out of bed and getting back into bed movement
The upper graph shows the original output and the lower graph shows the integrated values.

(Solid black line: upper left side / broken blue line: lower right side)

- Turning over movement

When we asked the subject to turn over from right to left, the left-side sensor output generated positive signals and the right-side sensor output generated negative signals. For the movement in the opposite direction, the output signals showed converse signs. The amplitude of the foot-side sensors was always lower than that of the head-side sensors. Figure 5 shows the output for the turning movement. The subject turned from right to left at around 31 s, and from left to right at around 38 s.

When the subject turned to the right while sitting up in bed, the sensor showed a similar signal to that when turning over while lying down.

The dominant frequency in the movement for turning over while lying down was less than 3 Hz. The spectrum for frequencies less than 3 Hz and that for about 10 Hz was conspicuous for the movement of turning while sitting up.

The integrated values of the sensor output always show a positive constant value when the moving direction is toward the sensor and vice versa. This always occurred at any position.

Figure 6 shows that the subject moved his left leg from the center to the left. The upper graph is a 'lifting case' and the lower is a 'non-lifting case'. The upper shows larger output values compared to the lower.

For the non-lifting motion, the right sign differs from the left.

Figure 6. Left leg movement

(Solid black line: upper left / broken red line: upper right
/ dotted green line: lower left / broken blue line: lower right)

- Resting peacefully

The output signals when the subject rested peacefully were much less than those for any of the movements. There were peaks in microvibration for a period at around 1 s. The signals from the head-side output were proportional to those from the foot-side output.

Figure 7 shows the spectrum during the subject's breathing.
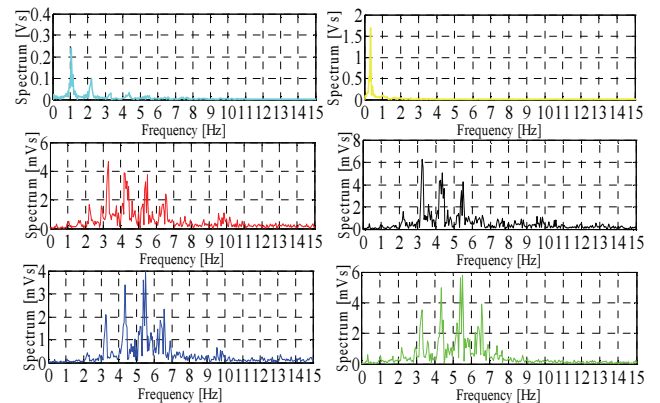
Figure 7. Spectrum for the signals when resting peacefully

(Sky blue line: pulse oximeter / yellow line: low-frequency microphone
/ red line: upper right / black line: upper left
/ blue line: lower right/ green line: lower left)

Figure 5. Turning movement
The upper graph shows the head side and the lower graph shows the foot side.

(Solid black line: upper left / broken red line: upper right
/ dotted green line: lower left / broken blue line: lower right)

- Moving one leg

The difference between lifting and not lifting the leg was the presence or absence of an intense peak. The lifting up motion showed an intense peak.

The output signals of the foot-side sensor were large. This was the clearest characteristic for distinguishing the different movements. The scale relationship for the output is as follows:

In the case of moving to the left:

{lower left} > {lower right and upper left} > {upper right}

In the case of moving to the right:

{lower right} > {lower left and upper right} > {upper left}

In the case of moving to the center:

{lower} > {upper}

From Figure 7 for the pulse oximeter signals, the spectrum shows a fundamental peak at 1.05 Hz and its harmonics. The spectrum for the output signal from the low-frequency

microphone shows a conspicuous peak at around 0.35 Hz. These are the heartbeat and respiration components, respectively. The output from the ceramic sensors included the spectrum for both the heart rate and respiration rate.

We picked out the signals from the 3–6-Hz components from the ceramic sensor output, and calculated their absolute value and then low-pass filtered them by moving average. The calculated output is shown in Figure 8. The components in the frequency range from 3–6-Hz included the same feature of the pulse oximeter, which is nothing more than the heart rate frequency. The top row of Figure 8 is the direct output from the pulse oximeter as the reference for the heartbeat. The signals from the second to fourth row on the left side of Figure 8 show the calculated output from the four ceramic sensors. The right side of Fig. 8 shows the spectrum for the left signals.

From these, the calculated output from the four ceramic sensors shows the same characteristics as the reference pulse oximeter output.
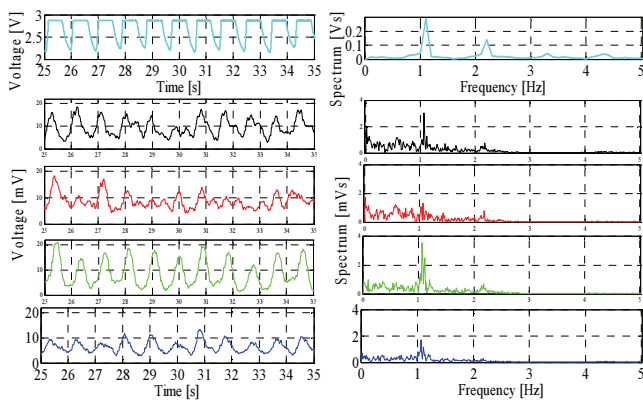
Figure 8. Heartbeat, output after calculation and frequency

(Sky blue line: pulse oximeter / black line: upper left / red line: upper right / green line: lower left / blue line: lower right)
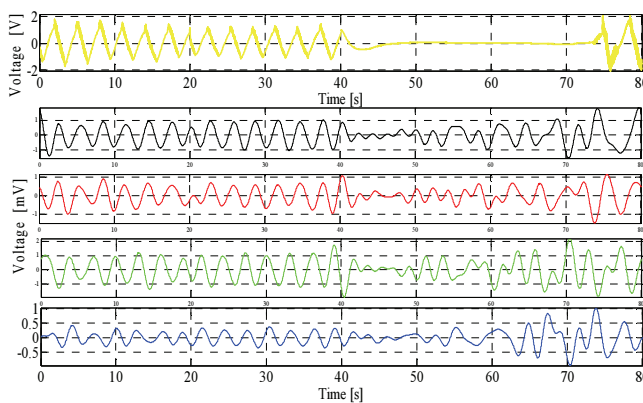
Figure 9. Respiration and filtered outputs

(Yellow line: low-frequency microphone / black line: upper left / red line: upper right / green line: lower left / blue line: lower right)

We also picked out the 0.1–0.5-Hz components. Figure 9 shows this data and the respiration rate reference from the low-frequency microphone. The head-side output is synchronized with the microphone output as the same phase,

whereas the foot-side signal, even synchronized, shows the opposite characteristics during breathing. Although the subject stopped breathing from 40 s to 75 s, the sensor output speared some signal.

The feature of the inverse phase between the head-side and foot-side output is also shown for the case of heartbeat rate.

C. Considerations

From the experiment on body movement, we could see that the features of the signals for each movement were different. Thus, it is possible to determine from the signals which body movement is occurring. The sign of the signal shows the direction of the motion, and the amplitude shows the magnitude of the motion.

(1) When the signs of the upper and lower sensors are different, the subject is sitting up or lying down.

(2) When the signs of all sensors are the same, the subject is getting out of bed or getting back into bed.

Similarly, all other motions can be determined.

Furthermore, judging from a comparison with the references, the heartbeat and respiration are measured. For the respiration, there are signals during the absence of breathing, due to some small body movement. The feature of the heartbeat and respiration signals is the inverse phase between the head-side and foot-side output.

V. CONCLUSIONS

A. Results

The experimental results show the differences between each position movement. They can be estimated from the change in the vibration measured by the four sensors, which yields information on the subject's change in sleeping position and movement during the night.

B. Conclusion

We determined how the four ceramic sensors set under the legs of the bed generate the output signals for different body movements of the subject in the bed.

Heartbeat and respiration rate can also be measured by a simple digital process.

The heartbeat rate is obtained by applying bandpass filtering and moving average to the absolute value of the filtered output. The heartbeat signal is clearly obtained by a bandpass filter with cut-off frequencies of 3 and 6 Hz.

Respiration is easily measured using a bandpass filter with cut-off frequencies of 0.1 and 0.5 Hz.

REFERENCES

[1] Medical Project Co., Ltd. http:www.medicpro.co.jp/guide.pdf

Noninvasive Bed Sensing of Human Biosignals via Piezoceramic Devices Sandwiched Between the Floor and Bed

Shoko Nukaya, Toshihiro Shino, Yosuke Kurihara*,

Kajiro Watanabe, *Member, IEEE and* Hiroshi Tanaka

Abstract— This paper describes a novel bed sensing method for noninvasive, constraint-free, subliminal detection of biosignals. The sensor system detects the heartbeat, respiration, body movement, position change and scratching motion of a person lying or sleeping on the bed. These biosignals provide not only basic medical information but also sophisticated details about sleep conditions. Thus, the bed sensing method can be used to monitor the health condition of people sleeping at home as well as that of patients in the hospital. Furthermore, the bed sensor system can detect emerging changes in the physical condition of a person, whether at home or in the hospital. The basic device used for sensing is piezoceramic bonded to stainless steel plate sandwiched between the floor and the four corners of the bed. Thus, no special bed is required. The device, which detects the biosignals generated as mechanical vibrations, has a wide dynamic range and high SN ratio enabling the detection of microvibrations from the heartbeat by the change in acting force, without saturation from body movements. It accurately detects the person's heartbeat and respiration as well as body movement and even the number of scratching motions. The device is suitable for various health monitoring applications including sleep and medical monitoring for circulatory system disorders as well as diseases characterized by itching.

Index Terms— noninvasive biosensing, bed sensing, piezoceramic, heartbeat, respiration, position change, scratching

Manuscript received May 15, 2009. *Asterisk indicates corresponding author.*

S. Nukaya is with the Division of Advanced Therapeutical Sciences Tokyo Medical and Dental University, 1-5-45 Yushima, Bunkyo-city, Tokyo 113-8510, Japan (e-mail: nukaya@bioinfo.tmd.ac.jp).

T. Shino is with the Graduate School of Hosei University, 3-7-2 Kajinocho Koganei-shi, Tokyo 184-8584, Japan.

*Y. Kurihara is with the Dept. of Computer and Information Science, Faculty of Science and Technology, Seikei University, 3-3-1 Kichijoji-kitamachi, Musashino-shi, Tokyo 180-8633, Japan (e-mail: yosuke-kurihara@st.seikei.ac.jp).

K. Watanabe is with the System Control Engineering Department, Faculty of Engineering, Hosei University, 3-7-2 Kajinocho Koganei-shi, Tokyo 184-8584, Japan.

H. Tanaka is with the University Center for Information Medicine Tokyo Medical and Dental University, 1-5-45 Yushima, Bunkyo-city, Tokyo 113-8510, Japan.

I. INTRODUCTION

IN THE aging society, it is important for senior citizens to maintain and improve their health and to lead active lives instead of lying in a hospital bed. Monitoring of biosignals in various situations at home whether outdoors or in the bedroom is helpful for daily health management. The use of wrist actigraphy provides information not only on activity cycles during the day but also on sleep cycles at night. Various studies have been carried out in conjunction with activity and sleep cycles [1], [2], [3]. We recently presented an ambient intelligent approach to ubiquitous health monitoring at home for detection of biosignals from a person on flooring, on a tatami mat, in the bathtub, or in the lavatory at home [4] based on the pneumatic method [5]. This method also detects biosignals in the daytime. Furthermore, we expanded this idea to outside the home through the use of a mobile phone by designing a low-frequency microphone for detecting biosignals [6]. A method that complements the detection of nighttime biosignals is the bed sensor method, typical examples of which can be found in literature [7], [8], [9], [10], [11], [12]. One of the bed sensor methods detects body movement, heartbeat and respiration through mechanical vibration using, for example, a highly sensitive accelerometer, or pressure vibration within a mattress into which a highly sensitive pressure sensor is plugged. However, when the gain of the sensor was set to detect the very small vibrations of the heartbeat, the large vibrations from body movement saturated the sensing device. Furthermore, even though the sensor is sensitive, a preamplifier with high gain and filters was required to enhance the heartbeat signal.

This paper describes a bed sensor method with a wide dynamic range and high SN ratio enabling the detection of microvibrations from the heartbeat by the change in acting force when a person is lying on the bed, without saturation from body movement and without a preamplifier, thus without any voltage source. The sensing device generates voltage corresponding to the biosignals of the heartbeat, respiration, body movement, changes in position and scratching motions of a person on the bed.

This article has been accepted for publication in a future issue of this journal, but has not been fully edited. Content may change prior to final publication.

NUKAYA, SHINO, KURIHARA, WATANABE AND TANAKA: BED SENSING VIA PIEZOCERAMIC DEVICES　　　　2

II. BED SENSOR SYSTEM

A. System

Figure 1 shows the proposed bed sensor system. Piezoceramics bonded to stainless steel plates are set beneath each of the four feet of the bed to support the weight of the bed and the person on it. Since piezoceramics have capacitive characteristics, the output voltage in the steady state is zero-biased and changes from zero voltage.

The variables and constants for the piezoceramic devices and the system shown in Figure 1 are defined as follows:

[Piezoceramics]

A [C/m] or [N/V]: force factor of the piezoceramic device
M [kg]: mass of bed and person on it
k [N/m]: stiffness constant of the metal stainless steel plate
d [Ns/m]: damping coefficient of the metal plate
C [F]: capacitance between the piezoceramic devices
R [Ω]: input resistance of the processor
t [s]: time
$x(t)$ [m]: resultant displacement of stainless steel plate
$f(t)$ [N]: force generated by the devices
$q_i(t)$ [C]: electric charge generated by external strain or bend to the ceramics
$q(t)$ [C]: resultant electric charge in the ceramics
$x_{hr}(t)$, $x_{hl}(t)$, $x_{fr}(t)$, $e_{fl}(t)$ [m]: displacement of device plate set at the head and right corner, head and left corner, foot and right corner, and foot and left corner, respectively
$e_{hr}(t)$, $e_{hl}(t)$, $e_{fr}(t)$, $e_{fl}(t)$ [V]: output voltage due to $x_{hr}(t)$, $x_{hl}(t)$, $x_{fr}(t)$, $x_{fl}(t)$, respectively
$P_{fh}(t)$ [Vs]: integrated value of the difference of $e_{fl}(t) - e_{hl}(t)$
$P_{rl}(t)$ [Vs]: integrated value of the difference of $e_{hr}(t) - e_{hl}(t)$

[Bed]

G, G': center of gravity (CG)
$F_H(t)$ [N]: forces pushing the bed by heartbeat
$F_R(t)$ [N]: forces pushing the bed by respiration motion
g [m/s^2]: magnitude of acceleration due to gravity
M [kg]: weight of the bed with a person on it
L [m]: length of the bed
L_f [m]: length from CG to foot side of the bed
L_h [m]: length from CG to head side of the bed
W [m]: width of the bed
W_l [m]: length from CG to left side of the bed
W_r [m]: length from CG to right side bed of the bed
$l(t)$ [m]: displacement of CG of the bed from the head to foot direction due to change in position of person on the bed
$w(t)$ [m]: displacement of CG of the bed from the left to right direction due to change in position of person on the bed
d_H [m]: distance from the heart to CG
d_R [m]: distance from the diaphragm for respiration to CG
$\theta_{fh}(t)$, $\theta_{rl}(t)$: sinking angle of the bed from the head to foot direction and from the left to right direction, respectively

From the system shown in Figure 1, we measured the heartbeat and respiration from output $e_{hr}(t)$, $e_{hl}(t)$, $e_{fr}(t)$ or $e_{fl}(t)$. Furthermore, in order to detect changes in position and scratching motions, we integrated the difference between two

$$P_{fh}(t)=\int_0^t \{e_{fl}(\tau) - e_{hl}(\tau)\}d\tau$$
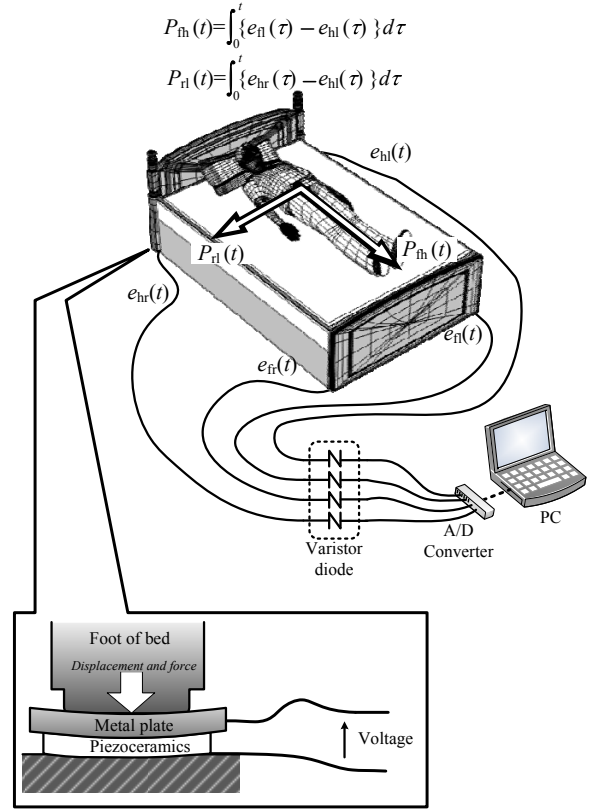
$$P_{rl}(t)=\int_0^t \{e_{hr}(\tau) - e_{hl}(\tau)\}d\tau$$

Fig. 1. Bed sensor method using piezoceramics

outputs $e_{hl}(t)$, $e_{fl}(t)$ from the left side and $e_{hl}(t)$, $e_{hr}(t)$ as follows:

$$P_{fh}(t) = \int_o^t \{e_{fl}(\tau) - e_{hl}(\tau)\}d\tau$$
$$P_{rl}(t) = \int_o^t \{e_{hr}(\tau) - e_{hl}(\tau)\}d\tau \tag{1}$$

B. Theoretical Model of the System

Figure 2 shows a situation where a person is lying on the bed. The location of the heart is at distance d_H from the CG and the diaphragm for respiration is at distance d_R from the CG. The heartbeat and respiration motions push the bed via forces $F_H(t)$ and $F_R(t)$ at these positions, respectively. Furthermore, the person moves toward the foot side of the bed as well as toward the right side of the bed and the CG shifts from G to G' for displacement $l(t)$ and $w(t)$, and the foot side sinks at angle $\theta_{fh}(t)$ and the right side sinks at angle $\theta_{rl}(t)$, respectively, as shown in Figure 2.

First, we considered the bed motion and piezoceramic output from the foot and head side. Suppose the shift $l(t)$ is very short and $l(t) << L, L_f, L_h$, thus the sinking angle $\theta_{fh}(t)$ around G and G' is the same. Assuming uniform mass for the bed with a person on it, the inertia moment I_{fh} of the bed around the CG is given by the bed size and weight, then the damping and spring for rotary motion of the bed are as follows:

This article has been accepted for publication in a future issue of this journal, but has not been fully edited. Content may change prior to final publication.

NUKAYA, SHINO, KURIHARA, WATANABE AND TANAKA: BED SENSING VIA PIEZOCERAMIC DEVICES 3

(a) Side view

(b) Sole side view

Fig. 2. Model of bed

$$I_{fh} = M \cdot \frac{L_f - l}{3L} \cdot (L_f - l)^2 + M \cdot \frac{L_h + l}{3L} \cdot (L_h + l)^2 \cong \frac{M}{3L}(L_f^3 + L_h^3)$$

$$D_{fh} = d\{(L_f - l)^2 + (L_h + l)^2\} \cong d(L_f^2 + L_h^2)$$

$$K_{fh} = k\{(L_f - l)^2 + (L_h + l)^2\} \cong k(L_f^2 + L_h^2)$$

(2)

The rotary motion around G or G' from a steady state condition is then given by:

$$I_{fh}\frac{d^2\theta_{fh}(t)}{dt^2} + D_{fh}\frac{d\theta_{fh}(t)}{dt} + K_{fh}\theta_{fh}(t) = Mgl(t) + d_H F_H(t) + d_R F_R(t) + Lf(t)$$

(3)

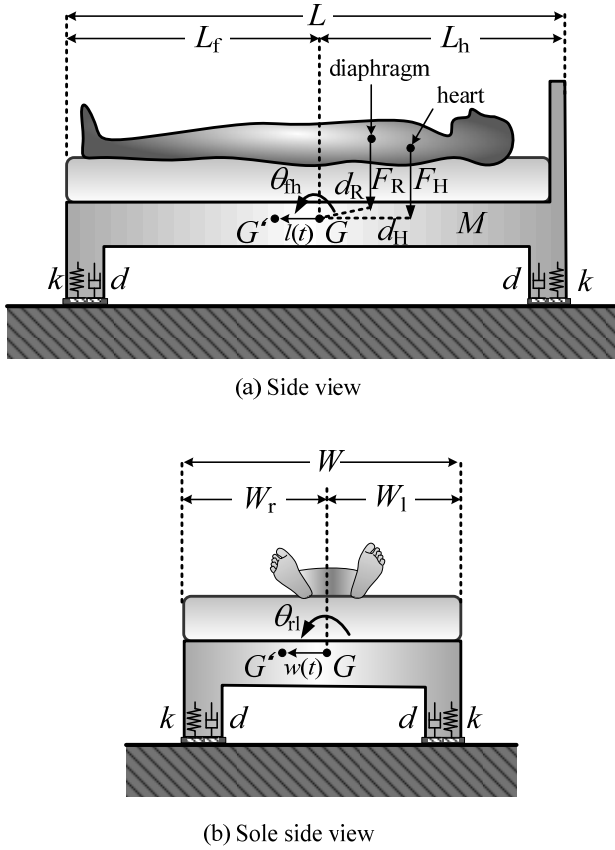The displacement of the stainless steel plate of the piezoceramic devices at the foot and head side are given as follows:

$$x_f(t) = (L_f - l)\theta_{fh}(t) \cong L_f\theta_{fh}(t)$$

$$x_h(t) = -(L_h + l)\theta_{fh}(t) \cong -L_h\theta_{fh}(t)$$

(4)

The displacement drives the piezoceramic devices with reversible characteristics between static and electrostatic as follows:

$$q_i(t) = Ax_f(t) = AL_f\theta_{fh}(t)$$

$$R\frac{dq(t)}{dt} + \frac{1}{C}q(t) = \frac{1}{C}q_i(t)$$

(5)

$$e_f(t) = R\frac{dq(t)}{dt}$$

$$f(t) = -Ae_f(t)$$

Figure 3 shows the equivalent block diagram representation.

The transfer functions are defined as follows:

$$G_1(s) = \frac{A}{C}, \quad G_2(s) = \frac{sCR}{1 + sCR}, \quad G_3(s \mid L_f) = \frac{\dfrac{L_f}{I_{fh}}}{s^2 + \dfrac{D}{I_{fh}}s + \dfrac{1}{I_{fh}}\left\{K_{fh} + \dfrac{sRLL_f A^2}{(1 + sCR)}\right\}}$$

(6)

Then, output e_f with respect to input forces $Mgl + d_H F_H + d_R F_R$ is given:

$$e_f = G_1(s) \cdot G_2(s) \cdot G_3(s \mid L_f)(Mgl + d_H F_H + d_R F_R)$$

(7)

Similarly, from Eqs. (4) and (7), the output voltage from the head side is given by:

$$e_h = -G_1(s) \cdot G_2(s) \cdot G_3(s \mid L_h)(Mgl + d_H F_H + d_R F_R)$$

(8)

These outputs correspond to the outputs of $e_{hl}(t)$, $e_{hr}(t)$, $e_{fl}(t)$, and $e_{fr}(t)$ in Figure 1.

C. Measurement of Heartbeat, Respiration and Body Movement

Since we could select a large input resistance R such as 1 to 10 MΩ, which is usual, the cut-off frequency $\dfrac{1}{2\pi CR}$ of $G_2(s)$ is sufficiently lower than the frequency range of the fundamental and higher components of the heartbeat. Furthermore, we could also select a resonance frequency

$$f = \frac{1}{2\pi}\sqrt{\frac{K_{fh} + (LL_f A^2 / R)}{I_{fh}}} = \frac{1}{2\pi}\sqrt{\frac{3Lk(L_f^2 + L_h^2)}{M(L_f^3 + L_h^3)}}$$

(9)

of the transfer function $G_3(s)$ around the components of the heartbeat, so that output voltages $e_f(t)$ and $e_h(t)$ include the enhanced heartbeat signals. For the low-frequency range where $f < \dfrac{1}{2\pi CR}$, from Eqs. (2), (6), (7) and (8) in the time domain, we obtained the following approximations:

$$e_f(t) = AR\frac{L_f}{k(L_f^2 + L_h^2)}\frac{d}{dt}\{Mgl(t) + d_H F_H(t) + d_R F_R(t)\}$$

$$e_h(t) = -AR\frac{L_h}{k(L_f^2 + L_h^2)}\frac{d}{dt}\{Mgl(t) + d_H F_H(t) + d_R F_R(t)\}$$

(10)

This article has been accepted for publication in a future issue of this journal, but has not been fully edited. Content may change prior to final publication.

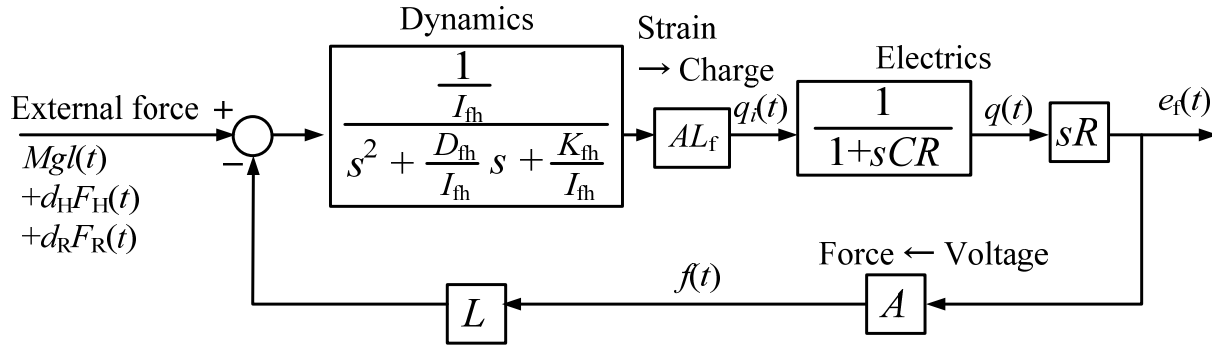NUKAYA, SHINO, KURIHARA, WATANABE AND TANAKA: BED SENSING VIA PIEZOCERAMIC DEVICES   4

Fig. 3. Block diagram of piezoceramic sensor device with resistive load

Similarly, output voltages $e_l(t)$ and $e_r(t)$ due to shifting of the body to the left or right side and heartbeat and respiration, can be obtained as follows:

$$e_r(t) = AR \frac{W_r}{k(W_r^2 + W_l^2)} \frac{d}{dt} \{Mgw(t) + d_H F_H(t) + d_R F_R(t)\}$$

$$e_l(t) = -AR \frac{W_l}{k(W_r^2 + W_l^2)} \frac{d}{dt} \{Mgw(t) + d_H F_H(t) + d_R F_R(t)\} \tag{11}$$

Thus, Eq. (12) can be derived:

$$P_{fh}(t) = \int_o^t \{e_{fl}(\tau) - e_{hl}(\tau)\} d\tau = AR \frac{L}{k(L_f^2 + L_h^2)} \{Mgl(t) + d_H F_H(t) + d_R F_R(t)\}$$

$$P_{rl}(t) = \int_o^t \{e_{hr}(\tau) - e_{hl}(\tau)\} d\tau = AR \frac{W}{k(W_r^2 + W_l^2)} \{Mgw(t) + d_H F_H(t) + d_R F_R(t)\} \tag{12}$$

When body movements occur, because
$Mgl(t) >> d_H F_H(t) + d_R F_R(t)$ and
$Mgw(t) >> d_H F_H(t) + d_R F_R(t)$, Eq. (12) can simply be rewritten as:

$$P_{fh}(t) = \frac{ARLMg}{k(L_f^2 + L_h^2)} l(t)$$

$$P_{rl}(t) = \frac{ARWMg}{k(W_r^2 + W_l^2)} w(t) \tag{13}$$

where each is linearly proportional to the shift in the CG at the foot to the head side and at the left to the right side, from which we can estimate the movement of the person on the bed.

III. VERIFICATION EXPERIMENTS

A. Measurement Device and System

Figure 4 shows the measurement system. The piezoceramic device, 20 mm in diameter, was bonded to a brass metal plate with a diameter of 25 mm. This is the same device used for a buzzer and costs half a dollar. The device was then bonded to stainless steel plate with a thickness of 1 mm and diameter of 50 mm. A washer with a thickness of 2 mm, inner radius 15 mm and outer radius 25 mm was set under the plate and the bottom was covered by an aluminum plate the same size as the stainless
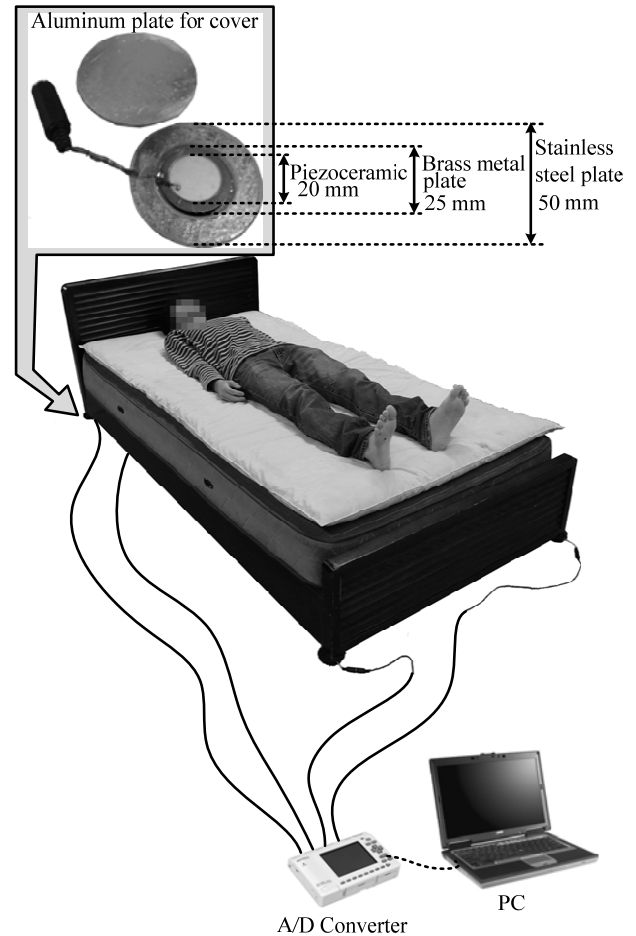
Fig. 4. Measurement system

steel disk above. Force factor A of the device was 1×10^{-3} C/m and capacitance was 0.01 µF. Four devices were set between the floor and the four bottom corners of the bed, as shown in Figure 4. The bed is a coil cushion bed weighing 60 kg and measuring 1.0×2.1 m. The data from the four devices was measured and A/D-converted at a sampling time of 1 ms and scale range of ±1 V using a data logger (NR-2000, Keyence Co. Ltd.).

The noise level without passive low-pass filtering was 10 mV, which is almost a humming noise. With the passive low-pass filter the noise level was reduced to 5 mV.

This article has been accepted for publication in a future issue of this journal, but has not been fully edited. Content may change prior to final publication.

NUKAYA, SHINO, KURIHARA, WATANABE AND TANAKA: BED SENSING VIA PIEZOCERAMIC DEVICES 5
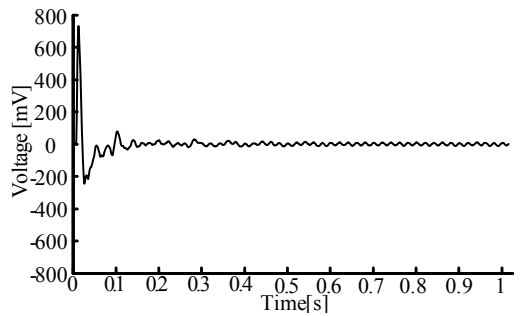
(a) Impulse response by hammering the frame of bed

P 1 = 10. 73 Hz
P 2 = 13. 66 Hz
P 3 = 22. 44 Hz
P 4 = 33. 17 Hz
P 5 = 44. 76 Hz
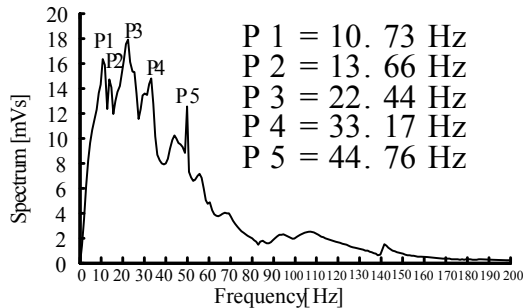
(b) Frequency characteristics of bed vibration

Fig. 5. Impulse response and frequency response of the bed sensor system

(a) Pulse oximeter for reference

(b) Output from ceramics

Fig. 6. Heartbeat signal

(a) Low frequency microphone

(b) Output from ceramics

Fig. 7. Respiration signal

First, to determine the dynamics of the bed system, we lightly hammered the center of the bed and acquired the output $e_{hr}(t)$. Figure 5 shows the time and frequency response calculated by FFT for 1024 data items.

The resonance frequency of the system is 10.73 Hz, which shows the overall dynamics of the bed sensor system including the resonance characteristics of the sensor device and the natural frequency of the bed vibrations.

B. Signal Processing

The data $e_{hr}(t)$, $e_{hl}(t)$ and $e_{fr}(t)$, $e_{fl}(t)$ acquired through A/D conversion was band-pass filtered using a bandwidth ranging from 3 to 7 Hz. The output signal from the band-pass filter was full-wave rectified and low-pass filtered at a moving average of 150 data items to obtain the heartbeat component. Since the respiration frequency is around 0.3 Hz, the respiration signal was obtained by band-pass filter with a bandwidth ranging from 0.1 to 0.5 Hz.

IV. EXPERIMENTAL RESULTS

A. Heartbeat and Respiration

Figure 6 shows the heartbeat signal. Figure 6(a) is the signal measured by a pulse oximeter for reference. Figure 6(b) is the band-pass-filtered signal from the piezoceramic device set at the foot, left corner $e_{fl}(t)$. The signal level is around 10 mV, for which the SN ratio is 40 dB. The periods of both waves are the same and are synchronized. The output signal from the piezoceramics includes the low-frequency components of respiration. The other three outputs show similar waveforms as
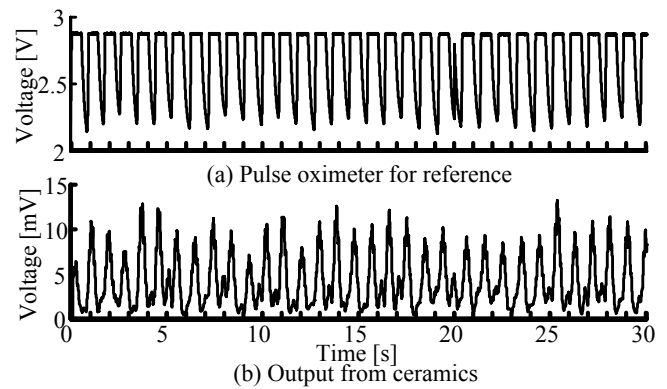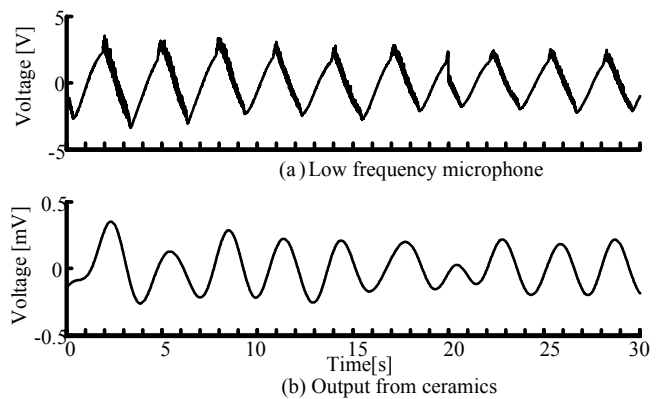
$e_{fl}(t)$ and thus we can measure the heartbeat from any of the four devices.

Figure 7 shows the respiration signal. Figure 7(a) is the respiration blowing pressure from the nasal cavity measured by a low-frequency microphone. Figure 7(b) is the band-pass-filtered signal from the piezoceramic device set at the head, right corner. The signal level of the $e_{hr}(t)$ was 0.5 mV, for which the SN ratio is 14 dB. The periods of both waves are the same and are synchronized.

The outputs from the other three devices show the same period. Both outputs from the head side are synchronized, but those at the foot side are the negative value of the head side outputs. This is because the diaphragm of the person was above the center of gravity of the bed cushion.

B. Turning Over on the Bed

Figure 8 shows a situation where a person is lying on his back, then turns over to the right side, to the left side and then returns to lying on his back again. The outputs from the four devices were not saturated by this movement. The graph in Figure 8 shows the change in $P_{fh}(t)$ in the upper part and that in $P_{rl}(t)$ in the lower part. Since the head-feet motion was slight, $P_{fh}(t)$ changes only a little, whereas $P_{rl}(t)$ changes following the body movement. When the person starts turning over to the right, $P_{rl}(t)$ starts increasing from zero to positive value; when the person maintains the same position, $P_{rl}(t)$ remains a constant positive value; when the person turns back to the center, $P_{rl}(t)$
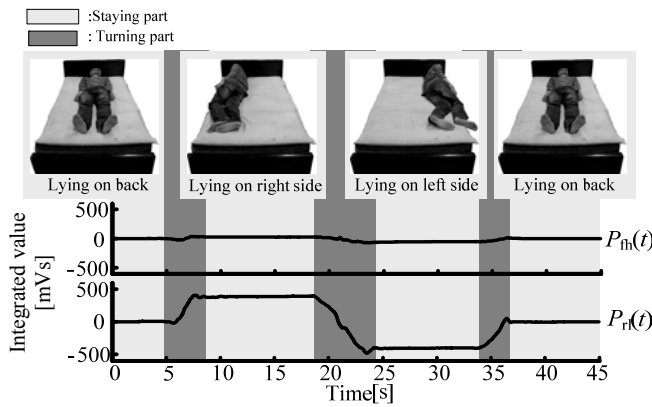
Fig. 8. Turning movement

Fig. 10. Sitting up and lying down motion using left hand

Fig. 9. Sitting up and lying down motion without using hands

decreases to zero; and when he starts turning over to the left, $P_{rl}(t)$ decreases to a negative value; when he stays in the same position, $P_{rl}(t)$ remains a constant negative value; and finally, when he turns back to the center, $P_{rl}(t)$ also increases to zero. The change in $P_{rl}(t)$ is proportional to that of the center of gravity of the bed or the moving direction of the person on the bed.

Figure 9 shows a situation where a person changes from a lying position to a forward sitting position and then lies down again. The person sits 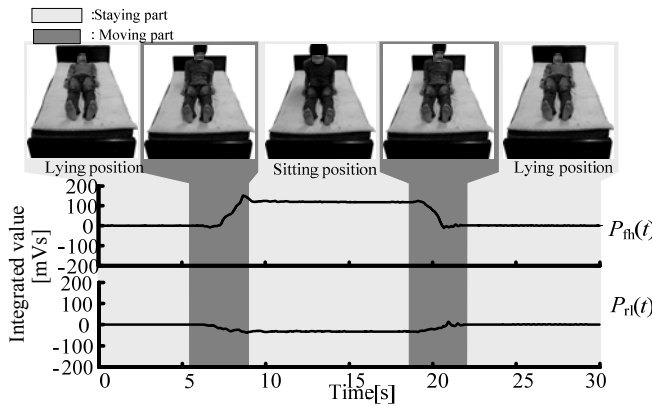up without using his hands. Again, the outputs from the four devices were not saturated by these motions. In the graph in Figure 9, the change in $P_{fh}(t)$ and $P_{rl}(t)$ is shown in the upper and lower row, respectively. Since there was only a slight motion from the left to right side when sitting up, $P_{rl}(t)$ changed only a little. In contrast, when the person starts to sit up, $P_{fh}(t)$ starts increasing to a positive; when he stays in the same position, $P_{fh}(t)$ remains a constant positive value; when he lies down again, $P_{fh}(t)$ decreases to zero. The change in $P_{fh}(t)$ is proportional to that of the center of gravity of the bed or the moving direction of the person on the bed.

Figure 10 shows the motion of sitting up and then lying down again using the left hand for support. Again, the outputs from the four devices were not saturated. $P_{fh}(t)$ shows similar changes to those in Figure 9, whereas $P_{rl}(t)$ shows a negative value when the left hand pushes against the bed, which means that the center of gravity of the bed shifts to the left side. When the person made the same motion using the right hand, $P_{fh}(t)$

showed similar changes to those in Figure 10, but $P_{rl}(t)$ shows a positive value when the right hand pushes against the bed.

C. Scratching

Figure 11 shows what happens when the person scratches his belly on the left side using the fingers of his right hand. Before scratching, the person had his hand at the side of his body on the bed. Thus, when he began scratching, his hand moved slightly to the head side. The lower figures in the graph from top to bottom show the change in angular velocity of the finger motion, $P_{fh}(t)$ and $P_{rl}(t)$, respectively.

When the person started the scratching motion, the average value of $P_{rl}(t)$ decreased. This is because his hand moved to the left and the center of gravity of the bed shifted to the left. The scratching frequency of $P_{fh}(t)$ and $P_{rl}(t)$ is the same as that of angular velocity of the finger motion and they are synchronized. The finger motion and $P_{fh}(t)$ and $P_{rl}(t)$ under various scratching motions were measured and compared. They show similar waves, as shown in Figure 11.

V. DISCUSSION

From the aspect of the medical system design, in comparison with our previous works [4], [5], the proposed bed sensor system has the following features.

The system uses four piezoceramic devices sandwiched between the floor and the bottom four corners of the bed. The devices are distortion sensors that work without an electric power supply; they generate voltage proportional to the time-derivative of the distortion and they are highly sensitive. The system A/D-converts the biosignals directly from the devices without using an electrical preamplifier. We used the system to measure the heartbeat at an SN ratio of 40 dB, respiration at 14 dB, position changes without saturation, and scratching motions of a person on the bed. The output from motions of getting into bed and getting out of bed, which is not shown, was of course measured as large signals, but without saturation. The device has a wide dynamic range. Furthermore, because the device is battery-free and generates the output voltage, it can be used not only for biosensing but also as an event trigger signal for a biosignal microprocessor, which in

This article has been accepted for publication in a future issue of this journal, but has not been fully edited. Content may change prior to final publication.

NUKAYA, SHINO, KURIHARA, WATANABE AND TANAKA: BED SENSING VIA PIEZOCERAMIC DEVICES　　　7

(a) Scratching motion
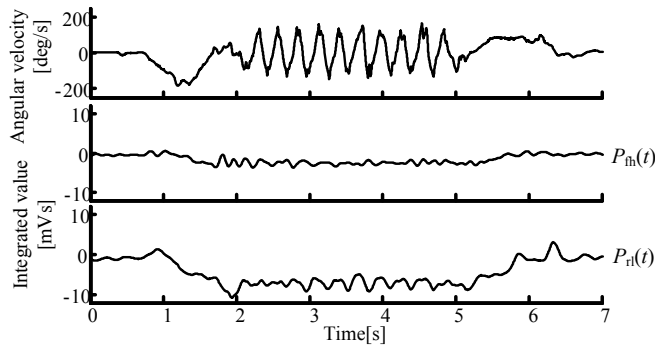
(b) Scratching

Fig. 11. Scratching the belly on the left side using the fingers of the right hand, and angular velocity of finger motion and change in motion, $P_{\mathrm{fh}}(t)$ and $P_{\mathrm{rl}}(t)$.

practice is very effective for developing equipment driven by a small-capacity battery for a period as long as a year.

From the heartbeat and body movements measurable by the sensor devices, we were able to estimate the sleep stages [8]. The shift in the center of gravity of the bed with a person on it was estimated by outputs $P_{\mathrm{fh}}(t)$ and $P_{\mathrm{rl}}(t)$. The shift in the center of gravity is proportional to the displacement from the movement of the person on the bed. Information on the different movements can be used to assist patients who are trying to get out of bed, as just one example. In the case of diseases, especially skin disorders, characterized by itching, the bed sensor method makes it possible to measure the frequency and intensity of scratching motions during the night, which is otherwise very difficult to ascertain.

From the clinical application aspect, because the sensors are set between the floor and the corners of the bed, it is more non-invasive and unconsciousness for subjects than the conventional bed sensing system in the literatures [7] - [12].
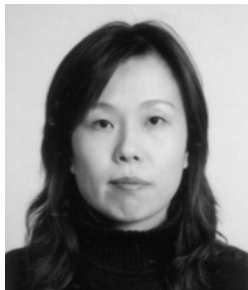
VI. CONCLUSIONS

This paper described a novel biosignal sensing method using four piezoceramic devices sandwiched between the floor and the four corners of the bed, which guarantees noninvasive, constraint-free, subliminal biomeasurement. The devices are battery-free and generate voltages corresponding to the heartbeat, respiration, position change, and scratching motion of a person on the bed. The wide dynamic range of the sensor enables the detection of mechanical microvibrations from the heartbeat as voltage of 10 mV to vibrations from getting into and out of bed as voltage of several volts without saturation and with a high SN ratio. Due to the high sensitivity of the device, a preamplifier was not required to obtain the biosignals. These features of the device are effective for developing biosensing

equipment with low power consumption driven for at least one year by a small battery.

The devices clearly detect the heartbeat at an SN ratio of 40 dB, and respiration at an SN ratio of 14 dB. Furthermore, from the integrated value of the difference in voltage generated by the head-side device and that by the foot-side device, and from that by the left side and right side of the bed, a change in position of the person on the bed was detectable. Detection of scratching motions of the person on the bed was also possible with accuracy. As one of the bed biosensing methods, the proposed method is valid in terms of cost performance, i.e., the device is the same one used for a buzzer costing half a dollar, realization of low power equipment, i.e., the device is battery-free and driven without a preamplifier, and accuracy and variety of biosensing, i.e., detection ranges from micro biovibration signals to giant signals without saturation.

REFERENCES

[1] Standards of Practice Committee, American Academy of Sleep Medicine; T. Morgenthaler, et al., "Validity in Actigraphic Sleep Assessment," *SLEEP*, vol.30, no.4, pp.519-529, 2007

[2] B. Sivertsen, et al., "A Comparison of Actigraphy and Polysomnography in Older Adults Treated for Chronic Primary Insomnia," *SLEEP*, vol. 29, no. 10, pp.1353-1356, 2006

[3] N. L. Johnson, et al., "Sleep Estimation Using Wrist Actigraphy in Adolescents With and Without Sleep Disordered Breathing: A Comparison of Three Data Modes," *SLEEP*, vol. 30, no. 7, pp. 899-905, 2007

[4] K. Watanabe, Y. Kurihara and H. Tanaka, "Ubiquitous Health Monitoring at Home – Sensing of Human Biosignals on Flooring, on Tatami Mat, in the Bathtub, and in the Lavatory," *IEEE SENSORS JOURNAL*, vol. 9, no. 12, pp.1847-1855, December 2009

[5] K. Watanabe, T. Watanabe, H. Watanabe, H. Ando, T. Ishikawa and K. Kobayashi, "Noninvasive measurement of heartbeat, respiration, snoring and body movement of a subject in bed via a pneumatic method," *IEEE Trans. Biomed. Eng.*, vol. 52, pp. 2100-2107, 2005.

[6] K. Watanabe, Y. Kurihara, T. Nakamura and H. Tanaka, "Design of a Low-Frequency Microphone for Mobile Phones and Its Application to Ubiquitous Medical and Healthcare Monitoring, *IEEE SENSORS JOURNAL*, vol. 10, no. 5, pp. 934-941, March 2010

[7] J. Alihanka and V. Vaahtornanta, "A static charge sensitive bed. A new method for recording body movement during sleep," *Electroencephalogr. Clin. Neurophysiol.*, vol. 46, pp. 731-734, 1979

[8] T. Watanabe and K. Watanabe, "Noncontact Method for Sleep Stage Estimation," *IEEE Trans. Biomed. Eng.*, vol. 51, no. 10, pp. 1735-1748, 2004

[9] N. Bu, N. Ueno and O. Fukuda, "Monitoring of respiration and heartbeat during sleep using a flexible piezoelectric film sensor and empirical mode decomposition," *Proc. IEEE Eng. Med. Biol. Soc.*, pp. 1362-1366, 2007

[10] M. Ishijima, "Monitoring of Electro-cardiograms in Bed without Utilizing Body Surface Electrodes," *IEEE Trans. Biomed. Eng.*, vol. 40, no. 6, pp. 593-594, 1993

[11] X. Zhu, W. Chen, T. Nemoto, Y. Kanemitsu, K. Kitamura, K. Yamakoshi and D. Wei, "Real-time monitoring of respiration rhythm and pulse rate during sleep," *IEEE Trans. Biomed. Eng.*, vol. 53, no. 12, pp. 2553-2563, 2006

[12] D. C. Mack, J. T. Patrie, P. M. Suratt, R A. Felder and M. A. Alwan, "Development and preliminary validation of heart rate and breathing rate detection using a passive, ballistocardiography-based sleep monitoring system," *IEEE Trans. Inf. Technol. Biomed.*, vol. 13, no. 1, pp. 111-120, 2009

This article has been accepted for publication in a future issue of this journal, but has not been fully edited. Content may change prior to final publication.

NUKAYA, SHINO, KURIHARA, WATANABE AND TANAKA: BED SENSING VIA PIEZOCERAMIC DEVICES 8

Shoko Nukaya Shoko Nukaya received B.E. degree from Waseda University, Tokyo, in 1992. She joined Sony Corporation. For 12 years, as a software engineer, She had been developing consumer mobile products. In 2005, she recieved M.S. degree from Eastern Michigan University, MI, US. After graduation, she joind Nokia Corportation. Since 2010, she has started the research at Tokyo Medical and Dental University Graduate School as a PhD student. Her major interests are healthcare innovation by utilizing IT.

Toshihiro Shino received the B.E. degrees in system control engineering from Hosei University, Tokyo, Japan, in 2010. Now he belongs to graduated school Hosei. His current interest is biomeasurment.

Yosuke Kurihara received M.E. and Ph.D. degrees from Hosei University, Tokyo, in 2003 and 2009, respectively. From 2009 to present, he served as Assistant Professor at the Seikei University. His research interests include sensor method, bio-sensing, system information. He is a member of Japanese Society for Medical and Biological Engineering, etc.

Kajiro Watanabe received the M.E. and Ph.D. degrees from the Tokyo Institute of Technology, in 1968 and 1971, respectively. From 1969 to 1971, he served as a Research Assistant at Faculty of Engineering Hosei University. From 1971, he served the Lecture; from 1974 to 1984, as an Assistant Professor; and from 1985 to present, as the Professor. From 1980 to 1981, he served as the Visiting Associate Professor at Oakland University, Rochester, MI, and from 1981 to 1982 as the Research Associate at the University of Texas, Austin. In the industrial filed, he acts as an authorized C.E. He is Chief Researcher of the several projects conducted by the Ministry of Economy, Trade, and Industry Japan. His major interest is the control and instrument and he is currently interested in bio-measurement, sports measurement, robotics, fault diagnosis, vehicle, environmental monitoring, and intelligent control. He holds 75 patents, has 15 publications in the control engineering field and more than 332 referenced journals and conference proceedings. Dr. Watanabe is a member of the Society of Instrument and Control Engineers.

Hiroshi Tanaka received D.M. and Ph.D. degrees from the University of Tokyo, in 1981 and 1983, respectively. From 1982, he served as a lecture at University of Tokyo; from 1987, as an Assistant Professor at Hamamatsu University School of Medicine; from 1991 to present, as a Professor at Department of Medical informatics Tokyo Medical and Dental University. From 1995, he is a Director General at University Center for Information Medicine Tokyo Medical and Dental University. From 2006, he is a Director of Biomedical Science PhD Program, the Chief Manager and President of the JAMI, and Chairperson of the JHITI.

Development of Unconstrained Biosignal Bed Sensing Method Using Piezoceramics to Detect Body Movement and Scratching Motion

Toshihiro Shino[1], Shoko Nukaya[2], Yosuke Kurihara[3], Kajiro Watanabe[1] and Hiroshi Tanaka[2]

[1]Department of System Engineering, Hosei University, Tokyo, Japan
(Tel: +81-42-387-6251)
[2]Division of Advanced Therapeutical Sciences, Tokyo Medical and Dental University, Tokyo, Japan
(Tel: +81-3-5803-0376)
[3]Department of Computer and Information Science, Seikei University, Tokyo, Japan
(Tel: +81-422-37-3738)

Abstract: This paper describes a novel bed sensing method for unconstrained detection of body movement and scratching motion through biosignal measurement. The bed sensing method can be used to monitor a person's health condition at home or in the hospital. Moreover, this system is able to detect the frequency of scratching motion. Conventional methods that use infrared cameras or acceleration sensors impose physical and/or psychological stress on the patient. We have developed an unconstrained biosignal bed sensing device using piezoceramics. Piezoceramic sensors are bonded to stainless steel plates sandwiched between the floor and the four legs of the bed. The sensors accurately detect body movement and scratching motions through the acquisition and measurement of biosignals. The device is suitable for various health applications including monitoring of sleep and diseases characterized by itching.

Keywords: Unconstrained sensing, bed sensing, piezoceramics, body movement, scratching.

1. INTRODUCTION

Staying healthy and active is essential for maintaining quality of life. Monitoring of biosignals, such as during outdoor activity or while sleeping, contributes to health management. The use of wrist actigraphy provides information on activity cycles during the daytime and sleep cycles at night. Hospitals often monitor nighttime scratching motion as a mechanical reaction to itching during sleep. Various studies have been conducted on the motion of scratching and its detection, including in conjunction with activity and sleep cycles [1, 6-8]. Scratching is typically measured by using an infrared video camera, accelerometer or gyrometer. An effective approach for detecting nighttime biosignals is the bed sensor method, and several different examples can be found in literature [9-14]. In these methods, body movement, heartbeat and respiration is detected through mechanical vibration using, for example, a highly sensitive accelerometer or a pressure sensor that is plugged into the mattress. This paper describes a noncontact bed sensing method that does not rely on a voltage source. The sensing device generates voltage corresponding to the biosignals or motions of the person on the bed.

2. OBJECT OF MEASUREMENT

Scratching motion is measured in order to estimate the intensity of itching, especially during sleep. In clinical practice, an infrared video camera is generally used to monitor the location, pattern, and frequency of scratching. This information is compiled into an index referred to as TST%, which is the ratio of total scratching time (TST) to total recording time during sleep. The data is correlated to the degree of pruritus in skin diseases such as atopic dermatitis [15, 16]. The more severe the disease is, the greater the frequency of scratching by the patient. Furthermore, a characteristic pattern in atopic dermatitis patients is that the head is scratched most frequently [7].

Numerous methods have been proposed for measuring scratching motion. They include the use of infrared video cameras and other recording devices to measure the motion or the sound of scratching and the acceleration of wrist movement and its angular velocity. An electromyograph can be used to measure electrical activity of the muscles in the forearm. Other devices can measure the change in pressure of the back of hand and its expansion and contraction, motion of the fingers, and so forth [7, 8, 15-24].

3. BED SENSING SYSTEM

Figure 1 shows the details of the built-in piezoceramic sensor employed in this system. The sensor is 20 mm in diameter and is firmly affixed to a brass metal plate, which is 25 mm in diameter. This device is typically used for a buzzer. The device is bonded to a stainless steel plate, which is 1 mm thick and 50 mm in diameter. Under the stainless steel plate is a washer, which has an inner radius of 15 mm, outer radius of 25 mm and thickness of 2 mm. The bottom is covered by an aluminum plate that is the same size as the stainless steel plate.

The characteristics of this sensor are as follows: 1×10^{-3} C/m, which is the displacement of electrical charge by piezoelectricity. The capacitance is 0.01 μF. Due to the capacitive characteristics of piezoceramics, the output voltage in the steady state is zero-biased and changes from zero voltage.
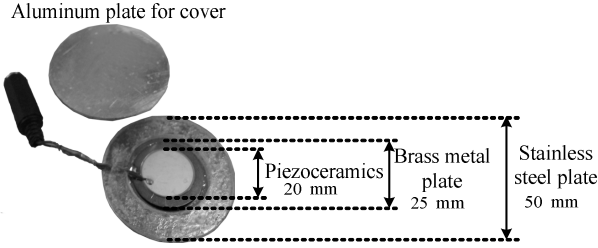
Fig. 1 Built-in piezoceramics sensor

4. EXPERIMENTAL SYSTEM

Figure 2 shows the proposed bed sensing system. Four piezoceramic sensors are used, one under each leg of the bed. The bed is a coil cushion type weighing 60 kg and measuring 1.0×2.1 m. The output from $e_{hr}(t)$, $e_{hl}(t)$, $e_{fr}(t)$ and $e_{fl}(t)$ is measured and A/D-converted at a sampling interval of 1 ms and scale range of ±1 V using a data logger (NR-2000, Keyence Co. Ltd.).
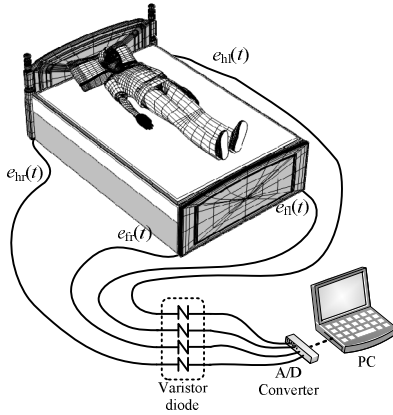

Fig. 2 Bed sensing system

We assume that the center of gravity of bed and subject follows his motion. It affects the force which each leg push the floor. We think it has symmetrical characteristics. For example, when the person on the bed turns over to the right, it increases in right side, and it decreases in left side. And the outputs are in proportion to the force. So, in order to detect body movement, we integrated the difference as follows:

$$P_{fh}(t) = \int_o^t \{e_{fl}(\tau) - e_{hl}(\tau)\} d\tau$$
$$P_{rl}(t) = \int_o^t \{e_{hr}(\tau) - e_{hl}(\tau)\} d\tau \qquad (1)$$

We made a video recording to be used as a reference for this experiment. To measure scratching motion, we used a conventional electromyograph and acceleration sensor (RF-ECG, Medical Electronic Science Institute Co., Ltd.), angular velocity sensor (FMS-001, Fujitsu), microphone (MX4843A, Primo Co. Ltd.), ceramic sheet (Flicker, Measurement Specialties Inc.) and strain gauge. The subject in this experiment was right-handed, so the sensors were set on his right hand, as shown in Fig. 3.

Details on the sensors are given in Subsections 4.1–4.6.
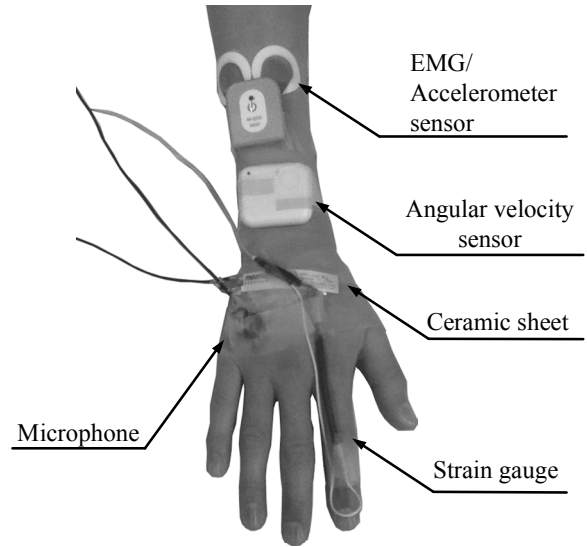
Fig. 3 Scratching sensors on right hand

4.1 Electromyograph [22]

This sensor measures changes in myogenic potential. We affixed it to the subject's forearm, as shown in Fig. 3. The two round objects are electrodes. The square object is the core, which transmits data to a PC by wireless Bluetooth. The core size is 40×35×7.2 mm. Sampling frequency is 204 Hz. This is not a medical instrument.

4.2 Acceleration sensor [8, 20, 21]

This measures the acceleration of the forearm. It is embedded in the EMG sensor and also uses Bluetooth. Sampling frequency is 204 Hz and the scaling range is ±3 G. The output includes gravitational acceleration.

4.3 Angular velocity sensor [21]

This sensor is 40×45×13 mm in size and it also uses wireless Bluetooth. The sampling interval is 2 ms. It is fixed on the forearm by surgical tape. This sensor has differential properties, so the output in the steady state is zero-biased and changes from zero degrees per second.

4.4 Microphone [17-19]

This method is used to record the sound made by the scratching motion. The system was originally developed for mouse monitoring and was later applied to humans.

The microphone is fixed to the back of the hand by surgical tape. The output is transmitted through an amplifier (MX4836, Primo Co. Ltd) and A/D-converted at a sampling interval of 1 ms and scale range of ±10 V using the data logger.

4.5 Ceramic sheet [23]

This is used to measure the change in pressure of the back of the hand, where it is fixed. The output is A/D-converted at a sampling interval of 1 ms and scale range of ±1.0 V using the data logger. The output voltage in the steady state is zero-biased and changes from zero voltage, due to the differential properties.

4.6 Strain gauge [24]

This measures the degree of finger bending. It is fixed by tape, along the index finger. The register value of this gauge changes from 1 to 2 kΩ. It has a source voltage, which is 9 V. It is designed so that the output is less than 5 V. The sampling interval is 1 ms and the scale range is ±5 V using the data logger.

5. EXPERIMENTAL RESULTS

In this experiment, we measured the motions for turning over, sitting up, lying down and scratching. As the starting position, the subject is lying on his back at the center of the bed and his arms and legs are straight, as shown in Fig. 2.

5.1 Turning over

We asked the subject to turn over from the center position to his right side and then turn from his right side to his left side and finally to return to the center.

Figure 4 shows the $P_{rl}(t)$ and $P_{fh}(t)$ of the turning over movement. The change in $P_{rl}(t)$ is indicated by the broken line and $P_{fh}(t)$ by the solid line, from Eq. (1). $P_{rl}(t)$ changed following each turning movement, whereas $P_{fh}(t)$ hardly changed.

When the subject starts turning over to his right side, $P_{rl}(t)$ starts increasing from zero to a positive value. When the subject turns back to the center, $P_{rl}(t)$ decreases to zero, and then further decreases to a negative value when the subject turns to the left. When the subject stays in the same position, $P_{rl}(t)$ remains at a constant value.

The change in $P_{rl}(t)$ is proportional to the right and left direction of the motion on the bed.
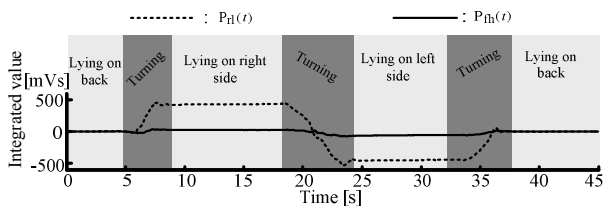

Fig. 4 $P_{rl}(t)$ and $P_{fh}(t)$ of turning over movement

5.2 Sitting up and lying down

In this situation, the subject changes position from lying on his back to sitting forward and then lying down again.

We measured two cases. In the first one, the subject sits up and lies down without using his hands. In the second case, the subject changes position using his left hand for support.

Figure 5 shows the $P_{rl}(t)$ and $P_{fh}(t)$ of sitting up and lying down. Figure 5(a) shows Case 1 (without using hands) and (b) shows Case 2 (using left hand). The lines are as defined for Fig. 4.

In Case 1, since the subject sits up without using his hands, there is only a slight motion in the right and left direction so $P_{rl}(t)$ changes only a little. While the subject

is in the process of sitting up, $P_{fh}(t)$ increases to a positive value; while he stays in the same position, $P_{fh}(t)$ remains a constant positive value; when he lies down again, $P_{fh}(t)$ decreases to zero. The change in $P_{fh}(t)$ is proportional to the motion in the foot and head direction.

In the second case, where the subject uses his left hand, $P_{fh}(t)$ changes similarly to the first case. However, $P_{rl}(t)$ shows a negative value during movement. At that time, the subject pushed his left hand against the left side of the bed while in the process of sitting up. So the weight on the bed moved to the left side, the same as when turning over to the left side.

Contrarily, when the subject uses his right hand, $P_{rl}(t)$ shows the opposite shape; it shows a positive value. In this case, $P_{fh}(t)$ also showed similar changes.

(a) Case 1 Without any hand

(b) Case 2 With left hand
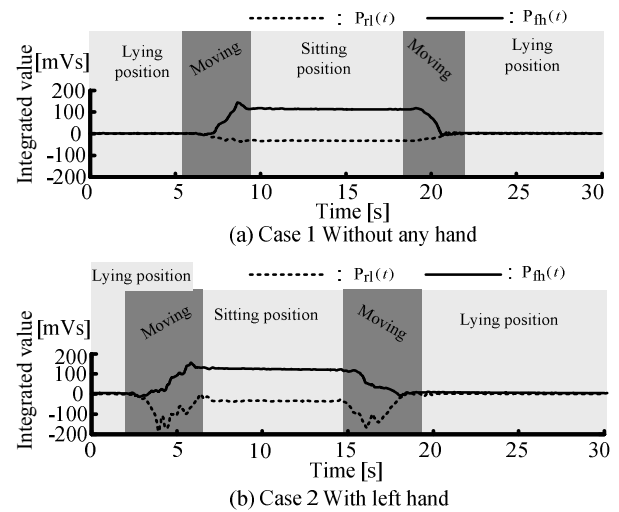
Fig. 5 $P_{rl}(t)$ and $P_{fh}(t)$ of sitting up and lying down

5.3 Scratching

Here, the subject was asked to move his right hand to his right cheek, and use his fingers to scratch his cheek twenty times and then return to his original position with his arm at his side on the bed. Scratching one time is one scratching stroke.

Figure 6 shows the results of one period of scratching. From top to bottom in the graph, the change is shown for the EMG, ceramic sheet, microphone, strain gauge, acceleration (X-, Y-, and Z-axis), angular velocity (X-, Y-, and Z-axis), $e_{hl}(t)$, $e_{hr}(t)$, $e_{fl}(t)$ and $e_{fr}(t)$.

The subject scratched between about 2 s and 8 s. At the beginning and end, from about 1 to 2 s and 8 to 9 s, the subject's right arm was moving, which generated a large change in the output from all sources. When the subject was resting quietly, the output hardly changed. All sensors show a cyclic change following the scratching motion.
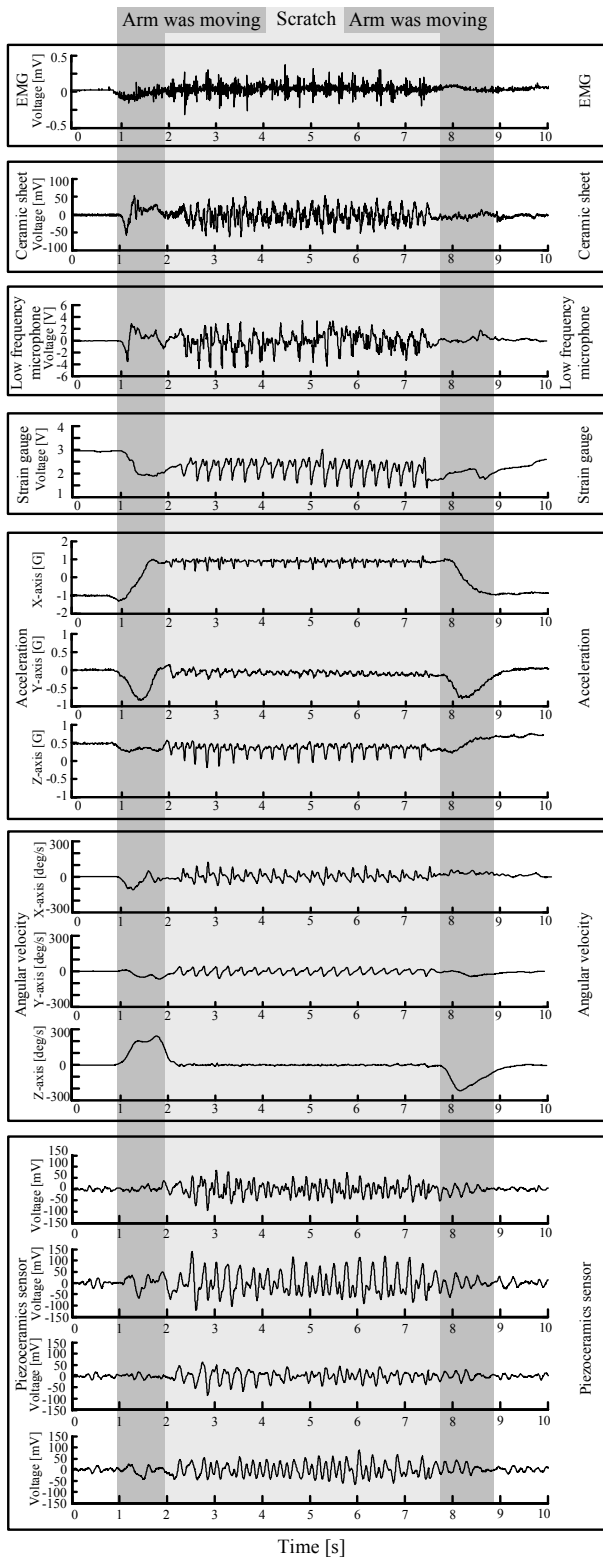
Fig. 6 Results for scratching motion

6. DISCUSSION

The sensors are set beneath the bed, so there is less awareness of their presence compared to conventional bed sensing and scratching monitoring systems [1-10].

Displacement of the person on the bed can be estimated by $P_{fh}(t)$ and $P_{rl}(t)$. This information would be valuable

for assisting a patient who, for example, is trying to get out of bed. It is also possible to estimate the sleep stages from the body movements measurable by the sensor devices [12].

In the case of skin diseases characterized by itching, this method enables contact-free measurement of scratching frequency during sleep, which is normally very difficult to ascertain. This system can measure the period of scratching motion, and calculate the total scratch time (%) automatically for objective monitoring and the acquisition of detailed information.

Our system uses four devices which are distortion sensors that do not require electric power supply; as the devices are bent, they generate a proportional voltage. In this system, the signals are converted from analog to digital directly without using an electrical preamplifier. This property makes it possible to use the system as an event trigger signal for a microprocessor. In practice, this is very effective for developing equipment.

7. CONCLUSIONS

We proposed a new bed sensing method using piezoceramic devices set under the legs of the bed, which guarantees subliminal measurement. The devices are battery-free and generate voltage corresponding to the motion of the person on the bed. The device is effective for developing bed sensing equipment with low power consumption.

Using the integrated value of the difference, $P_{rl}(t)$ and $P_{fh}(t)$, a change in position of the person on the bed was detectable. Scratching motions were also accurately detected. As a bed biosensing method, the proposed system is valid in terms of cost performance, accuracy and variety of sensing, and realization of low power equipment.

REFERENCES

[1] Standards of Practice Committee, American Academy of Sleep Medicine; T. Morgenthaler, et al., "Validity in Actigraphic Sleep Assessment", *SLEEP*, vol.30, no.4, pp.519-529, 2007

[2] B. Sivertsen, et al., "A Comparison of Actigraphy and Polysomnography in Older Adults Treated for Chronic Primary Insomnia," *SLEEP*, vol. 29, no. 10, pp.1353-1356, 2006

[3] K. Watanabe, Y. Kurihara and H. Tanaka, "Ubiquitous Health Monitoring at Home – Sensing of Human Biosignals on Flooring, on Tatami Mat, in the Bathtub, and in the Lavatory," *IEEE SENSORS JOURNAL*, vol. 9, no. 12, pp.1847-1855, December 2009

[4] K. Watanabe, T. Watanabe, H. Watanabe, H. Ando, T. Ishikawa and K. Kobayashi, "Noninvasive measurement of heartbeat, respiration, snoring and body movement of a subject in bed via a pneumatic method," *IEEE Trans. Biomed. Eng.*, vol. 52, pp. 2100-2107, 2005.

[5] K. Watanabe, Y. Kurihara, T. Nakamura and H. Tanaka, "Design of a Low-Frequency Microphone for

Mobile Phones and Its Application to Ubiquitous Medical and Healthcare Monitoring, *IEEE SENSORS JOURNAL*, vol. 10, no. 5, pp. 934-941, March 2010

[6] N. L. Johnson, et al., "Sleep Estimation Using Wrist Actigraphy in Adolescents With and Without Sleep Disordered Breathing: A Comparison of Three Data Modes," *SLEEP*, vol. 30, no. 7, pp. 899-905, 2007

[7] T. Ebata, et al., "The characteristics of nocturnal scratching in adults with atopic dermatitis", *British Journal of Dermatology* Vol. 141, pp.82-86, 1999.

[8] T. Ebata, et al., "Use of a wrist activity monitor for the measurement of nocturnal scratching in patients with atopic dermatitis", *British Journal of Dermatology* Vol. 144, pp.305-309, 2001.

[9] J. Alihanka and V. Vaahtornanta, "A static charge sensitive bed. A new method for recording body movement during sleep," *Electroencephalogr. Clin. Neurophysiol.*, vol. 46, pp. 731-734, 1979

[10] T. Watanabe and K. Watanabe, "Noncontact Method for Sleep Stage Estimation," *IEEE Trans. Biomed. Eng.*, vol. 51, no. 10, pp. 1735-1748, 2004

[11] N. Bu, N. Ueno and O. Fukuda, "Monitoring of respiration and heartbeat during sleep using a flexible piezoelectric film sensor and empirical mode decomposition," *Proc. IEEE Eng. Med. Biol. Soc.*, pp. 1362-1366, 2007

[12] M. Ishijima, "Monitoring of Electro-cardiograms in Bed without Utilizing Body Surface Electrodes," *IEEE Trans. Biomed. Eng.*, vol. 40, no. 6, pp. 593-594, 1993

[13] X. Zhu, W. Chen, T. Nemoto, Y. Kanemitsu, K. Kitamura, K. Yamakoshi and D. Wei, "Real-time monitoring of respiration rhythm and pulse rate during sleep," *IEEE Trans. Biomed. Eng.*, vol. 53, no. 12, pp. 2553-2563, 2006

[14] D. C. Mack, J. T. Patrie, P. M. Suratt, R A. Felder and M. A. Alwan, "Development and preliminary validation of heart rate and breathing rate detection using a passive, ballistocardiography-based sleep monitoring system," *IEEE Trans. Inf. Technol. Biomed.*, vol. 13, no. 1, pp. 111-120, 2009

[15] T. Ebata, H. Aizawa, R. Kamide, "An Infrared Video Camera System to Observe Nocturnal Scratching in Atopic Dermatitis Patients," *British Journal of Dermatology* Vol. 23, pp. 155-155, 1996.

[16] H. Izumi, T. Ebata, Y. Sato, H. Aizawa, R. Kamide, M. Niimura, "A Simplified Method for the Measurement of Nocturnal Scratching with an Infrared Video Camera," *The Skin* Vol. 39, pp. 560-563, 1997.

[17] K. Umeda, Y. Noro, T. Murakami, K. Tokime, H. Sugisaki, K. Yamanaka, I. Kurokawa, K. Kuno, H. Tsutsui, K. Nakanishi, H.Mizutani. "A novel acoustic ecaluation system of scratching in mouse dermatitis: Rapid and specific detection of invisibly rapid scratch in an atopic dermatitis model mouse," *Life Science* Vol. 79, pp. 2144-2150, 2006.

[18] Y. Kawabe. K. Aritake, Y. Noro, K. Umeda, H. Mizutani, "A Study of sensor for Detection of Human Scratching Behavior during Sleep," *Tokai of society related to electricity branch union rally* O-329, 2007.

[19] M. Konishi, K. Aritake, Y. Noro, K. Umeda, H. Mizutani, "A Study of sensor for Detection of Human Scratching Behavior during Sleep," *Tokai of society related to electricity branch union rally* O-322, 2008.

[20] H. Yokoi, Y. Noro, K. Umeda, H. Mizutani, "Detection of Human Scratching Behavior during Sleep with Acceleration sensor," *Tokai of society related to electricity branch union rally* O-323, 2008.

[21] R. Felix, S. Shuster, "A New method for the measurement of itch and the response to treatment," *British Journal of Dermatology* Vol. 93, pp. 303-312, 1975.

[22] J. A. Savin, W. D. Paterson, I.Oswald, "SCRATCHING DURING DLEEP," *THE LANCET* Vol. August 11, pp. 296-297, 1973.

[23] K. Endo, H, Sumitsuji, T. Fukuzumi, J. Adachi, T. Aoki, "Evaluation of Scratch Movements by a New Scrath-Monitor to Analyze Nocturnal Itching in Atopic Dermatitis," *Acta Derm Venereol (Stockh)* Vol. 77, pp. 432-435, 1997.

[24] T. Aoki, H. Kushimoto, Y. Hishikawa, J. A. Savin, "Nocturnal scratching and its relationship to the disturbed sleep of itchy subject," *Clinical and Experiment Dermatology* Vol. 16, pp. 268-272, 1991.

Unconstrained Bed Monitoring System for Scratching Motion

Toshihiro Shino
Department of System Engineering
Hosei University
Tokyo, Japan
toshihiro.shino.jg@stu.hosei.ac.jp

Yosuke Kurihara
Department of Computer and Information Science
Seikei University
Tokyo, Japan
yosuke-kurihara@st.seikei.ac.jp

Shoko Nukaya
Division of Advanced Therapeutical Sciences
Tokyo Medical and Dental University
Tokyo, Japan
nukaya@bioinfo.tmd.ac.jp

Kajiro Watanabe
Department of System Engineering
Hosei University
Tokyo, Japan
bob@hosei.ac.jp

Hiroshi Tanaka
Division of Advanced Therapeutical Sciences
Tokyo Medical and Dental University
Tokyo, Japan
tanaka@cim.tmd.ac.jp

Abstract

This paper describes a novel bed sensing method for monitoring scratching motion. This bed sensing method can be used to monitor a person's health condition at home or in the hospital. Moreover, the system can detect the frequency of scratching motion. Conventional methods that use infrared cameras or acceleration sensors can impose physical and/or psychological stress on the patient. Our proposed method applies an unconstrained biosignal bed sensing device using piezoceramics. Piezoceramic sensors are bonded to stainless steel plates sandwiched between the floor and the four feet of the bed. In carrying out the validation experiment, the total scratching time (TST) was measured using this sensing device. The results were compared with the TST obtained from conventional and more constrained scratching measurement devices, such as cameras, electromyograph (EMG) sensors, ceramic sheets, microphones, strain gauges, acceleration sensors, and gyro sensors. The experiment indicated that the sensors positioned close to the subject's head, where the scratching points are closer, were capable of determining the TST at an accuracy nearly equal to or greater than that obtained by all the conventional sensors except for the gyro sensors.

Keywords-Scratching; total scratching time; bed monitoring; unconstrained sensing; piezoceramics

1   INTRODUCTION

Itching can develop as a symptom of various skin diseases affecting patients, who scratch the itchy points to alleviate the itch. Skin inflammation, however, can become worse from the scratching [1]. Moreover, since the itch occurs irregularly, the patient unconsciously scratches while sleeping.

The gravity of skin diseases accompanied by itching is related to the frequency of the itch [2]. Therefore, measurement of the scratching is effective in diagnosing skin diseases. Since patients can control the scratching while they are awake, a more accurate evaluation would be made by monitoring the scratching motion while they are asleep.

In one of the methods for evaluating scratching motion, infrared cameras are used to capture images while the patient is sleeping, and the ratio of the total scratching time (TST [%]) to the total measurement time [1, 3] is used as an index. This method, however, is not suitable for daily monitoring, since it infringes on the patients' privacy and it also requires a large-scale system.

Given these circumstances, various smaller-scale methods have been proposed for evaluating scratching motion during sleep. For the most part, they are aimed at recording the motion or the sound of scratching, or the acceleration of wrist movement and its angular velocity. An electromyograph can be used to measure the electrical activity of the muscles in the forearm. Other devices can be used to measure the change in pressure at the back of the hand, the expansion and contraction motions of the hand, finger motions, etc. [1-11]. These methods, however, are somewhat bothersome as the sensors must be attached directly to the patient's arms.

This paper describes a novel system for unconstrained monitoring of scratching motion during sleep, by applying piezoceramic sensors.
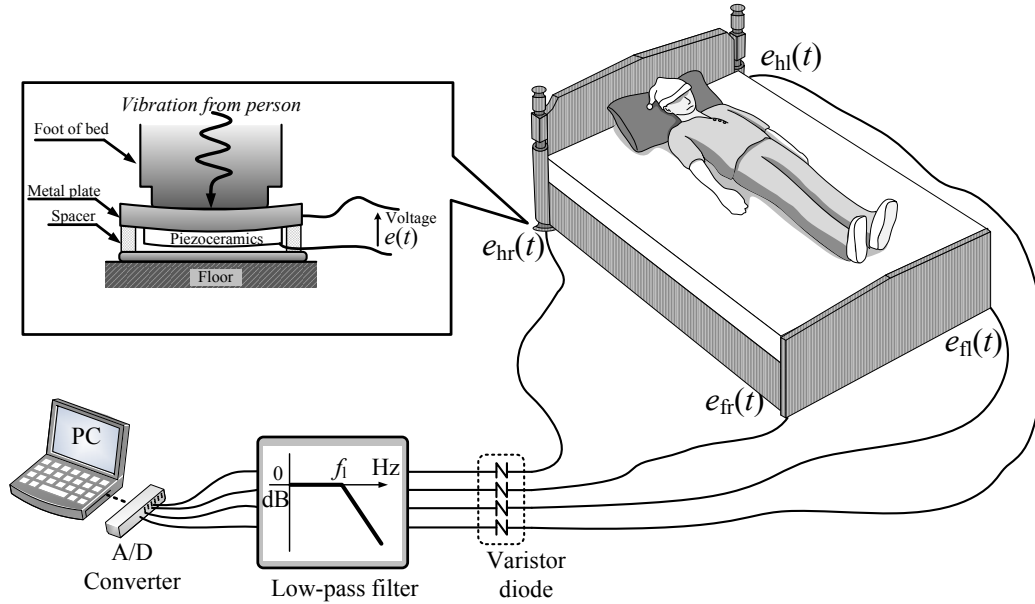
Fig. 1 Bed monitoring system

2 BED MONITORING SYSTEM

2.1 Sensing device

Figure 1 shows the proposed system in which a piezoceramic sensor is attached to the upper metal plate and spacers are inserted between the sensor and the lower metal plate. When the leg of the bed is placed on the upper plate, the weight compresses the plates.

When a person is lying on the bed, the force from the vibrations that accompany the heartbeat, respiration, and body movements is transferred through the bed cushion to the piezoceramic sensor, which then generates output voltage proportionate to the force. This output voltage, obtained as $e(t)$, is the linear sum of the heartbeat component $S_h(t)$, body movement component $S_b(t)$, and high-frequency noise $n(t)$.

$$e(t) = S_h(t) + S_b(t) + n(t) \quad (1)$$

If the person lying on the bed makes a scratching motion, it appears as $S_b(t)$ in Eq. (1). Therefore, this component must be extracted from $e(t)$. Since the amplitude of $S_h(t)$ is smaller than that of $S_b(t)$, $S_b(t)$ can be obtained by eliminating the high-frequency noise $n(t)$ through a low-pass filter of f_l [Hz].

Since the output from the piezoceramic sensor is proportionate to the magnitude of the conveyed force, measurement taken under a single leg of the bed results in a low S/N ratio when the patient scratches a point far from that particular bed leg. Therefore, in this experiment, piezoceramic sensors were placed under all four legs of the bed in order to secure a certain level of S/N ratio regardless of the point of scratching. As shown in Fig. 1, the output data from the four sensors $e_{hl}(t)$, $e_{hr}(t)$, $e_{fl}(t)$, and $e_{fr}(t)$ is transferred through varistor diodes that provide

protection against high voltage, and through a low-pass filter to eliminate the high-frequency noise. The data is then imported to a PC after A/D conversion.

2.2 Calculation of total scratching time (TST)

After obtaining the total measurement time, T_{total}, and the total scratching time, $T_{scratch}$, the ratio of TST [%] is calculated as follows:

$$TST = (T_{scratch} / T_{total}) \times 100 \ [\%] \quad (2)$$

3 VALIDITY EXPERIMENT

3.1 Experimental system and subject

Figure 2 shows the inner structure of the piezoceramic sensor used for the proposed system. The ceramics in this sensor is 20 mm in diameter and is firmly affixed to a brass metal plate, which is 25 mm in diameter. This device is typically used for a buzzer. The device is bonded to a stainless steel plate of 1 mm in thickness and 50 mm in diameter. Under the stainless steel plate is a washer with an inner radius of 15 mm, outer radius of 25 mm, and thickness of 2 mm. The bottom is covered with an aluminum plate that is the same size as the stainless steel plate.

The sensor has the following characteristics: 1´10-3 C/m, which is the displacement of electrical charge by piezoelectricity. The capacitance is 0.01 µF. Due to the capacitive characteristics of piezoceramics, the output voltage in the steady state is zero-biased and changes from zero voltage.

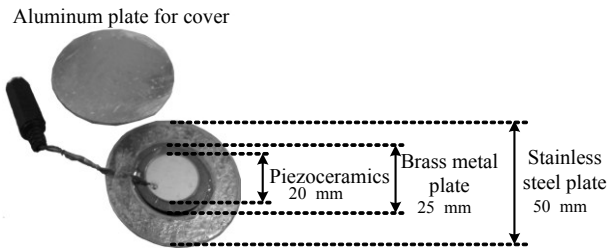Figure 3 shows the experimental system. The bed is a coil cushion type weighing 60 kg and measuring 1.0´2.1 m.

Fig. 2 Inner structure of a piezoceramics sensor

Fig. 3 Experimental system

Four piezoceramic sensors are placed under the four legs of the bed. The outputs $e_{hr}(t)$, $e_{hl}(t)$, $e_{fr}(t)$ and $e_{fl}(t)$ measured using the piezoceramic sensors go through the low-pass filter to remove the high-frequency noise component. The cutoff frequency f_l of the low-pass filter is set to 12 Hz. The output signals from the low-pass filters are A/D-converted, in which the sampling interval is set to 1 ms and the scale range to ±1 V using a data logger (NR-2000, Keyence Co. Ltd.).

In order to compare the accuracy of the proposed system with that of conventional methods, we used the sensors described below to simultaneously record the scratching motions, changes in myogenic potential, 3-axis acceleration and angular velocity of the forearm, scratching sounds, pressure changes at the back of the hand, and expansion and contraction motions of the fingers, as shown in Fig. 3 [1-11].

For recording the scratching motions, a video camera (EX-F1, Casio) was fixed on a camera stand to capture images of the right hand of the subject.

Changes in myogenic potential of the forearm were measured using an EMG sensor (RF-ECG, Medical Electronic Science Institute Co., Ltd.) of 40´35´7.2 mm in size that was affixed to the subject's forearm. The EMG data was transmitted to the PC via wireless Bluetooth at a sampling frequency of 204 Hz.

Acceleration of the forearm was measured using a 3-axis accelerometer (RF-ECG, Medical Electronic Science Institute Co., Ltd.) embedded in the EMG sensor. Each axis was set as shown in Fig. 3. The scaling range of the accelerometer is ±3 G. This accelerometer also measures gravitational acceleration.

Angular velocity of the forearm was measured using a 3-axis gyro sensor (FMS-001, Fujitsu). The gyro sensor is 40´45´13 mm in size, and the data is also transmitted via wireless Bluetooth at a sampling interval of 2 ms. The gyro sensor was fixed to the forearm with surgical tape so as to set the axes as shown Fig. 3. The gyro sensor has differential properties, so the output in the steady state is zero-biased and changes from zero degrees per second.

In order to measure the sounds from scratching, a microphone (MX4836, Primo Co. Ltd) was fixed to the back of the hand with surgical tape. The output data was transmitted through an amplifier and A/D-converted at a sampling interval of 1 ms and scale range of ±10 V using a data logger.
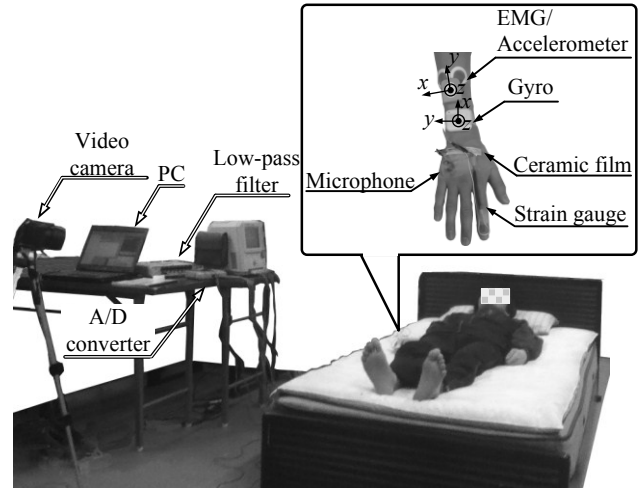
For the pressure changes on the back of the hand, a ceramic sheet (Flicker, Measurement Specialties Inc.) was used. The output data was A/D-converted at a sampling interval of 1 ms and scale range of ±1.0 V using a data logger. The output voltage in the steady state is zero-biased and changes from zero voltage, due to the differential properties.

For the expansion and contraction of the fingers, a strain gauge was used to measure the degree of finger bending. The strain gauge was fixed along the forefinger with surgical tape. The measurement circuit for the strain gauge was designed so as to make the output less than 5 V. The sampling interval was kept to 1 ms and the scale range to ±5 V using the data logger.

The subject in this experiment was male, approximately 170 cm in height and 50 kg in weight, and did not suffer from any sleep disorders. Since the subject was right-handed, the sensors were set on his right hand.

3.2 Experimental procedures

As the starting position, the subject is lying on his back at the center of the bed with his arms and legs straight, as shown in Fig. 3.

The subject scratched his right cheek 20 times, because patients with atopic dermatitis most frequently scratch the head area as a characteristic pattern [1]. He then returned his arm back to the starting position. After a 5-s pause, the subject once again scratched his cheek 20 times in a row. The set of scratching motions was repeated 35 times.

Since scratching is a reciprocating motion of the fingers, the sensor extracts the cyclically changing periods as scratching time in its data output. The total scratching time for all 35 sets is defined as $T_{scratch}$, and the ratio of TST [%] is calculated using Eq. (2). The entire procedure described above was carried out using all the sensors, and the errors among the sensors were compared using as a reference the TST data obtained from the video camera images.

4   EXPERIMENTAL RESULTS

Figure 4 shows the results from one scratching motion example. The graphs show the data from the EMG, ceramic sheet, microphone, strain gauge, acceleration (X-, Y-, and Z-axis), angular velocity (X-, Y-, and Z-axis), and the proposed sensors ($e_{hl}(t)$, $e_{hr}(t)$, $e_{fl}(t)$ and $e_{ff}(t)$). The $S_b(t)$ equals zero in Eq. (1) between 0 and 1 s in Fig. 4, since the subject's hand is stationary beside his body. The sensors $e_{hl}(t)$, $e_{hr}(t)$, $e_{fl}(t)$ and $e_{ff}(t)$, therefore detect the heartbeat component of $S_h(t)$, while the other sensors show no indication of this component. The wave shape between 1 and 2 s corresponds to the hand motion toward the face. During this period, the sensor $e_{ff}(t)$ beneath the right foot generates $S_b(t)$, and the $S_b(t)$ then appears at the sensor $e_{hr}(t)$ beneath the right side of the pillow. The wave shapes of most of the sensors fluctuate greatly during this period. The wave shape between 2 and 7.5 s corresponds to the 20 times of scratching motion, and the $S_b(t)$ at $e_{hl}(t)$, $e_{hr}(t)$, $e_{fl}(t)$ and $e_{ff}(t)$ is synchronized with the scratching motion and shows large cyclical fluctuations. During this period, $S_b(t)$ can be confirmed since it is larger than $S_h(t)$. The comparison among $e_{hl}(t)$, $e_{hr}(t)$, $e_{fl}(t)$ and $e_{ff}(t)$ shows that the outputs from $e_{hl}(t)$ and $e_{hr}(t)$, which are closer to the head, have a larger-amplitude wave shape than those from $e_{fl}(t)$ and $e_{ff}(t)$, which are closer to the feet. Moreover, the output from $e_{hr}(t)$, which is positioned beneath the right side of the head, becomes the largest among the four, since the subject scratches his right cheek. Therefore, the more distant the piezoceramics sensors are from the scratching point, the smaller their output signals are. The other sensors also show cyclical signals synchronous with the scratching motions. The wave shape between 7.5 and 9 s corresponds to the hand motion retuning to the original position. During this period, rather smooth fluctuations appear, similar to that during the period between 1 and 2 s. Between 9 and 10 s, the subject's hand once again becomes stationary beside his body, and the heartbeat component of $S_h(t)$ is also detected again. The other sensors show no indication of this component, which is the same thing that happened between 0 and 1 s. Table 1 shows the scratching times obtained from all the sensors and their respective errors with the scratching time confirmed by the video camera images. With the EMG, the wave shapes for the first arm motion and for the scratching motion look similar, making it difficult to divide the time frames. Therefore, the error resulted in +1.16 s. With the ceramic sheet, microphone, and strain gauge, the wave shapes for the first arm motion and for the scratching motion are clearly different, making it easy to divide the time frames. Therefore, errors of +0.02, +0.05, and +0.11 s were obtained, respectively. With the acceleration, the beginning of the scratching motion is not clear against the X-axis, and dividing the time frames is somewhat difficult. Its error was +0.06 s. Against the Y-axis, the boundary between the arm motion and the scratching motion was not easy to confirm, and the error was −0.22 s. Against the Z-axis, the arm motion appeared smooth, making it difficult to divide the time frame for the scratching motion. The error of the Z-axis was +0.18 s. With the angular velocity,

Fig. 4 Results for one bout scratching motion

the time of stopping the scratching motion was difficult to determine against the Y-axis, and its error was +0.48 s. Against both the X-axis and Z-axis, the arm motion and the scratching motion were clearly identifiable, thus making it easy to divide the time frames. The error was +0.42 and +0.03 s, respectively. With the ceramics sensor, it was difficult to divide the arm motion and the scratching
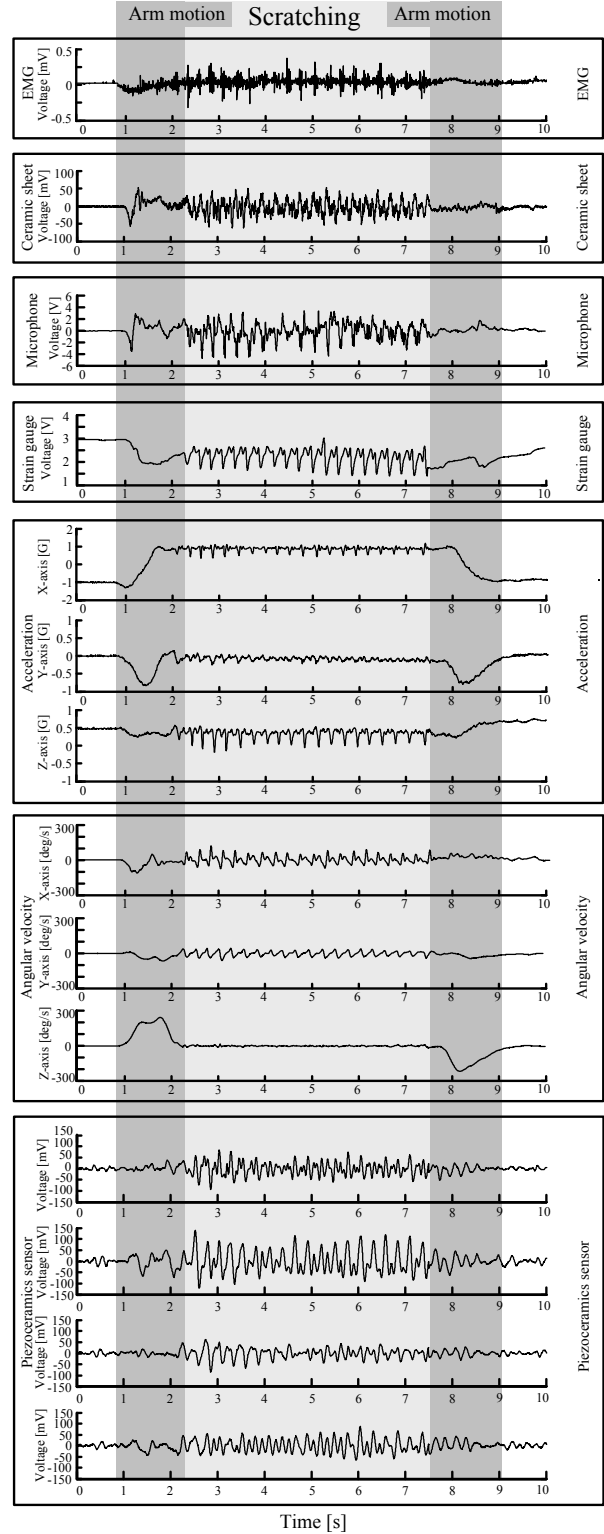
TABLE I
TIME DURING SCRATCHING AND ERROR IN FIGURE 4

Sensor		Time during scratching [s]	Error [s]
Video camera		5.22	-
EMG		6.38	1.16
Ceramic sheet		5.24	0.02
Microphone		5.27	0.05
Strain gauge		5.33	0.11
Acceleration	x	5.28	0.06
	y	5.00	-0.22
	z	5.40	0.18
Angular velocity	x	5.64	0.42
	y	5.70	0.48
	z	5.25	0.03
Piezoceramics sensor	e_{hl}	5.20	-0.02
	e_{hr}	5.37	0.15
	e_{fl}	6.22	1
	e_{fr}	6.34	1.12

TABLE II
$T_{SCRATCH}$ AND TOTAL SCRATCHING TIME AND EACH ERROR

Sensor		$T_{scratch}$ [s]	Error [s]	TST [%]	Error of TST [%]
Video camera		179	-	46.5	-
EMG		228	49	59.2	12.7
Ceramic sheet		177	-2	46.0	-0.5
Microphone		176	-3	45.7	-0.8
Strain gauge		186	7	48.3	1.8
Acceleration	x	159	-20	41.3	-5.2
	y	151	-28	39.2	-7.3
	z	162	-17	42.1	-4.4
Angular velocity	x	178	-1	46.2	-0.3
	y	178	-1	46.2	-0.3
	z	167	-12	43.4	-3.1
Piezoceramics sensor	e_{hl}	176	-3	45.7	-0.8
	e_{hr}	186	7	48.3	1.8
	e_{fl}	204	25	53.0	6.5
	e_{fr}	201	22	52.2	5.7

motion. The errors were −0.02 s with $e_{hr}(t)$, +0.15 s with $e_{hl}(t)$, +1.00 s with $e_{fr}(t)$, and +1.12 s with $e_{fl}(t)$.

The total recording time T_{total} was 385 s, and the total scratching time $T_{scratch}$ was measured with each sensor. The TST was calculated using Eq. (2).

Table 2 shows the $T_{scratch}$ and TST measured with all the sensors, and their respective errors with the $T_{scratch}$ and the TST confirmed by the video camera images. With regard to the TST errors in Table 2, the ceramic sensor e_{hl}, the closest to the scratching point on the face, showed the smallest error of −0.8%. The error with e_{fl}, near the left foot, showed the largest error of +6.5%, eight times larger than the error with e_{hl}.

In comparison with the other sensors, the smallest error was −0.3% for both the X-axis and Y-axis using the gyro sensors; and it was one-third of the error with e_{hl}. The largest error was 12.7% for the EMG, twice as large as the error for e_{fl}, which had the largest error among the ceramic sensors.

5   DISCUSSION

The reason that outputs e_{fl} and e_{fr} near the feet show the largest errors (see Table 2) is due to the small amplitude of their wave shapes during the scratching motions, which is the direct result of their distance from the scratching point. Thus, it was difficult to clearly identify the motion of the arm returning to the original position from the scratching motion. The errors with e_{hl} and e_{hr} were small because the amplitude of the wave shapes from the scratching motions were rather large, thus making it possible to clearly separate these wave shapes from those arising from the arm motions.

The gyro sensors showed the smallest errors since they directly measure the hand in the scratching motions. In contrast, the proposed unconstrained method measures the vibrations transmitted indirectly through the bed using ceramic sensors attached under the legs of the bed instead of directly applying the sensors to the hand or other body parts. This resulted in the larger errors compared with the gyro sensors.

6   CONCLUSIONS

In daily biosignal monitoring, it is important to carry out the measurements under unconstrained conditions.

In this paper, we proposed a novel sensing device using piezoceramic sensors to measure scratching motions in an unconstrained manner while the subject is sleeping. This device is composed of a piezoceramic sensor sandwiched between metal plates and placed under the legs of the bed. This device can measure microvibrations produced by the scratching motion of the subject on the bed. Furthermore, the TST, an important index for evaluating the scratching motions, could be calculated from the signals measured with the device.

In carrying out the validation experiment, the total scratching time (TST) was measured using the proposed sensing device. The results were then compared with the TST obtained from conventional and more constrained scratching measurement devices, such as cameras, electromyograph (EMG), ceramic sheets, microphones, strain gauges, acceleration sensors, and gyro sensors. As a result, the sensors positioned close to the subject's head, where the scratching points are closer, were capable of determining the TST at an accuracy nearly equal to or greater than that of all the conventional sensors except for the gyro sensor.

As future challenges, decreasing the TST errors and automatically extracting the TST remain to be solved. Another challenge is the establishment of a signal processing method to count the number of scratching motions for a more elaborate evaluation.

7   ACKNOWLEDGEMENT

8   REFERENCES

[1] T. Ebata, et al., "The characteristics of nocturnal scratching in adults with atopic dermatitis", British Journal of Dermatology Vol. 141, pp.82-86, 1999.

[2] T. Ebata, et al., "Use of a wrist activity monitor for the measurement of nocturnal scratching in patients with atopic dermatitis", British Journal of Dermatology Vol. 144, pp.305-309, 2001.

[3] H. Izumi, T. Ebata, Y. Sato, H. Aizawa, R. Kamide, M. Niimura, "A Simplified Method for the Measurement of Nocturnal Scratching with an Infrared Video Camera," The Skin Vol. 39, pp. 560-563, 1997.

[4] K. Umeda, Y. Noro, T. Murakami, K. Tokime, H. Sugisaki, K. Yamanaka, I. Kurokawa, K. Kuno, H. Tsutsui, K. Nakanishi, H.Mizutani. "A novel acoustic ecaluation system of scratching in mouse dermatitis: Rapid and specific detection of invisibly rapid scratch in an atopic dermatitis model mouse," Life Science Vol. 79, pp. 2144-2150, 2006.

[5] Y. Kawabe. K. Aritake, Y. Noro, K. Umeda, H. Mizutani, "A Study of sensor for Detection of Human Scratching Behavior during Sleep," Tokai of society related to electricity branch union rally O-329, 2007.

[6] M. Konishi, K. Aritake, Y. Noro, K. Umeda, H. Mizutani, "A Study of sensor for Detection of Human Scratching Behavior during Sleep," Tokai of society related to electricity branch union rally O-322, 2008.

[7] H. Yokoi, Y. Noro, K. Umeda, H. Mizutani, "Detection of Human Scratching Behavior during Sleep with Acceleration sensor," Tokai of society related to electricity branch union rally O-323, 2008.

[8] R. Felix, S. Shuster, "A New method for the measurement of itch and the response to treatment," British Journal of Dermatology Vol. 93, pp. 303-312, 1975.

[9] J. A. Savin, W. D. Paterson, I.Oswald, "SCRATCHING DURING DLEEP," THE LANCET Vol. August 11, pp. 296-297, 1973.

[10] K. Endo, H, Sumitsuji, T. Fukuzumi, J. Adachi, T. Aoki, "Evaluation of Scratch Movements by a New Scrath-Monitor to Analyze Nocturnal Itching in Atopic Dermatitis," Acta Derm Venereol (Stockh) Vol. 77, pp. 432-435, 1997.

[11] T. Aoki, H. Kushimoto, Y. Hishikawa, J. A. Savin, "Nocturnal scratching and its relationship to the disturbed sleep of itchy subject," Clinical and Experiment Dermatology Vol. 16, pp. 268-272, 1991.

Unconstrained Measurement System for Scratching by Limb and Estimation of Scratching Area

Toshihiro. Shino, Yosuke. Kurihara, Syoko. Nukaya, Kajiro. Watanabe, and Hiroshi. Tanaka

Abstract—This paper describes an unconstrained measurement system for scratching motion. We have proposed an unconstrained bed monitoring system by piezoceramic sensors that could detect heartbeat, respiration and body movement. The system could measure the bed vibrations due to the motion of the person on the bed. In this paper, we apply this unconstrained bed sensing method to the system for detecting scratching motion. The proposed sensors are placed under the bed feet. When the subject is lying on the bed, the output signals from the sensors are proportional to the magnitude of the vibration due to the body movement of the subject. Hence, it is possible to detect the subject's scratching motion from the output signals. Furthermore, also with output signals from the three ceramic sensors, the proposed system can detect the direction of the body movement, which enables us to estimate the scratched area.

We evaluated three scratching motions using the proposed system in the validity experiment as follows: Case 1 is the subject's scratching the right cheek with right hand; Case 2 is the subject's scratching the back after turning over, and; Case 3 is the subject's scratching the shin with another foot. As the results of the experiment, we identified the scratching signals that enable the determination when the scratching occurred. Furthermore, the difference among the amplitudes of the output signals enabled us to estimate where the subject scratched.

Keywords—body movement, itchy, piezoceramics, scratching, unconstrained bed monitoring.

I. INTRODUCTION

ITCHING can occur as a symptom of various skin diseases affecting patients, who scratch the itchy points to alleviate the itch. Skin inflammation, however, can become worse from the scratching [1]. The gravity of skin diseases accompanied by itching is related to the frequency of the itch [2]. So the more severe the disease is, the longer the scratching time by the patient. The scratching time information is compiled into an index referred to as TST%, which is the ratio of total scratching time (TST) to total recording time during sleep. The data is correlated to the degree of pruritus in skin diseases such as atopic dermatitis [3], [4]. Therefore, measurement of the scratching is effective in diagnosing skin diseases. Moreover, since the itch occurs irregularly, the patient unconsciously scratches while sleeping. Since patients can control the scratching while they are awake, a more accurate evaluation would be made by monitoring the scratching motion while they are asleep. In clinical practice, an infrared video camera is generally used to monitor the location, pattern, and frequency of scratching during sleep. Using camera, however, is not suitable for daily monitoring, since it infringes on the patients' privacy and it also requires a large-scale system.

Given these circumstances, various smaller-scale methods have been proposed for evaluating scratching motion during sleep. For the most part, they are aimed at recording the motion or the sound of scratching, or the acceleration of wrist movement and its angular velocity. An electromyograph can be used to measure the electrical activity of the muscles in the forearm. Other devices can be used to measure the change in pressure at the back of the hand, the expansion and contraction motions of the finger [1]-[12]. Furthermore, RF-ID can be used to measure limbs' monitoring in sleep diseases [13]. These methods, however, are somewhat bothersome as the sensors must be attached directly to the patient's arms or feet.

One of the effective approach for daily biosignals monitoring is measuring patients' biosignals without having to wear any sensors on their body. So, we have proposed a bed sensing method enabling the detection of the biosignals of the heartbeat, respiration, body movement and changes in position of a person on the bed [14].

This paper describes unconstrained scratching detection system based on our bed sensing method as mentioned above. Furthermore, proposed system can estimate where subject scratch during sleep.

II. BED SENSING SYSTEM TO DETECT SCRATCHING MOTION AND ESTIMATE SCRATCHING POSITION

Figure 1 shows the principle of our proposed system to measure scratching motion in which a piezoceramic sensor is attached to the upper metal plate and spacers are inserted

Toshihiro. Shino is with the Graduate School of Hosei University, 3-7-2 Kajinocho Koganei-shi, Tokyo 184-8584, Japan.

Yosuke. Kurihara, is with the Dept. of Computer and Information Science, Faculty of Science and Technology, Seikei University, Musashino-shi, Tokyo 180-8633 JAPAN. (e-mail: yosuke-kurihara@st.seikei.ac.jp).

Shoko. Nukaya is with the Division of Advanced Therapeutical Sciences Tokyo Medical and Dental University, 1-5-45 Yushima, Bunkyo-city, Tokyo 113-8510, Japan (e-mail: nukaya@bioinfo.tmd.ac.jp).

Kajiro. Watanabe is with the System Control Engineering Department, Faculty of Engineering, Hosei University, 3-7-2 Kajinocho Koganei-shi, Tokyo 184-8584, Japan.

H. Tanaka is with the University Center for Information Medicine Tokyo Medical and Dental University, 1-5-45 Yushima, Bunkyo-city, Tokyo 113-8510, Japan.

between the sensor and the lower metal plate. When the leg of the bed is placed on the upper plate, the weight compresses the plates.

When a person is lying on the bed, the force from the vibrations that accompany the person's body movements and scratching is transferred through the bed cushion to the piezoceramic sensor, which then generates output voltage proportionate to the force. Furthermore, as shown in Fig.1, three piezoceramic sensors are placed under the bed feet to estimate where the person scratches. By comparing with the amplitude of the output signals from each ceramic sensor, we can estimate the scratching position.

The output data from the three ceramic sensors $e_{hl}(t)$, $e_{hr}(t)$ and $e_{fl}(t)$ are transferred through varistor diodes that protect against high voltage, and through a low-pass filter to eliminate the high-frequency noise. The data is then imported to a PC after A/D conversion.

We assume that the center of gravity of bed and subject moves with the subject's movements. It affects the force which each leg push the floor. We think the forces have symmetrical characteristics. For example, when the person on the bed turns over to the right, it increases in right side, and it decreases in left side. And the outputs are in proportion to the force. So, in order to detect the displacement of the center of gravity, we integrated the difference of measured signals as follows:

$$P_u(t) = \int_o^t \{e_a(\tau) - e_{hl}(\tau)\}d\tau \tag{1}$$

$$P_d(t) = \int_o^t \{e_{hr}(\tau) - e_{hl}(\tau)\}d\tau$$
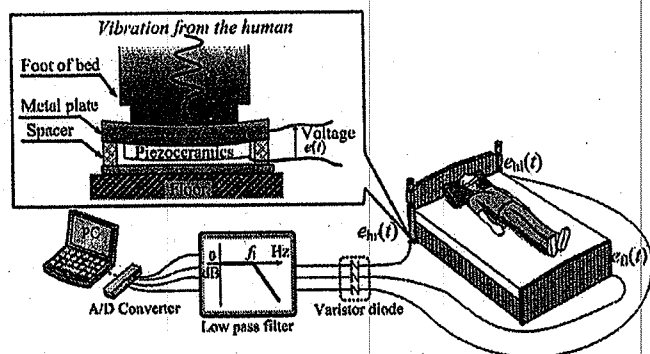

Fig. 1 Principle of proposed system

III. VALIDITY EXPERIMENT

A. Experimental System

Figure 2 shows the experimental system and inner structure of piezoceramic sensor used for the proposed system. The ceramics in this sensor is 20 mm in diameter and is firmly affixed to a brass metal plate, which is 25 mm in diameter. This device is typically used for a buzzer. The device is bonded to a stainless steel plate of 1 mm in thickness and 50 mm in diameter. Under the stainless steel plate is a washer with an inner radius of 15 mm, outer radius of 25 mm, and thickness of

2 mm. The bottom is covered with an aluminum plate that is the same size as the stainless steel plate.

The sensor has the following characteristics: 1×10^{-3} C/m, which is the displacement of electrical charge by piezoelectricity. The capacitance is 0.01 µF. Due to the capacitive characteristics of piezoceramics, the output voltage in the steady state is zero-biased and changes from zero voltage. The bed used in Fig. 3 is a coil cushion type weighing 60 kg and measuring 1.0×2.1 m. Three piezoceramic sensors are placed under the three legs of the bed. The outputs $e_{hr}(t)$, $e_{hl}(t)$ and $e_{fr}(t)$ measured using the piezoceramic sensors go through the low-pass filter to remove the high-frequency noise component. The cutoff frequency fl of the low-pass filter is set to 12 Hz.
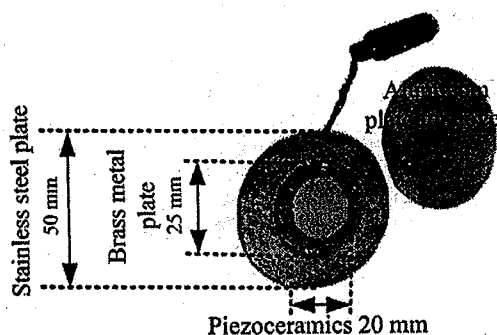
Fig. 2 Inner structure of a piezoceramics sensor
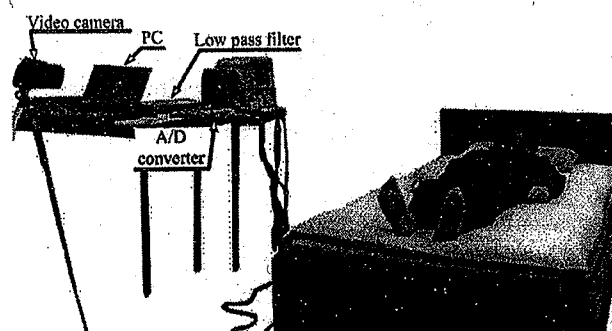
Fig. 3 Experimental system

The output signals from the low-pass filters are A/D-converted, in which the sampling interval is set to 1 ms and the scale range to ±1 V using a data logger (NR-2000, Keyence Co. Ltd.). The subject in this experiment was male, approximately 170 cm in height and 50 kg in weight, and did not suffer from any sleep disorders.

B. Experimental procedures

As the starting position, the subject is lying on back at the center of the bed with the arms and legs straight, as shown in Fig.3. The subject scratches three cases as follows.

(Case 1) The subject scratches his cheek 20 times. He then returns the arm back to the starting position. After a 5 sec pause, the subject once again scratches his cheek 20 times in a

72

row. The set of scratching motions is repeated 35 times.

(Case 2) The subject turns over and scratches his back 20 times by right hand. He then turns over again back to the starting position. After a 5 sec. pause, the subject once again acts same motion in a row. The set of scratching motions is repeated 35 times.

(Case 3) The subject scratches his left shin 10 times by his right foot. He then returns his right foot back to the starting position. After a 5 sec. pause, the subject once again scratches his left shin 10 times in a row. The set of scratching motions is repeated 5 times. Similarly, subject scratches his right shin 10 times by left foot. And subject repeated the scratching motion 5 times.

Since scratching is a reciprocating motion of the fingers, the sensor extracts the cyclically changing periods as scratching time in its data output.

IV. EXPERIMENTAL RESULTS

A. (Case 1) Results of scratching right cheek

Figure 4 shows the results of one period of scratching of right cheek. From top to bottom in the Fig.4 (a) shows $e_{hl}(t)$, $e_{hr}(t)$, $e_{fl}(t)$ and in Fig.4 (b) shows $P_{fh}(t)$ and $P_{rl}(t)$.

The subject scratched between about 4 s and 7.5 s. At the beginning and end, from about 3 to 4 s and 7.5 to 9 s, the subject's right arm was moving, which generated a large change in the output from all sources. When the subject was resting quietly, the output hardly changed. All sensors show a cyclic change following the scratching motion.

Between 0 and 3 s in Fig. 4(a), since the subject's hand is stationary beside his body, The sensors $e_{hl}(t)$, $e_{hr}(t)$ and $e_{fl}(t)$, therefore detect the heartbeat component. The wave shape between 3 and 4 s corresponds to the hand motion toward the face. The wave shape between 4 and 7.5 s corresponds to the 20 times of scratching motion, and $e_{hl}(t)$, $e_{hr}(t)$ and $e_{fl}(t)$ is synchronized with the scratching motion and shows large cyclical fluctuations. The comparison among $e_{hl}(t)$, $e_{hr}(t)$ and $e_{fl}(t)$ shows that the outputs from $e_{hl}(t)$ and $e_{hr}(t)$, which are closer to the head, have a larger-amplitude wave shape than those from $e_{fl}(t)$, which are closer to the feet. Moreover, the output from $e_{hr}(t)$, which is positioned beneath the right side of the head, becomes the largest among the three, since the subject scratches his right cheek. Therefore, the more distant the piezoceramics sensors are from the scratching point, the smaller their output signals are. The wave shape between 7.5 and 9 s corresponds to the hand motion retuning to the original position. During this period, rather smooth fluctuations appear, similar to that during the period between 3 and 4 s. Between 9 and 12 s, the subject's hand once again becomes stationary beside his body, and the heartbeat component is also detected again.

The length of the scratching period can be confirmed as the output signal changes with the scratching motion. When the subject's hand is stationary, both $P_{fh}(t)$ and $P_{rl}(t)$ fluctuated slightly centering around 0. Both $P_{fh}(t)$ and $P_{rl}(t)$ largely changed due to the arm motion, and slightly fluctuated in the

minus area during the scratching motions. The $P_{fh}(t)$ change toward the minus means the subject's center of gravity shifted toward the pillow, and the $P_{rl}(t)$ change toward the minus means the center of gravity shifted toward left: These gravity changes correspond to the motion of the subject's arm.
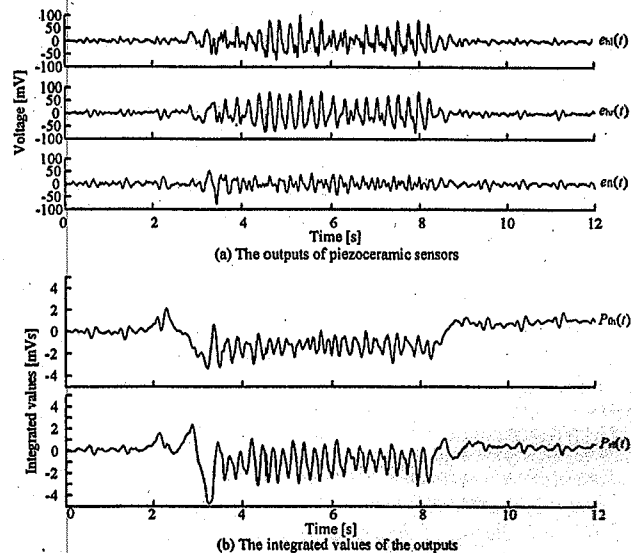

(a) The outputs of piezoceramic sensors

(b) The integrated values of the outputs

Fig. 4 Results of the scratching motion of right cheek by right hand

B. (Case 2) Results of scratching subject's back after turning over

Figure 5 shows the results of one period of scratching of the back. From top to bottom in the Fig.5 (a) shows $e_{hl}(t)$, $e_{hr}(t)$, $e_{fl}(t)$ and in Fig.5 (b) shows $P_{fh}(t)$ and $P_{rl}(t)$.

The subject, lying on the center of the bed, turned over toward the left side of the bed, scratched the back, and returned to the lying position on the back.

The output signals during the scratching fluctuated in synchronization with the hand motion, as with the scratching on the face. But unlike the scratching on the face, large fluctuations were shown before and after the scratching motion, due to the turning-over motion. Before the scratching, the sensors on the left side of the bed, $e_{hl}(t)$ and $e_{fl}(t)$, showed positive output signals due to the subject's turning over toward the left; and the sensor on the right side of the, $e_{hr}(t)$, showed negative output signals. After the scratching, the subject turned over toward the right and returned to lying position on the back. The output signals from the sensors became opposite from those before the scratching: sensors on the left negative, and the sensor on the right positive.

$P_{rl}(t)$ largely decreased due to the turning over toward the left, and increased as the subject returns to the original position. As the arm movement during the scratching was small, there was little change in the center of gravity of the bed. The change in $P_{fh}(t)$, though small, corresponded with each motion.
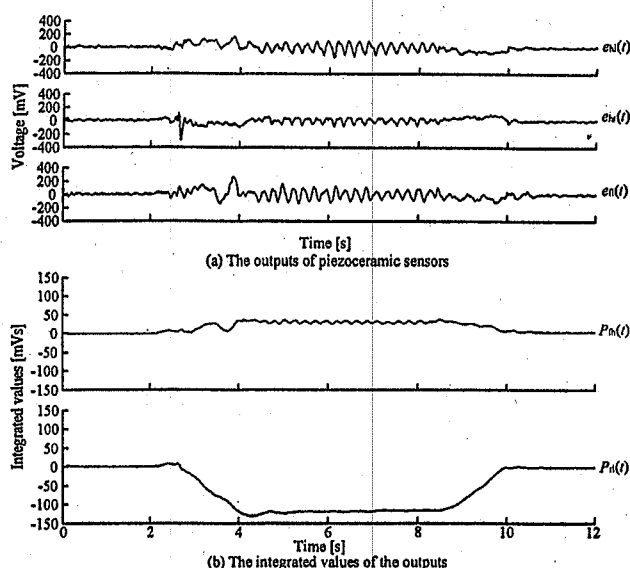
(a) The outputs of piezoceramic sensors

(b) The integrated values of the outputs

Fig. 5 Results of the scratching motion of the subject's back by right hand after turning over

C. (Case 3) Result of the scratching left side shin by right foot

Figure 6 shows the results of one period of scratching of the left side shin by right foot. From top to bottom in the Fig.6 (a) shows $e_{hl}(t)$, $e_{hr}(t)$, $e_{fl}(t)$ and in Fig.6 (b) shows $P_{fh}(t)$ and $P_{rl}(t)$.

As with the scratching motion above, cyclical output signals corresponding to the feet movements can be confirmed. When the feet move, the outputs from the sensors near the feet become larger than those from the ones near the pillow. The integral results showed the amplitude of $P_{fh}(t)$ was larger than that of $P_{rl}(t)$. Since the scratching motion of the foot is in the head-foot direction, the output of $P_{fh}(t)$ largely changed corresponding with the motion. As there was little movement toward right or left, there was little change in $P_{rl}(t)$ due to the transfer of the center of gravity, either.
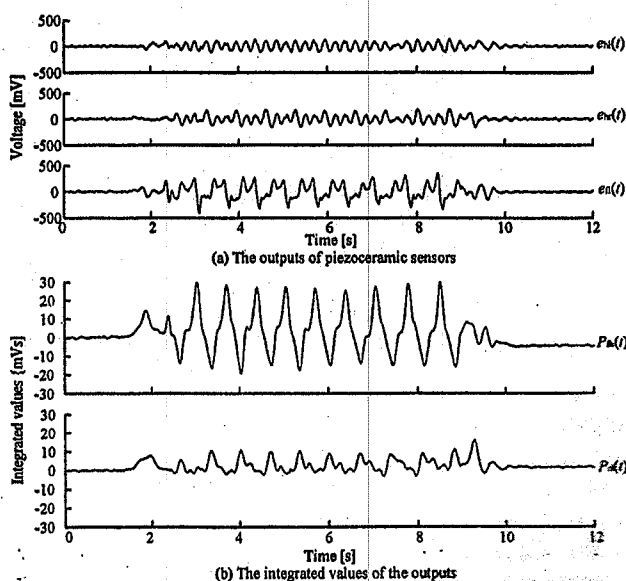

(a) The outputs of piezoceramic sensors

(b) The integrated values of the outputs

Fig. 6 Results of the scratch motion of the left shin by right foot

V. DISCUSSION

The measurement results from the scratching motions all showed cyclical signals with relatively large amplitude, which enables the measurement of the length of the scratching motions. The length of the scratching motion is correlated with the gravity of the skin disorders, and its index, TST%, can be obtained as shown below.

Let the total measurement time and the total scratching time be T_m and T_s respectively. The TST% is calculated as follows:

$$TST\% = \frac{T_s}{T_m} \times 100$$

This enables the unconstrained measurement and evaluation of the scratching motions while the patients are asleep.

The sensors are set beneath the bed, so there is less awareness of their presence compared to conventional bed sensing and scratching monitoring systems [1]-[12].

In the case of skin diseases characterized by itching, this method enables contact-free measurement of scratching frequency during sleep, which is normally very difficult to ascertain. This system can measure the period of scratching motion, and calculate the TST% for monitoring and the acquisition of detailed information.

The $P_{fh}(t)$ and $P_{rl}(t)$ in the equation (1) enables the acquisition of the data on the transfer of patient's center of gravity on the bed due to the body movements. The data can be applied to the estimation of the scratched area from the body movement before the scratching.

The positive and negative output of $P_{fh}(t)$ correspond to the head-foot direction and the foot-head direction of the transfer of the center of gravity: The positive and negative output of $P_{rl}(t)$ correspond to the left-right direction and the right-left direction of the transfer of the center of gravity. If the $P_{fh}(t)$ is larger than the $P_{rl}(t)$, the scratching is with a foot; and if not, it is with a hand.

The amplitude of $P_{fh}(t)$ while the foot is in a scratching motion is larger than that of $P_{rl}(t)$, because the output signals from the sensors near the feet are larger than the output signals from those near the pillow. Further enhancing the difference in the amplitude are the facts that: 1) there is little transfer of the center of gravity to the right or the left, and; 2) in the equation (1), $P_{rl}(t)$ only uses the output signals only from the sensors near the pillow for the calculation, while $P_{fh}(t)$ applies the output signals from those near the feet.

As the experiment in Case 3 shows, the proposed system not only enables the measurement of the itching through the scratching motions, but can be applied to observe abnormal motions of the limbs such as those accompanying the restless legs syndrome, which can cause insomnia. The proposed system has great advantage in its capability to carry out such measurements without directly touching the sleeping subject.

VI. CONCLUSIONS

In this paper, we proposed a novel sensing device using

piezoceramic sensors to measure scratching motions in an unconstrained manner while the subject is sleeping. This device is composed of a piezoceramic sensor sandwiched between metal plates and placed under the legs of the bed. This device can measure micro-vibrations produced by the scratching motion of the subject on the bed. The TST%, an important index for evaluating the scratching motions, could be calculated from the signals measured with the ceramic sensor devices. Furthermore, using the integrated value of the difference of output signals from three ceramic sensor devices, a change in position of the person on the bed could be detected.

VII. ACKNOWLEDGEMENT

REFERENCES

[1] T. Ebata, et al., "The characteristics of nocturnal scratching in adults with atopic dermatitis", British Journal of Dermatology Vol. 141, pp.82-86, 1999.

[2] T. Ebata, et al., "Use of a wrist activity monitor for the measurement of nocturnal scratching in patients with atopic dermatitis", British Journal of Dermatology Vol. 144, pp.305-309, 2001.

[3] T. Ebata, H. Aizawa, R. Kamide, "An Infrared Video Camera System to Observe Nocturnal Scratching in Atopic Dermatitis Patients," British Journal of Dermatology Vol. 23, pp. 155-155, 1996.

[4] H. Izumi, et al., "A Simplified Method for the Measurement of Nocturnal Scratching with an Infrared Video Camera," The Skin Vol. 39, pp. 560-563, 1997.

[5] K. Umeda, et al., "A novel acoustic ecaluation system of scratching in mouse dermatitis: Rapid and specific detection of invisibly rapid scratch in an atopic dermatitis model mouse," Life Science Vol. 79, pp. 2144-2150, 2006.

[6] Y. Kawabe. K. Aritake, Y. Noro, K. Umeda, H. Mizutani, "A Study of sensor for Detection of Human Scratching Behavior during Sleep," Tokai of society related to electricity branch union rally O-329, 2007.

[7] M. Konishi, K. Aritake, Y. Noro, K. Umeda, H. Mizutani, "A Study of sensor for Detection of Human Scratching Behavior during Sleep," Tokai of society related to electricity branch union rally O-322, 2008.

[8] H. Yokoi, Y. Noro, K. Umeda, H. Mizutani, "Detection of Human Scratching Behavior during Sleep with Acceleration sensor," Tokai of society related to electricity branch union rally O-323, 2008.

[9] R. Felix, S. Shuster, "A New method for the measurement of itch and the response to treatment," British Journal of Dermatology Vol. 93, pp. 303-312, 1975.

[10] J. A. Savin, W. D. Paterson, I.Oswald, "SCRATCHING DURING DLEEP," THE LANCET Vol. August 11, pp. 296-297, 1973.

[11] K. Endo, H. Sumitsuji, T. Fukuzumi, J. Adachi, T. Aoki, "Evaluation of Scratch Movements by a New Scrath-Monitor to Analyze Nocturnal Itching in Atopic Dermatitis," Acta Derm Venereol (Stockh) Vol. 77, pp. 432-435, 1997.

[12] T. Aoki, H. Kushimoto, Y. Hishikawa, J. A. Savin, "Nocturnal scratching and its relationship to the disturbed sleep of itchy subject," Clinical and Experiment Dermatology Vol. 16, pp. 268-272, 1991.

[13] C. Occhiuzzi and G. Marrocco, "The RFID Technology for Neurosciences: Feasibility of Limbs' Monitoring in Sleep Diseases," Information Technology in Biomedicine Vol. 14, No. 1, pp. 37-43, 2010.

[14] S. Nukaya, T. Shino, Y. Kurihara, K. Watanabe, H. Tanaka, "Noninvasive Bed Sensing of Human Biosignals via Piezoceramic Devices Sandwiched Between the Floor and Bed," Sensors Journal Early Access (http://ieeexplore.ieee.org/xpl/tocresult.jsp?isnumber=4427201).

Toshihiro Shino received the B.E. degrees in system control engineering from Hosei University, Tokyo, Japan, in 2010. Now he belongs to graduated school Hosei. His current interest is biomeasurment.

Yosuke Kurihara received M.E. and Ph.D. degrees from Hosei University, Tokyo, in 2003 and 2009, respectively. From 2009 to present, he served as Assistant Professor at the Seikei University. His research interests include sensor method, bio-sensing, system information. He is a member of Japanese Society for Medical and Biological Engineering, etc.

Shoko Nukaya received B.E. degree from Waseda University, Tokyo, in 1992. She joined Sony Corporation. For 12 years, as a software engineer, She had been developing consumer mobile products. In 2005, she recieved M.S. degree from Eastern Michigan University, MI, US. After graduation, she joind Nokia Corportation. Since 2010, she has started the research at Tokyo Medical and Dental University Graduate School as a PhD student. Her major interests are healthcare innovation by utilizing IT.

Kajiro Watanabe received the M.E. and Ph.D. degrees from the Tokyo Institute of Technology, in 1968 and 1971, respectively. From 1969 to 1971, he served as a Research Assistant at Faculty of Engineering Hosei University. From 1971, he served the Lecture; from 1974 to 1984, as an Assistant Professor; and from 1985 to present, as the Professor. From 1980 to 1981, he served as the Visiting Associate Professor at Oakland University, Rochester, MI, and from 1981 to 1982 as the Research Associate at the University of Texas, Austin. In the industrial filed, he acts as an authorized C.E. He is Chief Researcher of the several projects conducted by the Ministry of Economy, Trade, and Industry Japan. His major interest is the control and instrument and he is currently interested in bio-measurement, sports measurement, robotics, fault diagnosis, vehicle, environmental monitoring, and intelligent control. He holds 75 patents, has 15 publications in the control engineering field and more than 332 referenced journals and conference proceedings. Dr. Watanabe is a member of the Society of Instrument and Control Engineers.

Hiroshi Tanaka received D.M. and Ph.D. degrees from the University of Tokyo, in 1981 and 1983, respectively. From 1982, he served as a lecture at University of Tokyo; from 1987, as an Assistant Professor at Hamamatsu University School of Medicine; from 1991 to present, as a Professor at Department of Medical informatics Tokyo Medical and Dental University. From 1995, he is a Director General at University Center for Information Medicine Tokyo Medical and Dental University. From 2006, he is a Director of Biomedical Science PhD Program, the Chief Manager and President of the JAMI, and Chairperson of the JHITI.

Signal Processing Method for Extracting Scratching Time

T. Shino, Y. Kurihara*, S. Nukaya, K. Watanabe, Member, IEEE, and H. Tanaka

Abstract—**This paper describes a novel signal processing method for extracting scratching time. Scratching motion is often monitored in various ways to evaluate an itching which appears as a symptom of various diseases. It is known that the altitude of skin diseases accompanied by itching is related to the length of the scratching time. Various studies have been developed to measure the scratching motion. And we have proposed the bed sensing system which is able to monitor heartbeat, respiration and body movement involved scratching motion while a patient is sleeping on the bed. In this paper, our proposed processing method, capable of extracting the scratching time, is applied to many kinds of measurement devices.**

Index Terms—**auto extraction, total scratching time, noninvasive bed monitoring, piezo-ceramics.**

I. INTRODUCTION

ITCHING can develop as a symptom of various diseases affecting patients, who scratch the itchy points to alleviate the itch [1]. However skin inflammation can become worse from the scratching [2]. In the case of skin diseases accompanied by itching, an evaluation of the itching is important; this aims at diagnosing the gravity of skin diseases and monitoring curative effect. There are various measurement sensors which are developed for this purpose [2]-[3]. In general, monitoring the scratching motions is used to evaluate the degree of the itching. The scratching monitoring is based on the theorem that the gravity of skin diseases accompanied by itching is related to the length of the scratching time, and is effective in diagnosing skin diseases [4]-[5]. Because patients can control the scratching while they are awake, a more accurate evaluation would be made by monitoring the scratching motion while they are asleep. Recently, various measurement sensors have been proposed as objective and quantitative systems. For example, they are aimed at recording the scratching motions, or the acceleration of wrist movement and its angular velocity. A strain gauge can be used

to measure the expansion and contraction motions of fingers. An electromyograph can be used to measure the electrical activity of the muscles in the forearm. Other devices can be used to measure the change in the pressure on the back of the hand or the sound of the scratching [1]-[14]. We have proposed a noninvasive bed sensing device, using sets of piezo-ceramics under the bed feet, which is able to detect the heartbeats, respirations, body movement on the bed, and other biosignals [15]. The method for determining the scratching time, however, is bothersome, as the scorer has to look at the output wave shapes. This paper describes a novel signal processing method for extracting scratching time. We applied the proposed extracting process to the signals obtained from the scratching sensors: piezo-ceramics sensors, a strain gauge, an accelerometer, and a gyro sensor.

II. SCRATCHING MOTION AND PROBLEMS

A. Characteristics of scratching motion and bed vibrations

Fig. 1(a) shows the vibrations occurred on the bed and Fig. 1(b) shows scratching motions and their corresponding vibrations. When a subject is staying calmly, the hand of the subject is not moving, but the bed is vibrated by cyclical micro-vibration $s_h(t)$ produced by the heartbeat of the subject on the bed. When the subject feels itchy, s/he moves the arm forward to scratch the itching point. Then this arm motion causes vibration $s_b(t)$ whose cycle is long. The scratching motion oscillates the bed cyclically, and the vibration is larger than heartbeat. Since scratching is a reciprocating motion of the fingers, the sensor extracts the cyclically changing periods as scratching time in its data output. We call this vibration to be caused by scratch $s_s(t)$. The bed also vibrates due to the forces on the bed: natural vibration $s_v(t)$. When the scratching stops and the arm goes back, $s_b(t)$ occurs again. Since the natural vibration $s_v(t)$ could not stop immediately, two vibrations, $s_b(t)$ and $s_v(t)$, overlap. After these vibrations stop and the stable condition comes again, the bed is vibrated only by the micro-vibration $s_h(t)$ of heartbeat. In practice, though heartbeat vibration $s_h(t)$ never stops and does oscillate the bed, it is much smaller than the other vibrations. So, other than under the stable condition, the heartbeat vibration $s_h(t)$ could be disregarded. As described above, the subject's hand motion and the bed vibrations during the scratching motion are characterized by the frequency and amplitude. Especially during the scratching, the signals are cyclical and larger in amplitude than the heartbeat signal. These characteristics indicate that if the scratching period T_s [s] could be detected out of the vibration $s_s(t)$, we are capable of determining the TST%, an index for evaluating the

T. Shino is with the Graduate School of Hosei University, 3-7-2 Kajinocho Koganei-shi, Tokyo 184-8584, Japan.

*Y. Kurihara is with the Dept. of Computer and Information Science, Faculty of Science and Technology, Seikei University, 3-3-1 Kichijoji-kitamachi, Musashino-shi, Tokyo 180-8633, Japan (e-mail: yosuke-kurihara@st.seikei.ac.jp).

S. Nukaya is with the Division of Advanced Therapeutical Sciences Tokyo Medical and Dental University, 1-5-45 Yushima, Bunkyo-city, Tokyo 113-8510, Japan (e-mail: nukaya@bioinfo.tmd.ac.jp).

K. Watanabe is with the System Control Engineering Department, Faculty of Engineering, Hosei University, 3-7-2 Kajinocho Koganei-shi, Tokyo 184-8584, Japan.

H. Tanaka is with the University Center for Information Medicine Tokyo Medical and Dental University, 1-5-45 Yushima, Bunkyo-city, Tokyo 113-8510, Japan.
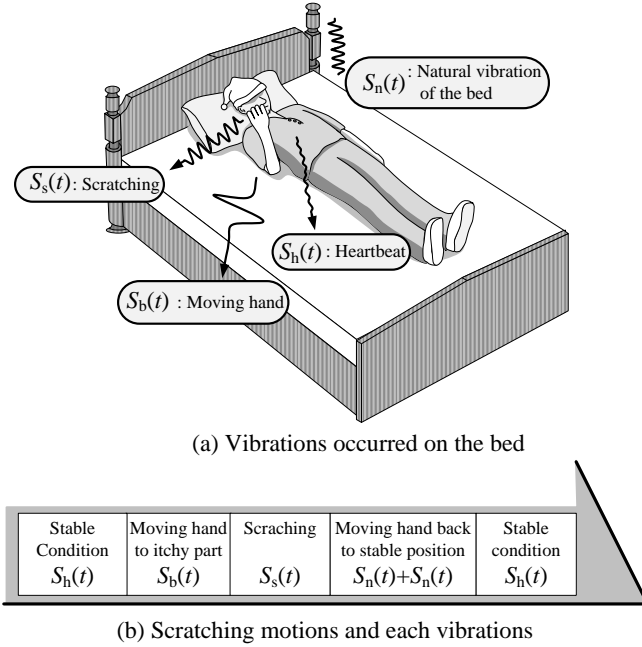
(a) Vibrations occurred on the bed

Stable Condition $S_h(t)$	Moving hand to itchy part $S_b(t)$	Scraching $S_s(t)$	Moving hand back to stable position $S_n(t)+S_n(t)$	Stable condition $S_h(t)$

(b) Scratching motions and each vibrations

Fig. 1 Bed vibrations from scratching motion on bed

Fig. 2 sensing system

itching. After obtaining the total scratching time T_s, we define the total measurement time T_m [s] and the number of scratching periods N, and the index of TST% is calculated as in eq. (1):

$$TST\% = \frac{\sum_{i=1}^{N} T_{si}}{T_m} \times 100 \qquad (1)$$

B. Sensing Devices

Fig. 2 shows the conventional sensing devices, described as following:

Strain gauge measures degree of finger bending. It is fixed along the index finger. The register value of this gauge changes depending on the degree of finger bending. The measurement of this register value makes it possible to monitor the scratching motion. The register value of the gauge does not change unless the finger bends. This device measures the signals $s_s(k)$, $s_b(k)$ and $s_n(k)$ above.

An accelerometer and an angular velocity sensor are fixed onto the forearm. These measure the acceleration and angular velocity of the forearm respectively. The output of the accelerometer includes the gravitational acceleration. These devices measure the signals $s_s(k)$, $s_b(k)$, and $s_n(k)$ above.

Piezo-ceramics sensors are set under the legs of the bed and measure all the vibrations of the bed. This sensor is with a wide dynamic range and high sensitivity enabling the detection of micro-vibrations from the heartbeat by the change in acting force when a person is lying on the bed, and of vibration from body movement without saturation. This device measures the signals $s_s(k)$, $s_b(k)$, $s_h(k)$, $s_v(k)$, and $s_n(k)$ above.
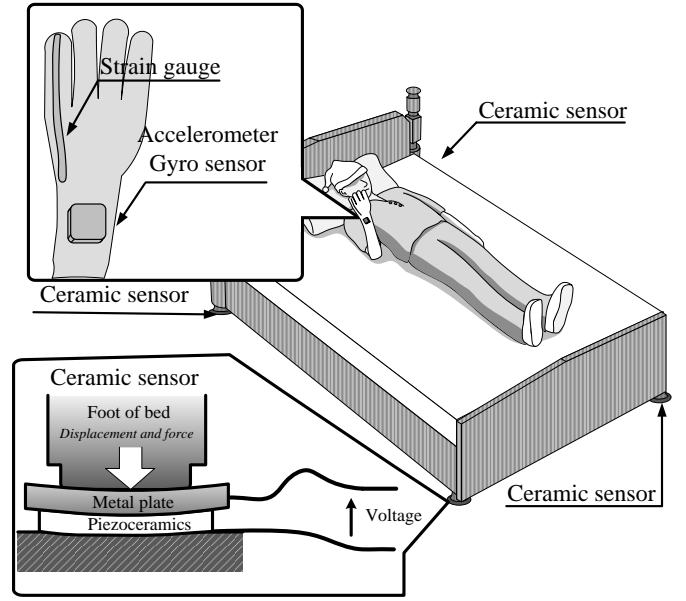
C. Signal processing

The analogue outputs from these sensors are measured and converted into a digital signal named $S(k)$ at a sampling time of dt. The variable k is defined as the digital time. If the output voltage $S(k)$ is the linear sum of the each signal and high-frequency noise $s_n(k)$ as shown in Eq. (2).

$$S(k) = s_s(k) + s_b(k) + s_h(k) + s_v(k) + s_n(k) \qquad (2)$$

Fig. 3 shows the relation between the amplitude and the frequency contained in the vibrations $s_s(k)$, $s_b(k)$, $s_h(k)$, $s_v(k)$, and $s_n(k)$ respectively. According to the characteristics described above, in order to extract the scratching period T_s, we exerted the following steps. However, other sensors than the piezo-ceramics sensor could not measure the heartbeat vibration $s_h(k)$ or the natural vibration $s_v(k)$, so $s_h(k) = 0$ and there is no need to follow the step 1 for these sensors.

(Step 1)

In order to attenuate the natural vibration $s_v(k)$, moving average $M(k)$ is calculated from Eq.(3). The value of q is degree.

$$M(k) = \frac{1}{2q+1} \sum_{i=k-q}^{k+q} S_{(i)} \qquad (3)$$

(Step 2)

The data for a certain period T are Discrete Fourier transformed from time domain to frequency domain. The frequency with the maximum spectrum during the period separates the transformed data into the lower-frequency periods and the other periods. The signal in the lower-frequency periods is $s_b(k)$ caused by arm motion and other body movements other than the scratching motion. The other periods contain the signals $s_s(k)$, $s_h(k)$ and $s_n(k)$. This process continues until the end
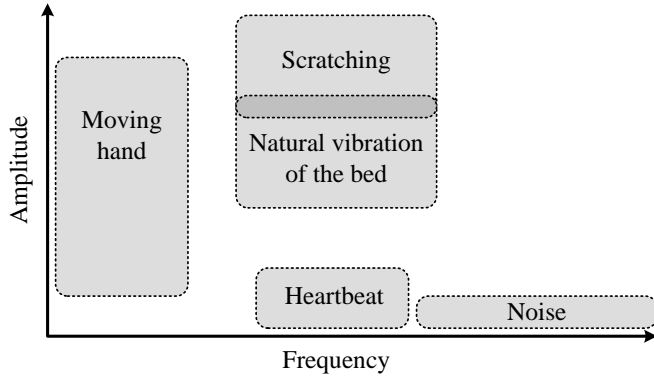
Fig. 3 Amplitude vs. frequency of each signal

of data, with the beginning of each T delayed by an interval L from the previous T.

(Step 3)

The other periods which are interpreted as in Step 2 are divided into $s_s(k)$, $s_h(k)$ and $s_n(k)$ using each amplitude. If the signals for a certain period have larger amplitude than the average amplitude value of past $s_b(k)$, these periods are $s_s(k)$, which is scratching period. Otherwise, the signals are $s_h(k)$ or $s_n(k)$.

Through these three steps, the scratching time which mainly contains the scratching signal $s_s(k)$ can be extracted.

III. VALIDATION EXPERIMENTS

A. Experimental System

Fig. 4 shows the experimental system. Strain gauge, accelerometer and gyro sensor are attached to the subject's right hand, and piezo-ceramics sensors are set beneath the four each bed foot as shown in Fig. 4. It is known that the more distant the piezo-ceramics sensors are from the scratching point, the smaller their output signals are [16]. The subject in this experiment was male, approximately 170 cm in height and 50 kg in weight, and did not suffer from any sleep disorders. We explained to the subject in sufficient detail to give consent to the experiment.

B. Experimental Procedures

We set the sampling interval dt of each sensor as following: the piezo-ceramics and the strain gauge to 1 ms, the gyro sensor to 2 ms, and the accelerometer sampling frequency to 204 Hz. In this experiment, we asked the subject to scratch the cheek, because patients with atopic dermatitis most frequently scratch the head area as a characteristic pattern [4]. The procedure of scratching is following:

As the starting position, the subject is lying on his back at the center of the bed with his arms and legs straight, as shown in Fig. 4. The subject scratched his right cheek 20 times using his right four fingers. He then returned his arm back to the starting position. After a 5-s pause, the subject once again scratched his cheek 20 times in a row. The set of scratching motions was repeated 35 times. The total scratching time for all 35 sets is
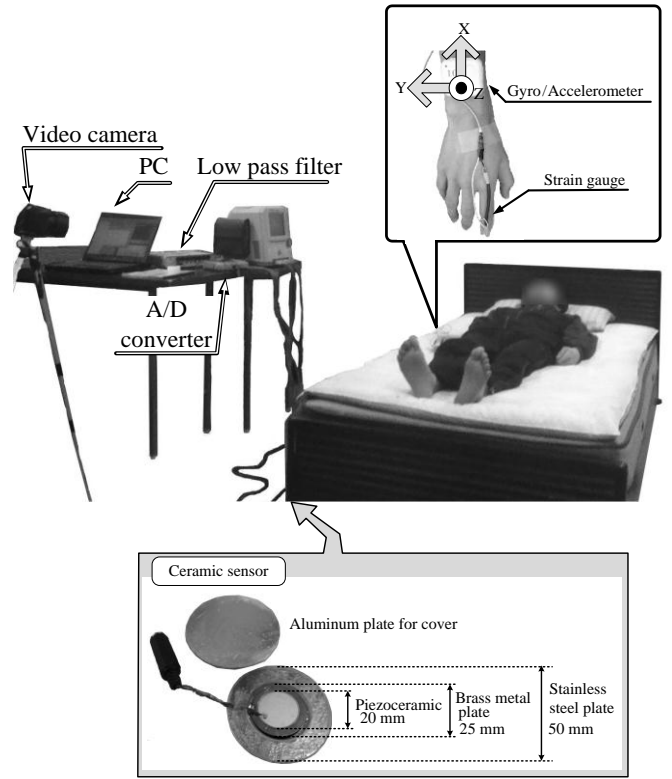

Fig. 4 Experimental system

defined as T_s, and the ratio of TST% is calculated. The entire procedure described above was carried out using all the sensors. While scratching, he pressed his fingers on the cheek moderately. The series of hand movements were performed smoothly. Sometimes he also turned over. In this experiment, we set N in Eq. (1) to 35 and q in Eq. (3) to 250. In step 2, T is set to 1 s, L to 0.5 s and the threshold frequency was the lowest one. Regarding the accelerometer and the gyro sensor, Z-axis and Y-axis were monitored respectively, because these axes change most largely. Using the results, T_s and TST% are obtained from both the proposed and conventional extracting methods. The T_s defined from captured image is true value of T_s. The root mean square error (RMSE) [s] among the sensors were compared using as reference the T_s and TST% data obtained from the video camera images. The error rate is defined from the ratio of RMSE [s] to total measurement time T_m.

IV. RESULTS

A. Measurement result

Fig. 5 shows an example of scratching periods decided from the captured images by reference camera, conventional method in which scorer look at wave shapes, and the proposed processing method. The gray areas mean the correct scratching period T_s defined by captured images. Fig. 5(a) and (b) show the results of piezo-ceramics sensors, (a) is set under the head side right corner and (b) is set under the head side left corner. The results of two piezo-ceramics sensors set under the foot side are the same as (a) and (b) respectively. Fig. 5(c) is the change of

the strain gauge fixed along the index finger, (d) is that of the Z-axis element of the accelerometer set onto forearm, and (e) is that of the Y-axis element of the gyro sensor set on forearm. The conventional method needs the scorer to divide the signal of the scratching motion from that of the other signals, especially the turning over motion.

With (a) and (b), the subject stayed calm between 0 and 1 s. At this time, piezo-ceramics sensor detected the heartbeat component of $s_h(t)$. When the subject turned from the left side of the bed to its center, between 1 and 3 s, the wave shape of the sensor (a) under the right side fluctuated to the positive in a long period. At the same time, the wave shape of (b) under the left side fluctuated slowly to the negative. This is because the center of the gravity of the subject on the bed shifted toward the left side. In the conventional method in which the scorer looks at the output wave shapes, the scorer was biased to misjudge that the signal was not from scratching but from other body movements. From 3 to 6.5 s, when the subject was stationary again, these sensors detected the heartbeat component of $s_h(t)$. Between 6.5 and 7 s, when he moved his hand toward his right cheek, the output changed slowly. While he scratched, from 7 to 9.3 s, the output changes were cyclical and had large amplitudes, as described in the second chapter. After scratching till 10 s, while his arm moved back to the starting position, the output signal contained the natural vibration $s_v(k)$. After the moving of his hand, he stayed calm again. By the conventional extracting method, the scorer had also judged the natural vibration $s_v(k)$ as the scratching signal $s_s(k)$. Using the proposed processing method, the scratching signal $s_s(k)$ can be separated from the natural vibration $s_v(k)$, whose effect is attenuated.

Regarding the result (c), while staying calm between 0 and 1 s, 3 and 6.5 s, and 10 and 11 s, the subject's finger did not move, so the output signals hardly changed. The strain gauge was not affected by the turning over movement. The median of the signal during the scratching motion was smaller than the other periods, not because of arm motion but of his finger bending to scratch. The changes of outputs during the scratching also were cyclical and had large amplitudes, as described in the second chapter. The proposed method, which applies the signal of strain gauge, is able to decide only the scratching time.

Regarding the result (d), the signal of the accelerometer hardly changed while the subject stayed calm; whereas the output fluctuated largely while he turned over on the bed. This is because the effect of gravitational acceleration changed with the change of sensor direction caused by the turning over motion. Before and after the scratching, his arm motion generated low-frequency signals. During the scratching motion, the output signal also changed largely and cyclically as described in the second chapter. The proposed method, which applies the signal of accelerometer, is able to define only the scratching time.

The result (e) is similar to that of (d). While the subject stayed stationary, the signal hardly changed. When he turned over, the output signal changed slowly and largely. Before the scratching, the signal also changed slowly and largely along with the turning over movement. After the scratching, the signal changed

(a) The output of piezoceramics sensor set under the head-side left corner

(b) The output of piezoceramics sensor set under the head-side right corner

(c) The output of straingauge set index finger

(d) The output of acceleration sensor set forearm

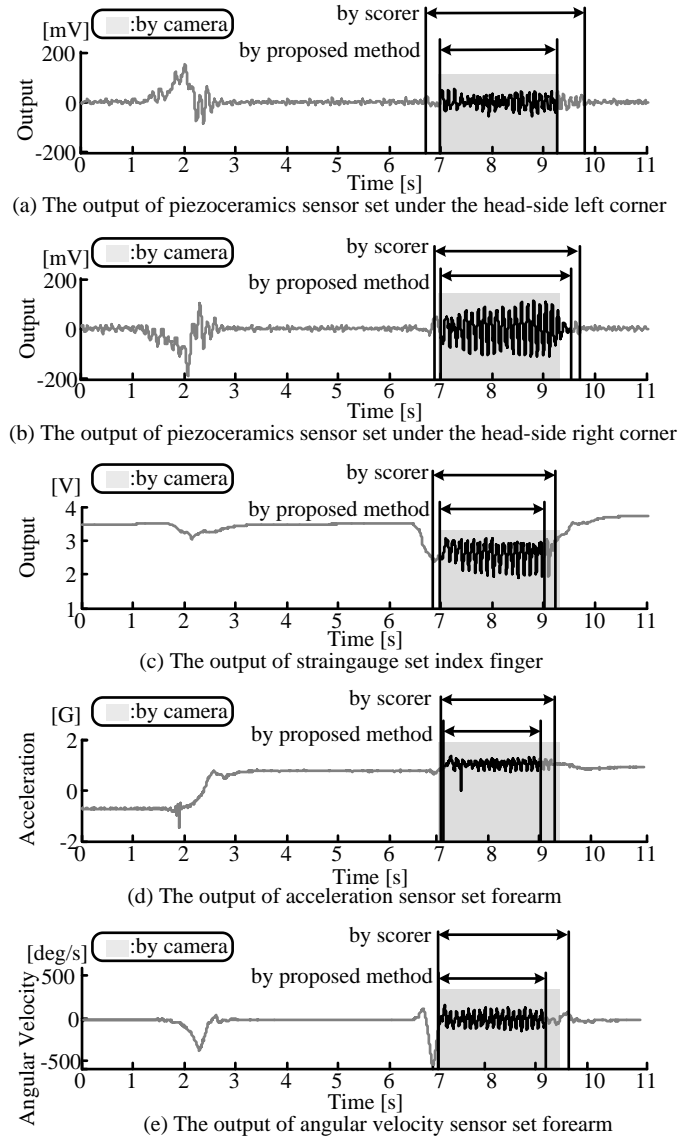(e) The output of angular velocity sensor set forearm

Fig. 5 Results of the scratching and turning over motion

slowly but smaller than before the scratching. During the scratching motion, the output signal also changed largely and cyclically as described in the second chapter. The proposed method, which applies the signal of angular velocity, is able to define only the scratching time.

B. Evaluation

Table 1 shows the RMSE and the error rate of each sensor; and table 2 shows the TST obtained from each sensor, the TST% and its error. The total measurement time T_m was 385 s and the correct total scratching time T_s was 179 s. By the conventional extracting method, in which the scorer looks at the output wave shapes, the wave shapes for the arm motion and for the scratching motion look similar regardless the type of the sensor used, making it difficult to divide the time frames. The T_s therefore included the time for moving the arm, resulted in enlarged TST%. The RMSE of the four piezo-ceramics sensors was less than 1 s, and the maximum error rate was 0.24 %.

TABLE I
RMSE AND THE ERROR RATE

Sensors	Method	RMSE [s]	Error rate
Piezo-ceramics,	Conventional	0.40	0.10
head side left	Proposed	0.68	0.18
Piezo-ceramics,	Conventional	0.64	0.17
head side right	Proposed	0.74	0.19
Piezo-ceramics,	Conventional	0.92	0.24
foot side left	Proposed	0.73	0.19
Piezo-ceramics,	Conventional	0.94	0.24
foot side right	Proposed	0.79	0.20
Strain gauge	Conventional	0.37	0.10
	Proposed	0.53	0.14
Accelaration	Conventional	0.64	0.17
Z-axis	Proposed	0.83	0.22
Angular velocity	Conventional	0.31	0.08
Y-axis	Proposed	0.54	0.14

TABLE II
TST, TST% AND THE ERRORS

Sensors	Method	TST [s]	TST%	Error [%]
Camera	Conventional	179.31	46.57	-
	Proposed	-	-	-
Piezo-ceramics,	Conventional	176.12	45.75	0.82
head side left	Proposed	168.50	43.77	2.81
Piezo-ceramics,	Conventional	186.17	48.36	-1.79
head side right	Proposed	184.50	47.92	-1.35
Piezo-ceramics,	Conventional	204.36	53.08	-6.51
foot side left	Proposed	187.50	48.70	-2.13
Piezo-ceramics,	Conventional	201.51	52.34	-5.77
foot side right	Proposed	163.50	42.47	4.11
Strain gauge	Conventional	185.24	48.11	-1.54
	Proposed	174.00	45.19	1.38
Accelaration	Conventional	162.62	42.24	4.33
Z-axis	Proposed	160.00	41.56	5.02
Angular velocity	Conventional	177.78	46.18	0.39
Y-axis	Proposed	169.00	43.90	2.68

Regarding the ceramics sensors set under the foot side, the RMSEs of the proposed extracting method became smaller than those of the conventional method. The errors of TST% obtained from the proposed method became smaller than those of the conventional method. With the sensor set under the foot side right, the TST from the conventional method was long, while that from the proposed method was short.

Both RMSEs from the strain gauge set along the subject's index finger were less than 0.6 s; both error rates were approximately 0.1 %. The TST from the conventional method was longer than that from the proposed method, which in turn was shorter than correct TST.

With the T_s of acceleration, the error rates obtained from both methods were about 0.2 %. The TST% calculated from both methods were at the same level.

Regarding the angular velocity, the RMSE from the proposed method was longer than the correct time by 0.2 s, and the error rates calculated from both methods were approximately 0.1 %. The TST of the proposed method was shorter than that of the conventional extracting method.

V. DISCUSSION

The errors calculated with the proposed signal processing method and with the conventional method with a scorer's observation are at the same level. The proposed extraction method can separate the scratching motion from the other motions, thus making it operational without the judgment as to whether a signal is caused by a scratching motion, whereas this judgment is needed for the conventional method. With the conventional method, the main reason for the T_s error is the difficulty to separate the scratching motion from other motions before and after the scratching. With the proposed extracting method, the T_s error depends on how long the period T is set in Step 2, or how to compare the amplitudes in Step 3. Step 2 is the process which separates the low frequency signal $s_b(k)$ out of the data obtained for a certain period, using its peak frequency with the data acquisition delay by an interval of L. In this step, the beginning and the end of T_s, required elements to calculate

TST%, depend on the period T and the interval L. Therefore, a shorter interval enhances the resolution and accuracy of T_s. In this experiment, the reason why the TST of the acceleration and of the angular velocity were judged in a shorter period also lies in the interval L. Step 3 is the process to compare the amplitudes of $s_h(k)$, $s_n(k)$, and $s_s(k)$ with the average value of past amplitude of low frequency signal $s_b(k)$. However the changes in the low frequency signal $s_b(k)$ were different from each other; the Step 3 could be improved to be adapted to each sensor.

VI. CONCLUSION

In this paper, we proposed the signal processing method for extracting the scratching time, and applied the method to the piezo-ceramics sensors, the strain gauge, the accelerometer, and the angular velocity sensor as conventional sensors to monitor the scratching motions. The base of this algorism is the characteristics that scratching motion generates cyclic larger-amplitude vibration and signals. This processing is able to calculate the TST%, which is the index of scratching evaluation, and its accuracy is the same as the conventional extracting method in which a doctor looks at the recoded wave shapes to decide the scratching time. In the case of using infrared video camera, calculating the TST% requires significant time, about the same as the measurement time. The proposed extracting method enables to extremely shorten the time to calculate the TST%. In summary, the proposed method can shorten the calculation time of T_s and keep the accuracy of extracting the scratching time. Shortened the calculating time could relieve the doctor of some burden and increase the time to care the patients. The proposed method can also be applied to the electronic medical recording, and there is no fluctuation due to the scratching time judgment, because it is digitally processed.

Our future works are the optimization of Step 2 of the certain time T for Fourier transferring and interval L for the determination of the TST resolution, and the development of comparison way for Step 3.

REFERENCES

[1] Y. Ishibashi, K. Yoshikawa, "The skin diseases with strong itch, the manual for discernment and therapeutics," 1991.

[2] R. Miyaji, A. Ikoma, "Forefront of medical dermatologists series: Frontiers itching," 2006.

[3] R. Miyaji, "Q&A Itching," 2007.

[4] T. Ebata, H. Aizawa, R. Kamide, M.Niimura, "The Characteristics of nocturnal scratching in adults with atopic dermatitis," *British Journal of Dermatology* Vol. 141, pp. 82-86, 1999.

[5] H. Izumi, T. Ebata, Y. Sato, H. Aizawa, R. Kamide, M. Niimura, "A Simplified Method for the Measurement of Nocturnal Scratching with an Infrared Video Camera," *The Skin* Vol. 39, pp. 560-563, 1997.

[6] J. A. Savin, W. D. Paterson, I. Oswald, "SCRATCHING DURING SLEEP," *The Lancet* Vol. August 11, pp. 296-297, 1973.

[7] T. Ebata, et al., "Use of a wrist activity monitor for the measurement of nocturnal scratching in patients with atopic dermatitis", *British Journal of Dermatology* Vol. 144, pp.305-309, 2001.

[8] H. Yokoi, Y. Noro, K. Umeda, H. Mizutani, "Detection of Human Scratching Behavior during Sleep with Acceleration sensor," *Tokai of society related to electricity branch union rally* O-323, 2008.

[9] N. V. Bergasa, D. W. Alling, T. L. Talbot, et al., "Effects of Naloxone Infusions in Patients with the Pruritus of Cholestasis," *Annals of Internal Medicin* Vol. 123, No. 3, pp. 161-167, 1995.

[10] Y. Kawabe. K. Aritake, Y. Noro, K. Umeda, H. Mizutani, "A Study of sensor for Detection of Human Scratching Behavior during Sleep," *Tokai of society related to electricity branch union rally* O-329, 2007.

[11] M. Konishi, K. Aritake, Y. Noro, K. Umeda, H. Mizutani, "A Study of sensor for Detection of Human Scratching Behavior during Sleep," *Tokai of society related to electricity branch union rally* O-322, 2008.

[12] T. Aoki, H. Kushimoto, Y. Hishikawa, J. A. Savin, "Nocturnal scratching and its relationship to the disturbed sleep of itchy subject," *Clinical and Experiment Dermatology* Vol. 16, pp. 268-272, 1991.

[13] J. R. Burch, P. V. Harrison, "THE MEASUREMENT OF ITCH," *Measurements we Couldn't Make Without a Micro*, pp. 9-12, 1988.

[14] K. Endo, H, Sumitsuji, T. Fukuzumi, J. Adachi, T. Aoki, "Evaluation of Scratch Movements by a New Scrath-Monitor to Analyze Nocturnal Itching in Atopic Dermatitis," *Acta Derm Venereol (Stockh)* Vol. 77, pp. 432-435, 1997.

[15] S. Nukaya, T. Shino, Y. Kurihara, K. Watanabe, H. Tanaka, "Noninvasive Bed Sensing of Human Biosignals via Piezoceramic Devices Sandwiched Between the Floor and Bed," Sensors Journal Early Access (http://ieeexplore.ieee.org/xpl/tocresult.jsp?isnumber=4427201).

[16] T. Shino, Y. Kurihara, S. Nukaya, K. Watanabe, H. Tanaka, "Unconstrained Bed Monitoring System for Scratching Motion," proceedings 24th International Conference on Computers and Their Application in Industry and Engineering, pp. 135-140, 2011.